

Design of a UHF Radio System for Small LEO Satellites

Erik Narverud

Master of Science in Electronics

Submission date: July 2007

Supervisor: Odd Gutteberg, IET

Co-supervisor: Morten Olavsbråthen, IET

Problem Description

Design, Prototype Development and Test of a Radio System intended for use in small, LEO Satellites.

Assignment given: 15. January 2007
Supervisor: Odd Gutteberg, IET

Design of a UHF Radio System for Small LEO Satellites

Erik Narverud

July 10, 2007

preface

During the autumn of 2006, three students from the Electronics and Telecommunications Institute at NTNU, one being the author of this thesis, undertook an assignment proposed by professor Odd Gutteberg, investigating the possibility of a new student satellite project at NTNU. The inspiring task culminated in a specification document, [1], outlining specification demands for a small satellite based on the CubeSat standard. Based on information from the Norwegian Space Center, two frequencies around 150 MHz and 437 MHz, with a bandwidth of 25 kHz each, was thought to be the likely communication channels for the satellite. Investigation of satellite antenna solutions for these frequency areas were therefore performed, and viable designs were created.

The project team saw the advantage of having two-way communication on both frequencies, in case of radio system failure. This master thesis has therefore focused on designing a two-way, half-duplex radio system for the UHF channel of the intended satellite system. The work is based on the requirements and limitations given in [1], and assumes the use of the antenna described in that report.

Because no dedicated project administration has existed during the spring of 2007, the students participating in the project has been largely responsible for it's organization. This work has been undertaken simultaneously with the radio system development. An account of the work, and an evaluation of the entire project, is therefore included in this report.

Both the technical and administrative work has been done in close collaboration with fellow student Roger Birkeland, who has been working on the VHF radio system. I would therefore like to thank him for an inspiring and rewarding semester, and especially for his aid in finalizing this report. My professor Odd Gutteberg has been a valuable source of information and support, and working with him has been a great pleasure. My supervisor Morten Olavsbråten, who has presented a solution to every problem I have laid before him, deserves much credit for his technical skills and enthusiasm. Institute Engineer Terje Mathisen and doctorate student Marius Ubostad deserves much gratitude for having assisted me in the use of laboratory equipment. Without the aid and support of the people above, this master thesis would not have been as inspiring and fun to work with, as it ultimately was.

Contents

I	UHF Radio System Design	1
1	Introduction	2
2	Communication and Transmission Theory	3
2.1	Wave Propagation	3
2.1.1	Free Space Wave Propagation	3
2.1.2	Visibility Time Calculation	6
2.1.3	Doppler Shift Calculation	6
2.1.4	Atmospheric Propagation Effects	6
2.1.5	Observed Noise Power and Antenna Noise Temperature	9
2.2	Passband Data Transmission Theory	9
2.2.1	Information theory	10
2.2.2	Spectral Shaping and ISI	12
2.2.3	Modulation techniques	14
3	RF design theory	20
3.1	RF Network Analysis	20
3.1.1	Transmission Lines	20
3.1.2	Impedance Matching and Network Describing Parameters	20
3.2	Noise and Distortion	21
3.2.1	System-Generated Noise	21
3.2.2	Distortion in RF Components	22
3.3	Space Environment Considerations for Electronic Engineering	23
3.3.1	Vacuum	23
3.3.2	Charged Particles	24
3.3.3	Launch Environment	26
4	Design Process	27
4.1	Design Considerations	27
4.1.1	Overall Design Choices	27
4.1.2	Requirements and Limitations	28
4.2	Design Alternatives	29
4.2.1	Fully Integrated Solution	29
4.2.2	Customized DSP design	30
4.2.3	Semi-integrated Design Without DSP	31
4.3	Final Design Layout	33
4.3.1	General Description	33
4.3.2	Peripheral Circuitry	36

4.3.3	Transmitter Section	38
4.3.4	Receiver Section	39
5	Link Budget Analysis	42
5.1	Noise Bandwidth Calculations	42
5.2	Uplink Analysis	43
5.3	Downlink Analysis	45
6	Prototype Construction, Testing and Measurements	47
6.1	Procedure	47
6.2	Transmitter Components	48
6.2.1	CMX980a Baseband Processor	48
6.2.2	AD8345 Quadrature Modulator and Upconverter	50
6.2.3	RF2878 Output Buffer Amplifier	52
6.2.4	RF5110 Power Amplifier Stage	54
6.3	Receiver Components	55
6.3.1	LFCN-490 Low Pass Filter	55
6.3.2	RF2878 Low-Noise Amplifier stage	56
6.3.3	Carrier Band pass Filter	58
6.3.4	RF2418 LNA and IF stage	60
6.3.5	PIF-40 IF Band Pass Filter	62
6.3.6	SA606 IF-to-Baseband section	63
6.3.7	GMSK Baseband Processor	66
6.4	Additional Circuitry and Components	66
6.4.1	HSWA2-30R Transmit/Receive Switch	66
6.4.2	Microcontroller and Interface Logic	68
7	Serial Interface and Software Development	70
7.1	CMX980 Serial Interface	70
7.1.1	overview	70
7.1.2	Serial Packet Formats	71
7.2	External Circuitry	71
7.2.1	External Shift Register Circuit	71
7.2.2	External Flip-Flop Synchronization Circuit	71
7.3	Software Functions	72
8	Development and Demonstration Circuit Designs	74
8.1	PI/4-DQPSK Transmitter Development Circuit	74
8.2	GMSK Receiver Development Circuit	78
9	Discussion	80
9.1	Design Choices	80
9.2	Transmitter section	81
9.3	receiver section	81
9.4	Logic section and software	82
10	Conclusion	83

II	Student Satellite Project	84
11	background	85
12	Project Work	86
12.1	Project Assignments and Master Theses Development	87
12.2	Student Presentations	87
12.3	System Design Review Arrangement	87
12.4	Technical Interchange Meetings	87
13	Project Database Development	88
14	Conclusion	89
III	Appendices	94
A	CMX980a Circuit Diagrams and Measurement Results	95
A.1	Circuit Diagrams	95
A.2	Measurement Results	98
B	AD8345 Circuit Diagrams	100
B.1	Circuit Diagrams	100
C	RF2878 Circuit Diagrams and Measurement Results	103
C.1	Circuit Diagrams	103
C.2	Measurement Results	105
D	RBP-400 Circuit Diagrams	107
E	LFCN490 Circuit Diagrams	109
F	RF2418 Circuit Diagrams and Measurement Results	111
F.1	Circuit Diagrams	111
F.2	Measurement Results, LNA section	114
F.3	Measurement Results, mixer section	116
G	PIF-40 Circuit Diagrams	120
H	SA606 Circuit Diagrams and Measurement Results	122
H.1	Circuit Diagrams	122
H.2	Measurement Results	127
I	HSWA2-30R Circuit Diagrams	129
J	RF5110g Circuit Diagrams	131
K	CMX980 serial Interface; Circuit diagrams, software and timing measurements	134
K.1	External logic Circuit Diagrams	134
K.2	Measured timing Diagrams	138
K.3	Microcontroller Software	140

L	Transmitter Development Circuit Simulation Results	145
M	Receiver Development Circuit Simulation Results	148
N	Student satellite Project Documents	150
	N.1 System Design Review; Invitation and Agenda(Norwegian)	150
	N.2 System Design Review; mechanical Systems Presentation	152
	N.3 System Design Review; UHF Radio System Presentation	156
	N.4 System Design Review; Account (Norwegian	161
	N.5 Future Assignments	170

Part I

UHF Radio System Design

Chapter 1

Introduction

This report concludes a master thesis concerning the design and prototype construction of a UHF half-duplex radio system, intended for use on board a small student satellite. The assignment is a continuance of a project assignment done during the fall of 2006, concerning the outline and specification of a new student satellite project at NTNU. Here, the wish for a downlink with a data rate high enough to transmit a VGA size image in a single pass, is presented. The report details performance-deciding parameters of satellite communication systems operating at UHF frequencies, and fundamental information theory. Theory and application of RF design is discussed, along with complications in electronic engineering due to space environment factors.

The report goes on to describe the design process and prototype development of a UHF transceiver intended for use in small, low power LEO satellites. Three alternative designs, based on commercially available components, are discussed, and a final design solution is chosen for further investigation through prototype development. The prototype system incorporates a 9600 bit/s *GMSK* uplink and a 9600 to 18000 bit/s $\pi/4 - DQPSK$ downlink, operating at frequencies around 430 to 440 MHz. The report concludes that this design is a viable solution, with good bandwidth efficiency, relatively low complexity and good power characteristics, provided that reasonably efficient local oscillators, linear power amplifiers and output networks are found. To aid future students in such work, and form a basis for the development process, receiver and transmitter development boards are presented.

Chapter 2

Communication and Transmission Theory

2.1 Wave Propagation

Although basic wave propagation theory will not be discussed in this report, the application of radio communication in satellite systems presents special problems that must be considered. The effect of the atmosphere on the signal can no longer be neglected, because of the very long pathway, and the presence of the ionosphere in the communication channel creates special attenuation phenomena not found in other forms of radio communication. All these factors, and more, must be taken into account when developing a reasonably correct link budget.

2.1.1 Free Space Wave Propagation

the *transmission equation* is the basis of all link design, and decides an invariable limit to the performance of any communication system. A short summary of its basic composition is given below, based on the more thorough explanation given in [2], chapter 4.2. When a transmitter generates an electromagnetic wave with an average power P_t Watts, and this wave is emitted with equal power in all directions, the emitted power will be dispersed as a sphere. If the transmitter antenna has the ability to focus the emitted power in a given direction, the antenna will contribute with a gain G_t , defined as the relation between the power emitted in that direction, and the total emitted power. For convenience it is hereby assumed that this direction is towards the receiver. The power per square meter of the emitted sphere, in the direction of the receiver, will therefore be

$$F = \frac{P_t G_t}{4\pi R^2} [W/m^2] \quad (2.1)$$

where $P_t G_t$ is commonly referred to as the *Effective Isotropic Radiated Power*, or *EIRP*, of the transmitting radio system. The receiver antenna will have an *Effective Area* $A_e = \eta_A A_r$, relating to the part of the emitted sphere that it is

able to absorb. This area is also directly related to the antenna gain as

$$G_r = 4\pi \frac{A_{e,r}}{\lambda^2} \quad (2.2)$$

When the effective area of the receiver antenna is inserted into 2.1, and substituted with the calculated gain from 2.2, the total received power can be expressed as in equation 2.3, known as the transmission or *Link Equation*.

$$P_r = P_t G_t G_r \left(\frac{\lambda}{4\pi R}\right)^2 [W] \quad (2.3)$$

The product $L_p = (4\pi R/\lambda)^2$ is called the *Path Loss*. In perfect vacuum, with no noise or absorption, the path loss will be the only degradation in a transmission path. Unfortunately, such a scenario is never present, and numerous other factors need to be added to the link budget if it is to match a real application.

Slant Range Calculation

The distance R in link equation, equals the line-of-sight distance between the transmitter and receiver, often called the *Slant Range*. The slant range will depend on the orbital parameters of the satellite relative to the position of the ground station, and therefore change with time and elevation angle. If the orbit is reasonably circular, which can be expected for a polar low earth orbit, the slant range can be calculated through the use of simple trigonometry. Figure 2.1 shows the parameters used. R_e is the earth radius at the ground station, R_s is the satellite orbit radius and el is the *Elevation*, i.e the angle between the slant range and the horizon. γ ("gamma") is the angle between the satellite nadir direction and the latitude of the ground station. From [2], page 33-34, where $d = R$ is the slant range, we have the slant range as

$$R = \sqrt{R_s^2 + R_e^2 - 2R_e R_s \cos(\gamma)} \quad (2.4)$$

From figure 2.1 we can calculate the relation between *gamma* and el to be

$$R_s \cos(\gamma) = R \sin(el) + R_e \quad (2.5)$$

By inserting 2.5 into 2.4 and rearranging, and recognizing that the orbit altitude $h = R_s - R_e$, one gets

$$R = R_e \left[\sqrt{\left(\frac{R_e + h}{R_e}\right)^2 - \cos^2(el)} - \sin(el) \right] \quad (2.6)$$

which is an expression for the slant range as a function of elevation angle and orbit height. It is important to remember that the earth radius changes with latitude, and this will have an effect on the slant range, as the orbit height of the satellite will be higher at the poles than at the equator. For LEO systems, using the true earth radius at the ground station latitude should be sufficiently accurate. With an earth radius of 6378 km, an orbit height of 800 km and an elevation angle of 20°, the slant range will be 1768.7 km.

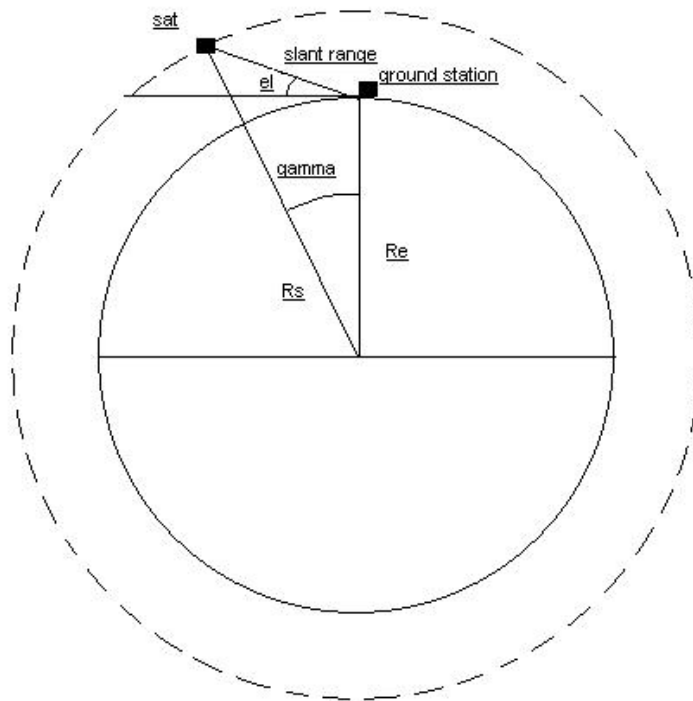


Figure 2.1: Variables of the Slant Range calculations

2.1.2 Visibility Time Calculation

A LEO satellite with a circular orbit will be visible over the ground station for a specific time, depending on the satellite orbit height and the minimum elevation of the ground station. The longest visibility time naturally occurs when the satellite passes directly overhead. By rearranging equation 2.5 we get an expression for γ as

$$\gamma = \arccos\left(\frac{R * \sin(el) + R_e}{R_e + h}\right) \quad (2.7)$$

Recognizing that γ defines an arc in the circular orbit, we can use Keplers laws for orbit period, given in [2] page 19, to find the time it takes for the satellite to pass this arc as

$$T_{visible} = \frac{speed}{distance} = 2\gamma \sqrt{\frac{(R_e + h)^3}{\mu}} \quad (2.8)$$

given that γ is expressed in radians. Equation 2.4 can then be used in combination with 2.7 and 2.8 to produce an expression for the maximum visibility period for a given elevation. At an elevation of 20° and an earth radius of 6378 km, the maximum visible time will vary between 4 and 7 1/2 minutes for orbits between 400 and 800 km.

2.1.3 Doppler Shift Calculation

The relative speed between the satellite and the ground station will generate a doppler shift on the received frequency. The largest shift will occur at the lowest elevation, when the satellite comes directly towards the ground station. When the orbit is highly inclined, the earths rotation speed will be negligible, and the doppler shift becomes

$$\delta f = \frac{V_t}{\lambda} = \frac{\sqrt{\mu/(R_e + h)} \cos(\gamma) \cos(el)}{\lambda} \quad (2.9)$$

as shown in [2], page 50. For an orbit height of 800 km and a minimum elevation angle of 20deg, the maximum doppler shift on a 437 MHz frequency equals about 9.9 kHz.

2.1.4 Atmospheric Propagation Effects

The atmosphere is a complicated, time-varying structure, responsible for significant degradations in the performance of a satellite communication channel. In [3], The radio Communications Sector of the International Telecommunications Union, *ITU-R*, has listed the most common atmospheric propagation effects that must be considered as:

- Absorption by atmospheric gases
- Absorption, scattering and depolarization by hydrometeors(ice and water particles)
- Emission noise from absorbing media

- Beam-divergence due to atmospherical refraction
- Phase decorrelation, due to irregular refractive index
- Fading and scintillation, due to slow and fast refraction changes, accordingly.
- Multipath fading
- Attenuation by obstacles near the ground station
- Varying elevation angle
- Ionospheric Dispersion
- Faraday Rotation
- Ionospheric phase and amplitude scintillation
- Ionospheric Refraction and Propagation Delay
- Ionospheric Absorption

Most of these losses are frequency dependent, and many do not apply at all for a UHF, narrowband, single-carrier system. Those that do, however, call for further investigation, so that the total channel loss can be determined to the best possible extent. This is especially true for ionospheric effects, who tend to increase with the wavelength. The ionosphere also causes more severe problems at higher latitudes, because of the higher values of charged particles in the atmosphere near the geomagnetic poles. Because the solar wind will affect the particles, ionospheric effects tend to be more powerful during the day than at night.

Tropospheric Gas Absorption, Refraction and Depolarization

Signal attenuation caused by absorption by atmospheric gases only becomes important at frequencies above 10 GHz, according to [3], and will therefore be assumed to produce zero degradation in the UHF band. The same goes for tropospheric scintillation and multipath fading. Because of the relatively low frequency, none of these phenomena will affect the system. At low elevation angles, the refractive index of the atmosphere may bend the focus beam of the antenna, but with a minimum elevation of 20 degrees, this is not an issue for the system of interest.

Attenuation and Noise from Hydrometeors

[3] gives a detailed calculation of rain and cloud attenuation. Rain attenuation is generally a complicated attenuation to calculate, as it is both frequency, distance and elevation dependent. On top of that, rainfall is a statistical occurrence, and it is usually modeled after yearly occurrence. In the case of a LEO satellite, possibly with several downlink stations and relatively high elevation angle, the usual rain intensity models will not be suitable. Fortunately, the rain attenuation increases with frequency, and at UHF frequencies it can usually be neglected. The same goes for depolarization caused by rain. Thus, the noise

emitted from rainfalls, which is a function of the attenuation according to [4], can also be reduced to the physical noise temperature of the raincloud. However, the physical temperature of a raincloud is significantly higher than that of a clear sky. This can be compensated by assuming a receiver antenna noise temperature of 290 deg K for the ground station. This will give a sufficient noise margin for most situations.

Ionospheric Refraction and Propagation Delay

In opposition to the tropospheric wave propagation, ionospheric propagation effects usually become more protrudent at lower frequencies. The ionospheric refraction is such an effect, varying with a factor $1/f^2$. However, [3] lists a typical refraction value of less than 0.16° at 250 MHz, which does not contribute significantly to any attenuation. The ionosphere will also generate a time delay (the source of GPS time inaccuracy, normally compensated by the use of two frequencies) with the same frequency dependence as the refraction. By interpolating the estimates of the time delay given in [3], a typical time delay of $1.3\mu s$ for 430 MHz can be found. This will not produce any significant distortion of the signal in the given system, as the bandwidth is too narrow, and the bit rate too low. The same goes for the dispersion caused by the ionosphere. At 500 MHz, the dispersion is specified by [3] to be 0.0032 pS/Hz, resulting in a total dispersion in a 25 kHz band of 80 pS. Even with more pessimistic assumptions, this will not affect the system significantly, because of the low baud rate.

Faraday Rotation

Faraday Rotation is an ionospheric phenomenon that causes a rotation of the signal polarity. The rotation estimates of [3] can be interpreted to give a rotation of

$$r = 360 \frac{3 * 10^{17}}{f^2} \text{ [Degrees]} \quad (2.10)$$

Thus, at 430 MHz, a rotation of about 580° can be expected. If a vertical linearly polarized signal is transmitted from a satellite, it may be horizontal at the receiver. An obvious solution to this problem is to use circularly polarized signals. However, the antennas of the satellite do not necessarily allow this, so the ground station should use a circularly polarized antenna configuration to receive the signal. This brings along a demand for a depolarization margin of 3 dB because of a maximum *polarization mismatch* of 45° , as explained in [5], page 123. If the satellite is rotating with a constant yaw, as is the case of most small LEO student satellites, this margin would have to be included anyway.

Ionospheric Absorption

Although the ionospheric absorption is normally estimated to be near zero for most commercial satellite links, this is not true for high-latitude ground stations and frequencies below 1 GHz. According to [3], the attenuation caused by this absorption is roughly inversely proportionate to the square of the frequency, as for most other ionospheric effects. From the values given in this recommendation for high latitudes, one can deduct that an attenuation of about 0.5 dB should be accounted for to provide good margins.

Ionospheric Scintillation

Aperiodic fluctuations in the ionosphere, known as *scintillation*, is very difficult to calculate. It occurs because of uneven electron accumulations in the ionosphere, and is most prominent at the equator and polar regions. The scintillation affects both phase and amplitude and depend upon solar activity, season and location. At rare occasions, signal amplitude variations can be higher than 20 dB for frequencies below 1 GHz. [3] presents tabular estimations of the scintillation for VHF and UHF frequencies at medium latitudes. At 500 MHz, the scintillation can be as high as 1 dB, 0.1% of the time. This number can be expected to rise for higher latitudes, so a margin of at least 3 dB to compensate for such random scintillation is recommendable for a 430 MHz link.

2.1.5 Observed Noise Power and Antenna Noise Temperature

The noise of a radio channel, if one assumes that the receiver is noise-free, is determined by the thermal noise observed by the antenna. Thermal noise power is defined to be proportional to the temperature T of the observed medium in Kelvin, scaled with Boltzmanns constant $k = 1.3806503 \cdot 10^{-23}$. This is true for any practical frequency, and the *observed* noise power of a radio system will be

$$N_{observed} = kTB [W] \quad (2.11)$$

and therefore proportional with the system bandwidth B . The noise temperature passed on through the receiver antenna is appropriately called the *Antenna Noise Temperature*. As explained in [5], chapter 4.3, it will be a function of the surrounding noise temperature and the directive properties of the antenna. Thus, for an antenna pointing towards Earth with a reasonably high gain, the observed temperature will usually be close to the noise temperature of the Earth. Though this temperature has some geographical variations, it is usually set to 290 Kelvin.

For a ground station antenna pointing out in space through a clear, night-time sky, the noise temperature may only be slightly higher than the cosmic background noise of about 3 Kelvin. In practice, however, the noise temperature of such an antenna will always be higher, due to the temperature of atmospheric gases, clouds, and surrounding media. In the design study, a temperature of 290 Kelvin is therefore assumed for the ground station antenna. Because of the relatively low gain of the satellite antenna, and because it is located in a cold environment, the uplink antenna noise temperature may be expected to be somewhat lower than 290 Kelvin. The *Antenna Efficiency*, describing the dissipative losses in an antenna, will reduce the received noise as well as the signal. In addition to observed noise, the total noise power is made up of the system noise of the receiver, an equally important degradation factor in the system.

2.2 Passband Data Transmission Theory

This section looks at the most important factors used to describe the performance of a transmission system. In essence, there are only three available

resources in a radio channel for transmitting a certain amount of data, namely time, power and bandwidth. If the bandwidth is fixed, and one seeks to transmit as much data as possible in a given period, the only option left is to divide the power of the channel between more data. The amount of power per data will then decrease proportionally, thus reducing the error margin. To keep a low bit error rate, the output power therefore has to be increased, but this conflicts with the interest of keeping power consumption low. A good design must therefore utilize as much of the available bandwidth as possible, while keeping power consumption to an acceptable level. The use of error-correcting codes can help to achieve a higher BER, at the expense of the number of information bits transmitted.

2.2.1 Information theory

Some important parameters, relating to the amount of information that can be transmitted in a communication system, are used to measure the performance of a radio system. This section gives a brief explanation of the ones used in this design study.

Bit Energy and Signal-To-Noise Ratio

The *Signal-To-Noise Ratio*, described mathematically as $SNR = \frac{C}{N}$ in [2], chapter 4.3, is the ratio between the average carrier signal power, denoted C or P , and the average noise power N contained within the bandwidth of the system. Hence, the noise is calculated from the total system noise temperature as

$$N = kT_{total}B = N_0B \text{ [W]} \quad (2.12)$$

where N_0 is the *Noise Power Spectral Density*. When the noise is distributed evenly in frequency and has a gaussian amplitude distribution, it is referred to as *Additive White Gaussian Noise*. A communication channel influenced purely by such noise is called an AWGN channel. Although other noise distributions occur to a certain extent, such as Rayleigh and Rice distributed noise, AWGN will usually be the most prominent. Section 5.5 of [6] shows the exact mathematical relations between signal and noise in an AWGN channel. The SNR is usually expressed in dB, and is the deciding factor of the quality of the communication system. However, though the signal power C is a physical measure of the signal amplitude, it does not say how the signal energy is distributed. [2], section 5.4, therefore states that if R_s symbols per second are transmitted over a carrier wave with an RMS power of C Watts, the average energy per symbol will be

$$E_s = C/R_s \quad (2.13)$$

If one recognizes that the energy of each symbol in the received signal can be divided amongst a number of bits, we find the *Bit energy* E_b to be related to the SNR and bit rate R_b as

$$E_b = E_s \frac{R_s}{R_b} = \frac{C}{R_b} \quad (2.14)$$

By using the information from equation 2.12 that $N_0 = \frac{N}{B}$ and combining this with equation 2.14, the *Bit Energy to Noise Spectral Density* ratio can be found,

expressed as

$$\frac{E_b}{N_0} = \frac{C}{N} \frac{B}{R_b} \quad (2.15)$$

The $\frac{E_b}{N_0}$ ratio, in contrast to the SNR, is an invariable measure of the transmission performance of a system, and can be used to directly compare systems with different modulation schemes.

Bit Error probability

The *bit Error probability*, normally denoted P_e , is a statistical measure of the probability for error in the receiver, based on the assumption that both the signal and noise in the radio system will be distributed across time and bandwidth in a way that can be statistically modeled. The *Bit Error rate*, or just BER, is the likelihood that a bit value is incorrectly detected by the receiver. Whether a symbol is detected correctly or not will depend on the minimum distance between the symbol values compared to the noise power. Because the noise adds directly to the signal value, a symbol may be incorrectly detected if the noise power at the time of detection is equal to or higher than half the minimum symbol distance. Hence, the BER will be dependent on the symbol constellation of the chosen modulation, as well as the $\frac{E_b}{N_0}$ ratio. As one can see from figure 2.2, the BER decreases exponentially when the signal strength is increased.

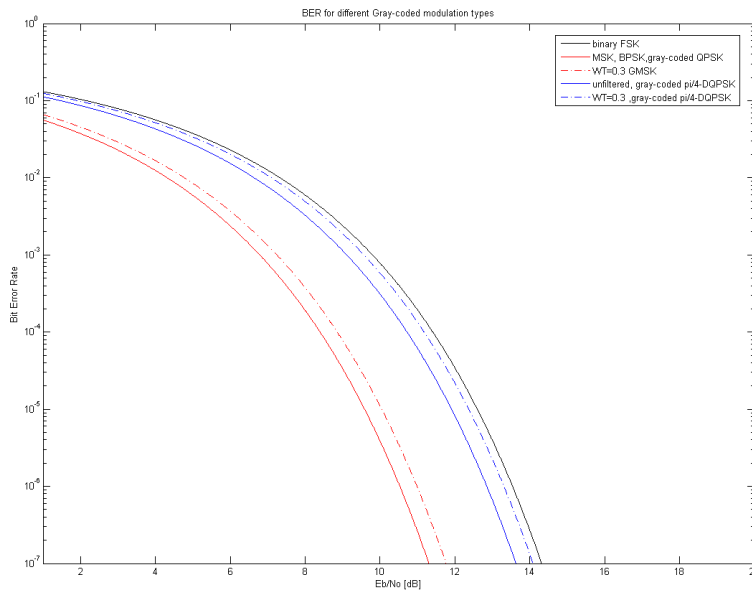


Figure 2.2: Bit Error Rates of relevant modulation schemes.

Statistically, there will always be a possibility of a bit error, so error detection should always be employed to ensure that corrupt data will be detected. Of course, The BER of a physical system will be largely dependent on the sensitivity and function of the receiver.

Power Spectral Density and Spectral efficiency

Bandwidth is a limited resource, and knowledge of the frequency used by a transmission system is crucial. As only a limited bandwidth will be allocated for a system, it is always interesting to see how a particular configuration exploits the available bandwidth. Because any modulated signal is made up from several frequency components, the shape of the symbols will affect the bandwidth occupied by the system.

The Fourier Transform of a deterministic signal will yield the *Power Spectral Density*, denoted *PSD*, of the signal as explained in [7], chapter 10. This is a function describing how the signal power is distributed in frequency. The *Bandwidth* of a signal is usually defined as the frequency area where the *PSD* magnitude is higher than half the maximum magnitude, and can therefore be referred to as the *-3dB Bandwidth* in some cases. Figure 2.3 shows power spectral densities for modulation schemes considered in this report, with a normalized bit energy E_b and a symbol rate R_s of 18 kBaud. According to [2], page 180, Assuming that the symbols are Nyquist filtered, the occupied bandwidth can generally be expressed as

$$W = R_s(1 + \alpha) [Hz] \quad (2.16)$$

where α , described in section 2.2.2, is called the *excess-bandwidth parameter*. The *Bandwidth efficiency* ν , defined in [6], page 142, is a measure of how much information that can be transferred through the system at a given bandwidth, and therefore becomes

$$\nu = \frac{R_b}{W} \quad (2.17)$$

2.2.2 Spectral Shaping and ISI

By appropriate filtering of the symbols in the baseband signal, one can effectively shape the frequency response of the signal. As explained in chapter 10 of [7], sharp edge symbol transitions will generate a large number of frequency components, very unfavorable for systems in adjacent frequency bands. One therefore seeks to reduce these unwanted frequency components by "smoothing" the transmitted symbols. Several filter shapes can be used, but the most common are *gaussian* and *Raised Cosine* filters. Applied to an originally square pulse shape, they will create pulse shapes with good spectral properties. In [8], page 397, The Gaussian pulse shape is defined as

$$h(t) = \sqrt{\frac{2\pi}{\log 2}} W * \exp \frac{-2\pi^2}{\log 2} (Wt)^2 \quad (2.18)$$

. Gaussian spectral shaping is further discussed in the GMSK part of section 2.2.3. A downside to the use of a gaussian spectral shaping filters, is the generation of *Inter-Symbol Interference*, or ISI. ISI occurs because some power from each symbol is scattered in time, affecting subsequent symbols and contributing to the overall noise power. A system incorporating spectral shaping will therefore generally have a higher spectral efficiency, but a lower SNR. This can be seen from figure 2.3 and 2.2, where gaussian filtered MSK has a smaller occupied

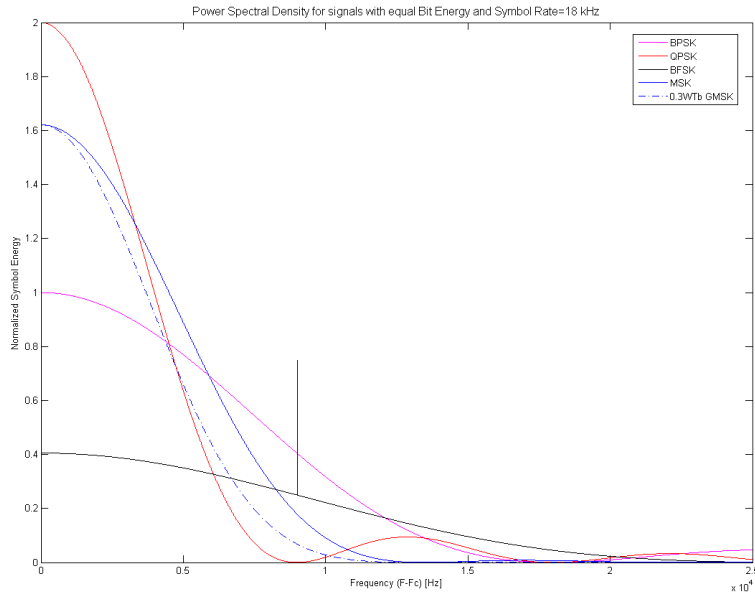


Figure 2.3: Power Spectral Density for different signals of equal bit energy and with Nyquist pulse shapes.

bandwidth, but higher error probability, than pure MSK. As described in [6], section 5.1.1, the *Nyquist Pulse Shape*,

$$g(t) = \frac{\sin(\pi t/T_b)}{\pi t/T_b} = \text{sinc}(t/T) \quad (2.19)$$

defines an ideal pulse shape that creates zero ISI with no excess bandwidth. This is possible because the pulse has zero crossings at every detection point of subsequent symbols. The Nyquist pulse is not usable in practice, however, because the infinite pulse length will make the time period available for correct detection, converge towards zero. However, the principle of zero-crossings in subsequent sampling moments can be applied to pulses with some degree of excess bandwidth. The most common pulse shapes with this property are the *Raised Cosine* pulse shapes, which is essentially a Nyquist pulse with an attenuating part:

$$g(t) = \text{sinc}(t/T) * \left[\frac{\cos(\alpha\pi t/T)}{1 - (2\alpha t/T)^2} \right] \quad (2.20)$$

Here, α is known as the *Roll-Off Factor* of the filter, and also decides the excess bandwidth created by the filter. When raised cosine filtering is employed in a transmission system, the square-root response of the raised cosine filter, abbreviated *RRC* for *square-Root Raised Cosine*, is commonly employed as a transmit and receive filter, making the overall response a raised cosine pulse shape. Although the RRC pulse satisfies the nyquist criterion, it must be remembered that ISI can only be neglected if the sampling moments are exact, which will never be completely true.

2.2.3 Modulation techniques

Below follows a description of different types of modulation that might be good alternatives for a low power LEO system with a 25 kHz available bandwidth. The chosen modulation types, GMSK and $\pi/4$ -DQPSK, are given a more thorough explanation. Bit Error Rates and Power Spectral Densities are compared in figures 2.2 and 2.3.

Frequency Shift Keying

Frequency Shift Keying, FSK, provide an easy way of designing a radio system with acceptable performance. This section will concentrate on Binary FSK only, although several bits per symbol might be transmitted with this modulation scheme. Like ordinary analog frequency modulation, known as FM, FSK uses a change in frequency to represent information. Unlike FM, orthogonal frequencies are used to distinguish between the digital symbols. A binary FSK transmitter can therefore easily be constructed with two frequency generators, being arbitrarily switched on and off, or with a single, fast changing oscillator that is set to vary between the two frequencies.

This modulation scheme can produce a continuous phase provided that the two frequency generators are synchronized, and one then gets *Continuous-Phase FSK*, CPFSK, often called *Sundes FSK* after it's inventor. As the detection and demodulation can be done with regular FM receiver technology, this enables a simple, power efficient and robust implementation, with a signal that does not produce rapid phase variations. A high-efficiency power amplifier may therefore be used without creating intermodulation problems. The nature of coherent CPFSK produces independent in-phase and quadrature components, and the Power Spectral Density of the signal is therefore a sum of the spectral density of the two components. In [8], page 385-386, the total baseband power spectral density is given as:

$$S_B(f) = \frac{E_b}{2T_b} \left[\delta \left(f - \frac{1}{2T_b} \right) + \delta \left(f + \frac{1}{2T_b} \right) \right] + \frac{8E_b \cos^2(\pi T_b f)}{\pi^2 (4T_b^2 f^2 - 1)^2} \quad (2.21)$$

As one can see from 2.21, two frequency components will be generated at the frequencies given by equation 2.22.

$$f_{1,2} = (f_c \pm 1/2T_b) \quad (2.22)$$

It therefore follows that the maximum bit rate per channel bandwidth must be

$$R_b \leq \frac{B}{2} \quad (2.23)$$

Thus, no more than 12500 *Bit/s* can be sent over a 25 kHz channel using CPFSK. The Bit Error Rate of CPFSK, shown in figure 2.2, is also inferior to most other modulation types. FSK needs twice as high signal to noise ratio as conventional BPSK and QPSK to achieve the same BER. The main advantage over other modulations schemes is therefore limited to lower system complexity and lower intermodulation products, provided that a continuous-phase scheme is used. FSK also has an additional advantage over phase shift keying in that it can be noncoherently detected, meaning that no knowledge of the carrier phase is necessary. However, as [8] points out, *differential PSK* still has a 3 dB advantage in E_b/N_0 over noncoherent FSK.

Gaussian Minimum Shift Keying

Minimum Shift Keying, MSK, is a frequency shift keying modulation scheme with substantially better noise performance than ordinary CPFSK. Being the ultimate choice for the uplink modulation scheme in this thesis, the way this noise performance is achieved, will be more closely investigated here. The main difference between Minimum Shift Keying and CPFSK, is that where the frequency change of CPFSK is instant in time, the MSK scheme changes its frequency linearly during the entire bit period, but keeps the signal envelope constant. The modulated signal can therefore be represented as a carrier signal with a continuous phase change, as shown in equation 2.24.

$$s(t) = \sqrt{\frac{2E_b}{T_b}} \cos [2\pi f_c t + \phi(t)] \quad (2.24)$$

The phase function equals that of equation 2.25, where a positive phase change equals 1 and a negative equals 0.

$$\phi(t) = \phi(0) \pm \frac{\pi h}{T_b} t \quad (2.25)$$

In MSK, the information is therefore not represented by two static frequencies, but by a continuous phase change on a center carrier. h is a factor deciding the magnitude of the phase change, and can be related to the frequency deviation of FSK through

$$h = T_b(f_1 - f_2) \quad (2.26)$$

h therefore represents the *Deviation Ratio* of the signal, and a 1 symbol will therefore increase the phase of the signal by πh , while a 0 will decrease the phase by the same amount. if h is 1, the phase change will always return to zero, as a change of $-\pi$ is equal to $+\pi$. By using a deviation ratio of $h = 1/2$, the instant phase will be a function of both the current and previous phase value. This increases receiver complexity, but also reduces the occupied bandwidth by 1/2 compared to orthogonal FSK. MSK can therefore be interpreted as CPFSK with a difference of half the bit rate between the signaling frequencies. On page 394-396, [8] uses the relations to CPFSK given above, to find the Power Spectrum Density of MSK as

$$S_{msk}(f) = \frac{32E_b}{\pi^2} \left[\frac{\cos(2\pi T_b f)}{(4T_b f)^2 - 1} \right]^2 \quad (2.27)$$

A bandwidth of half the bit rate is considered to be the minimum required bandwidth for coherent detection of FSK signals, as a lower h will produce interference between the signaling frequencies. As shown in [8], page 392-394, the Bit Error Rate of MSK can be found to be

$$P_e = \frac{1}{2} \operatorname{erfc} \left(\sqrt{\frac{E_b}{N_0}} \right) \quad (2.28)$$

for a white noise channel. This is the same BER as for BPSK and QPSK, and twice as good as ordinary CPFSK. Although pure MSK generates lower sidelobes than PSK, Gaussian symbol filtering is commonly employed to further

reduce out-of-band power, effectively generating *Gaussian* MSK, abbreviated to GMSK. The 3dB attenuation bandwidth of the Gaussian filter, W , defines the attenuation of the GMSK signal as shown in equation 2.29.

$$H(f) = \exp\left(-\frac{\log 2}{2}\left(\frac{f}{W}\right)^2\right) \quad (2.29)$$

The *time-bandwidth product* WT_b is commonly used as a design parameter for gaussian filtering. The effect of such filtering can be seen in the power spectrum plots in figure 2.3, where the pure MSK signal has substantially higher sidelobes than the GMSK signal with $WT_b = 0.3$. Unfortunately, the filtering generates a non-trivial degradation of the BER because of ISI. [8] gives an estimate of the degradation for a varying time-bandwidth product, and for $WT_b = 0.3$, the SNR must be increased by approximately 0.7 dB to maintain the BER of unfiltered MSK.

The difference in BER for a filtered and pure MSK signal can be seen in figure 2.2. In both cases, the theoretical minimum SNR needed for detection will be half the bit energy, but as the MSK constellation actually has four points, where two points represent one symbol, the total bit energy for MSK is twice as high as for ordinary FSK. MSK therefore has a BER equal to BPSK and QPSK, with a slight degradation if gaussian filtering is employed.

Binary and Quadratic Phase Shift Keying

Phase Shift Keying is a very common form of modulation in many modern mobile and satellite communications. The principle function of the modulation technique is to assign a phase value for each symbol in the constellation, while keeping the magnitude of the symbols constant. Intuitively, one can deduce that several symbols can be added to a PSK constellation, at the expense of accuracy, as there is only 360 degrees of phase available. However, by increasing the power of the signal, the mutual distance of the symbols can be kept constant. The bandwidth efficiency of PSK is therefore only limited by the available output power. The constellation map for *Binary* and *Quadratic* phase shift keying, is shown in figure 2.4. By interpreting the mutual distance between the symbols in the constellation, one can calculate the BER for both modulations to be equal that of MSK, given in equation 2.28 and plotted in figure 2.2. As seen, there is no theoretical degradation in SNR performance when the constellation is expanded, provided that the Bit energy is kept constant. The occupied bandwidth of M-ary PSK can therefore be expressed as

$$B = \frac{2R_b}{\log_2 M} \quad (2.30)$$

In terms of BER, PSK is better than the other modulation types discussed here. Unfortunately, there are important drawbacks. As knowledge of the carrier phase is critical for demodulation, PSK signals will always be coherent. The phase dependency can be removed by differentially encoding the signal, generating what is known as *DPSK*. In section 6.9, [8] calculates the BER for DPSK as

$$P_e = \frac{1}{2} \exp\left(-\frac{E_b}{N_0}\right) \quad (2.31)$$

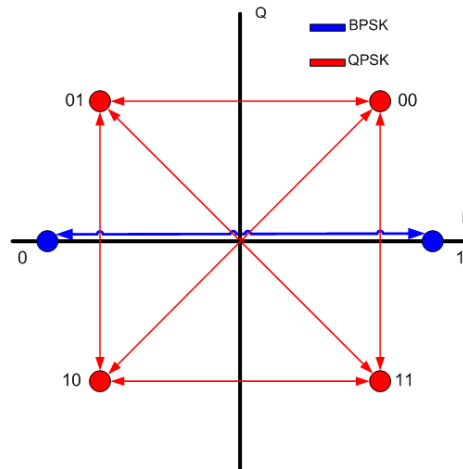


Figure 2.4: The symbol constellation of BPSK and QPSK

An important degrading factor of all PSK constellations, is that they possess *zero crossings*, meaning that the direct line between two constellation points move through a zero envelope amplitude. Hence, the signal may have rather large envelope variations, as any filtering due to amplifier nonlinearity or channel limitations will distort the signal, reducing the SNR and disturbing adjacent channels. QPSK therefore demands a system with a rather linear frequency response.

$\pi/4$ -shifted Differential Quadrature Phase Shift Keying

As the final choice of downlink modulation in this thesis, and a rather special modulation altogether, $\pi/4$ -shifted DQPSK, from here on referred to as $\pi/4$ -DQPSK, requires some special attention. If one uses the ordinary QPSK constellation shown in figure 2.4, and shifts its phase by $\pi/4$, one will achieve a similar constellation with equal properties. $\pi/4$ -shifted QPSK exploits this by using both the shifted-and unshifted QPSK constellation alternately, making each symbol jump between the two constellations. The result is the constellation shown in figure 2.5, where no symbol shifts pass through the center of the constellation map. This significantly reduces envelope variations caused by filtering and non-linearity in the signal channel, and makes for a spectral-efficient modulation scheme. Because the modulation will have a continuous phase shift even though no symbol change occurs, it can be noncoherently detected. Furthermore, it can be differentially encoded, resulting in $\pi/4$ -DQPSK. Although it can be tempting to use these features to design a very elegant and simple receiver, one should note that the accuracy of noncoherent detection may deteriorate if the signal channel is a varying multipath environment, as mentioned in [8], page 362-635. Because this is a nonlinear modulation, though it inherently has only small amplitude variations, good signal margins can only be achieved through the use of a reasonably linear output amplifier. At higher frequencies, amplitude levels may be randomly attenuated by the atmosphere, thus distorting the signal, but such attenuation is not that distinctive in the UHF band.

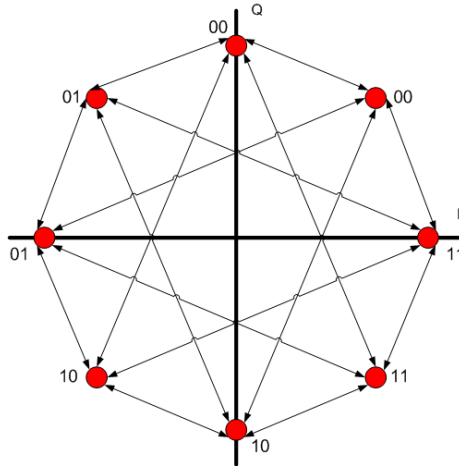


Figure 2.5: The symbol constellation of $\pi/4$ -shifted QPSK

The drawback of using this modulation in a low-power application, is the need for linear amplification, which in turn reduces the efficiency of the transmitter. However, the signal has substantially smaller envelope variations than ordinary QPSK, where statistically, 1/3 of the symbol changes are zero crossings. Ordinary QPSK has a 2.3 dB SNR advantage over $\pi/4$ -DQPSK, but this advantage in power is quickly lost because of the larger envelope variations of QPSK. This makes $\pi/4$ -DQPSK a good choice when the bit rate needs to be higher than the allocated bandwidth.

Because the signal constellation of $\pi/4$ -DQPSK is quadrature generated, and thus dependent on both phase and amplitude of two separate channels, many factors can affect the Bit Error Rate in a physical system, making it somewhat tricky to calculate. Figure 2.2 shows the BER for $\pi/4$ -DQPSK in an ideal AWGN channel, derived through a method presented in [9], where it is shown that the ideal case is equal to the BER of four-phase, gray-coded DPSK. Methods have been developed for calculating the BER when the system is influenced by different types of degrading phenomena such as gain imbalance, DC offset and I and Q channel phase imbalance. The articles [10], [11] and [12] demonstrate such solutions for calculating the BER for a system suffering of gain imbalance, DC offset or phase difference between the I and Q channel, respectively.

The TETRA Communication Standard

The link and power budget presents clear requirements to the radio system, especially when considering the narrow available channel of 25 kHz. $\pi/4$ -DQPSK modulation seems to fulfill, and even exceed, these requirements, given that the transmitter utilizes an efficient power amplifier. The modulation, being an advanced form of regular QPSK, is used in the TETRA system, short for *Terrestrial Trunked Radio* system, or *Trans European Trunked Radio System* as it was first introduced. The TETRA system is divided into 25 kHz subchannels, and transmits 36 kBit/s using $\pi/4$ -DQPSK on a carrier in the 400 MHz

band. The existence of commercial TETRA baseband processors, such as the CMX980a used in the final design, therefore presents integrated solutions, and good utilization of the allocated bandwidth through the use of $\pi/4$ -DQPSK modulation.

Chapter 3

RF design theory

As this project has included an extensive prototype development, the subject of RF design theory can not be omitted. In this chapter, parameters used to describe the physical properties and performance of the chosen components, are explained. The chapter also includes sections describing noise performance parameters and environmental factors that should be considered when designing electronics for space applications.

3.1 RF Network Analysis

3.1.1 Transmission Lines

At higher radio frequencies, *transmission line theory*, described in [5], chapter 2.1, must be used to design electronic circuits. This is because, at high frequencies, the RF signal in a circuit may be considered as a wave, traveling in the substrate between a microstrip line and the ground plane of a circuit board. This effect only becomes noticeable when the wavelength of the signal approaches the dimensions of the transmission line. Because the wavelength of UHF frequencies are usually significantly larger than most microstrip lines used in an electronic design, transmission line calculations may be omitted, provided that the designer has some knowledge of it's effect and keep the length of conductors small. Any further explanation of transmission line theory will therefore not be given here.

3.1.2 Impedance Matching and Network Describing Parameters

In order for a high frequency electric signal to be dissipated in a load, *Impedance Matching* must be incorporated into the network design. Because RF signals propagate along transmission lines as waves, a portion of an emitted wave may be reflected if the seen output impedance is not matched to the output of the source, thus reducing the power delivered to the load. The same applies if the load impedance is different from the network impedance that it is connected to.

At higher frequencies, matching can be achieved by using microstrip lines as capacitors and inductors. At UHF frequencies however, the long wavelengths call for the use of lumped elements, i.e. normal circuit components, to be used to

design the matching networks. A detailed explanation of matching techniques will not be given here, an readers may consult chapter 2.4 of [5] for a more thorough explanation. However, the parameters used to describe the measured impedance of a circuit will be discussed below.

Scattering Parameters

Scattering parameters, or just *S-parameters*, are parameters used to describe the voltage distribution of an unknown microwave circuit. They can also be calculated for a known system. In an network of N ports, N^2 S-parameters will exist. this is because the s-parameter is the ratio of the output voltage wave amplitude on one port, to the input voltage wave amplitude on another (or the same) port. On page 51, [5] defines an s-parameter as

$$S_{ij} = \frac{V_i^-}{V_j^+} |_{V_k^+ = 0 \text{ for } k \neq j} \quad (3.1)$$

which essentially is the ratio of the output voltage of port i to the incident voltage on port j . It follows naturally, that if S_{ij} is larger than unity, one has a voltage amplification from port j to port i . S-parameters are the most common parameters used to describe high frequency circuits, as they give information about both gain and impedance. Interpretations must be done with care, however, as the parameters are amplitude related only.

Voltage Standing Wave Ratio

3.2 Noise and Distortion

3.2.1 System-Generated Noise

In addition to the noise generated by surrounding media, the components of a radio system will also generate a substantial amount of noise. Keeping this noise at a low level is particularly important in the first stages of a receiver, as the noise will be further amplified through the circuit. This section takes a look at the most important aspects of receiver noise calculations.

Noise Figure

The noise performance of a component or system is commonly described by it's *Noise Figure*. On page 89, [5] defines the noise figure as

$$F = \frac{S_i/N_i}{S_o/N_o} \quad (3.2)$$

making the noise figure the relation between the input and output SNR. The noise figure will always be greater than 1. There is no such thing as a noiseless component.

Equivalent Noise Temperature

The *equivalent noise temperature* is a noise temperature relating to a specific noise power measured within a confined bandwidth. It is also related to the noise

figure through a specified reference temperature $T_0 = 290K$, and can therefore be expressed as

$$T_e = \frac{N_o}{GkB} = (F - 1)T_0 \quad (3.3)$$

where G is the gain of the system or component. This is the expression for equivalent noise temperature referred to the *input* of the component, with the noise power N_o being measured on the *output* of the component. The equivalent noise temperature can be calculated for a system of cascaded components through the following relation:

$$T_e = T_{e1} + \frac{T_{e2}}{G_1} + \frac{T_{e3}}{G_1 G_2} \dots \quad (3.4)$$

Of course, the same can be done with the noise figure, as explained in [5], page 92.

3.2.2 Distortion in RF Components

When a time-varying signal is transmitted through a certain component, the signal may be *distorted* by nonlinearities in the amplitude transfer characteristic of the component. For example, a sine wave of 1 V p-p can be transmitted without any degradation through a certain component, but if the amplitude is increased to 2 V, the sine wave shape may be *compressed*, because some of the increased input power is not being transmitted through the circuit. Generally, the transfer characteristic of any component can be modeled as a Taylor series

$$V_{out} = \sum_{k=0}^{\infty} a_k V_{in}^k \quad (3.5)$$

as shown on page 98 of [5]. Here the constant a_0 will correspond to a DC component, a_1 will be the linear gain, and the rest of the sum will be unwanted nonlinear products. The constants $a_k, k \geq 2$ will generally be negative, and because they will generally be smaller with increased k , it is normal to consider only the 2nd., 3rd., and to some extent, the 5th. order product. These products generate what is commonly known as *Intermodulation Distortion*, or IMD. Not only will this distortion reduce the SNR, but it will also generate unwanted components in adjacent frequency bands. Chapter 2 of [13] gives a comprehensive explanation of such distortion, and though it mainly focuses on amplifier linearity, the phenomenon is equally true for passive components with a gain of less than unity.

IMD products from Amplifier Nonlinearity

Intermodulation distortion will have a significant effect on the power spectral density of a signal, because a sine wave applied to a transfer characteristic with higher order products will generate frequency components related to these products. As shown in chapter 2.3 of [13], a *Two-Tone Test* can be performed to investigate amplifier nonlinearity. When two frequencies are applied to a component with a third-order linearity, the output will consist of these frequencies and an additional six unwanted components. A crucial downside to odd order

nonlinearities is that they will also have a negative in-band component, reducing the wanted signal power, while even order nonlinearities will only affect out-of-band frequencies and can therefore be reduced through filtering.

1-dB Compression Point

The 1-dB compression point is a parameter describing the power linearity of components. All components, passive or active, can only handle a certain amount of power without degrading the signal. Specifically, the 1-dB Compression point in a input-to output power plot, is defined as *The point where the actual characteristic of the component deviates with 1 dB from an ideal, linear characteristic.* It can be related to both the input and output power. It is therefore stressed that the 1 dB compression points of the components in a linear RF path should be substantially higher than the power of the signal. The voltage area below the 1 dB compression point is called the *Dynamic Area* of the component.

Third Order Intercept Point

Because third order nonlinearity is a degrading factor of the signal quality, a measure of the relation between this and the gain in an amplifier is desirable. The *Third Order Intercept Point*, often denoted *IM3*, is the point in an input-output voltage plot where the ideal linear response is intercepted by the linear product of the third harmonic constant, as shown on page 28 of [13]. The *IM3* point is therefore a measure of the ratio between the linear gain and the unwanted third order product.

3.3 Space Environment Considerations for Electronic Engineering

Space is an unfriendly place, compared to our familiar surroundings. When we leave our planet, the environment changes radically. The lack of gravitation, atmospheric pressure and radiation shielding introduces a new set of challenges, totally different from those of earth based engineering. The elements of space environment are numerous, as are the factors deciding how these elements work on a particular spacecraft. They pose radical and harmful effects on both man and machine, and knowledge of such effects is critical in order to make a satellite survive long periods in space. The following chapter takes a brief look on some important factors of space environment, and their effects on electronic systems.

3.3.1 Vacuum

The presence of a near vacuum environment brings with it complications to the engineer. These complications are numerous, and some may easily be overlooked, because the characteristics of certain materials change radically with the absence of atmospheric pressure.

Outgassing

At low pressure, certain substances may dissipate from their materials as gas, a phenomenon known as *outgassing*. Outgassing can lead to several fatal errors, as lubricants may dry up, and dissipated gas may condense and attach to other surfaces, or cause corrosion to other parts of the satellite. As a result one needs to take great care in selecting materials that do not contain volatile gases. For example, PCB plastics are strictly forbidden, as the chloride may escape and corrode other parts of the satellite. The components used in a radio system must therefore be checked to see whether they contain substances that can cause damage to the satellite.

Gas Residues

Another issue occurs when air gets trapped inside the satellite. The air may stay inside the structure for weeks after launch, seeping out little by little. Because this air contains moisture, condensation may occur, and ice will gather on cold surfaces of the satellite. This can be a problem as optical lenses or other sensors may become blurred by ice. A bigger issue occurs if moisture or gas gets trapped underneath electronic components. When it freezes, it may actually push the component off its pads, ripping the soldered connections apart. Surface-mounted devices with pads instead of pins can be particularly exposed to such events.

Thermal Conditions

Thermal control in space poses challenges because of the absence of atmosphere. Satellites, and especially their on board radio amplifiers, generate a lot of heat, and the satellite is also heated significantly by the sun. On earth, such problems are usually solved by transferring the heat to a colder medium like air or water. In space however, there is no material surrounding the satellite to which heat can be transferred. Therefore, if the spacecraft needs to rid itself of excess heat, it must apply the use of thermal radiators to turn the heat energy into electromagnetic radiation. Because the sun is the primary source of heat for satellites, accompanied only by earth radiation, good thermal control is needed to ensure that one side of the satellite does not overheat while the other side freezes up. A radio contains many heat sources that must be taken into account when thermal modeling of a satellite is performed, and heat must be efficiently removed from high power components, such as output stages. [14]

3.3.2 Charged Particles

although the term vacuum is commonly used to describe space, there is a lot of charged particles, such as protons and electrons, flying around out there. The particles are emitted by both the sun and other interstellar objects, and some may even be remains from the Big Bang. The amount of particles emitted by the sun, called the *Solar Wind*, varies according to the activity of the sun's surface. Solar flares may emit very high concentrations, resulting in *particle showers*.

Electrostatic Charging

Charged particles can create several harmful effects to a spacecraft, such as electrostatic charging. This occurs because the solar wind particles make up a charged plasma, towards which non-conducting parts of the satellite may build up an electric potential. This potential can discharge as static electricity, damaging electric circuits and creating data errors known as *bitflips*. Such events can cause both temporary errors, called *Single Event Upsets*, SEU's, and permanent, possibly fatal errors called *Latch Up*'s, depending on the satellite's ability to reboot the stricken system.[2]

Galactic Cosmic Radiation

Bitflips can also be the result of *Single Event Phenomenons*, SEP's, when high-energy particles like cosmic radiation, penetrate into memory circuits of the data systems, literally changing logical values. Galactic Cosmic Radiation consists of very high energy particles, and although they are extremely few, their energy is enough to cause problems in satellite computers such as SEU's and latch up.

Exposed Areas and Orbits

The earth's magnetic field will trap some of the charged particles, concentrating them in rings aligned perpendicular to the magnetic field, called the *Van Allen Belts*. An artistic impression of the belts is shown in figure 3.1. Fortunately, LEO satellites orbiting below 1500 km are not as vulnerable to such events because the inner Van Allen belt starts above this height. The Van Allen belts are in fact located at altitudes in between usual orbit altitudes, and although satellites with highly eccentric orbits pass through them at regular intervals, few satellites are exposed to these harmful belts for long durations.[14] However, though the highest particle concentrations occur at much greater altitude, trapped in the outer belts, charged particles will always exist to some degree in LEO orbits as well. Because the earth's magnetic field has large geographical variations, the amount of particles reach critical levels in certain areas. *The South-American Anomaly* is such an area, and operators often take preemptive actions to prevent damage on the satellite when it passes through this high-activity zone.

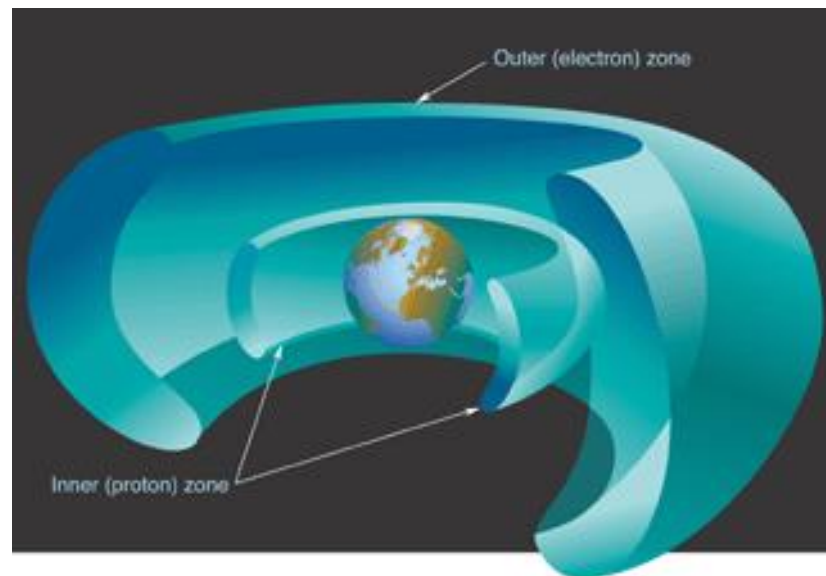


Figure 3.1: Schematic of the Van Allen Belts (courtesy of aero.org)

3.3.3 Launch Environment

Though the absence of gravity removes much of the physical demands on soldering and mountings of electronic circuits, this advantage is canceled out by the violent situation of a launch. Components should therefore be securely fastened. Fortunately, most electronic components are so light that the launch environment does not demand any extra measures to be put into use. However, one should be extra careful when using large, heavy components or cables and wires. The latter must be securely strapped down to ensure that they do not break off during the severe vibrations. Connectors are also prone to failure during launch, and permanent soldering should be used instead of connectors whenever possible. The vibrations generated during launch tend to be around 20 Hz to 2 kHz, according to [14] and care should be taken to ensure that mechanical components do not resonate at these frequencies.

Chapter 4

Design Process

This chapter describes the design process leading up to the final design, and the choices and considerations made. Although only one design was further developed in this thesis, the alternative designs presented in this chapter can be equally good solutions.

4.1 Design Considerations

The design process started with a research into what type of components were available on the commercial market. Several interesting products were evaluated to see if they could be used in a radio system, and an image of the possible design alternatives was gradually built up. At this stage, no decision had been made concerning modulation schemes, integration level, complexity or performance. The goal was to find a solution based on commercial products that would satisfy the design requirements, without being needlessly complicated or expensive. The study of previous student satellite radio designs gave valuable information concerning the choice of manufacturers, and what products they could offer. Before prototyping and testing commenced, a design review was held for all the participants of the satellite project. Several guests from national space technology companies, as well as from the University, attended the review and gave vital information and helpful hints to the students.

4.1.1 Overall Design Choices

Because of the possibility of a very power efficient and robust circuit, the use of radio system IC's in combination with suitable amplifier stages was closely investigated at the early stage of the design process. When the integrated baseband processors were discovered, a design was gradually built up around the use of these, as they seemed to be ideal choices. A milestone in the design process was an ingeniously simple solution; By choosing different modulation schemes for the uplink and downlink, a simpler, more power efficient transceiver could be made that still conformed very well with the design requirements.

Because of the inevitable lack of time in such a comprehensive project, it was decided at an early stage that prototyping of some design elements had to be abandoned, in favor of producing an operational development system. When

the choice of a non-linear modulation on the downlink was made, it became clear that the design of a power efficient, linear output amplifier with a suitable gain could not be completed in the available time period. The design of a good output diplexer, switch or matching network was therefore rendered impossible, as the PA output impedance would remain unknown. As a result, work on the antenna connection network was not carried on.

The last major component that could not be completed was the frequency generation units. Because of superior noise and stability characteristics, crystal oscillators was chosen in preference to synthesizer frequency generators used in the previous NCUBE projects. But as no specific frequency band were allocated at the time, it was decided not to order any oscillators, as they have to be specifically made with the desired frequencies. This design element was therefore not tested, although a suitable crystal oscillator was found.

4.1.2 Requirements and Limitations

The design is based upon the specification document [1] for a small student satellite, developed during the autumn of 2006. The specification outlines requirements with respect to power consumption, dimensions and weight. The design will aim to fulfill these demands to the greatest extent possible.

Required data rate

If one bases the required data rate on the need to transmit a VGA image in a single pass, the equation is simple. A raw VGA image consists of 800x600 pixels. If the image is in grayscale, the intensity of each pixel is described with one 8 bit word. In color images, each pixel has 3 primary colors, each of which is described with 8 bit words. The total size of a grayscale VGA image will therefore be 3.84 Mbit, and of a color image the size will be 11.52 Mbit. One must then take the visible time, calculated in section 2.1.2, into account. For an 800 km high orbit, and a minimum elevation angle of 20 degrees, the visible time will be about 450 seconds. For a grayscale image, the corresponding information data rate must therefore be a minimum of 8.54 kbit/s. The color image will require 25.6 kbit/s. Off course, when the satellite does not pass directly over the ground station, the visible time will decrease. Hence, the required bit rate will increase.

Power Budget Limitations

From the preliminary power budget for given in [1], the allowed power consumption for the 437 MHz system is a total of 3 W during transmission, and 0.20 W during reception. For a 3 V system, this equals current consumptions of 1 A during transmission and 66.7 mA during reception.

Mass and Volume Limitations

The satellite specification also outlines a preliminary mass budget, where a 437 MHz transmitter has been allowed a mass of 0.05 kg. although this is suspected to be a very difficult requirement to meet when a receiver is included as well, the total mass of the system will be kept in mind during the design study.

Pre-defined Peripheral Interfaces

There are two main external interfaces which need to be considered in the system design. The power supply has not yet been defined in the specification and will not be especially considered. One is the digital communication interface connecting the transceiver to the OnBoard Data Handling system of the satellite. The internal communication is performed over a two-wire bus, conforming with the I^2C standard developed by Philips. The transceiver must therefore be able to communicate over such a bus solution. The other interface is the antenna connection. During the autumn of 2006, the author developed a directive UHF antenna for the student satellite, described in [1]. The antenna has an impedance of 50 Ohm, meaning that it can be fed through a standard coaxial cable. A standard, 50 Ohm, broadband chip balun can be used to produce a differential feed on the antenna. The antenna gain is also used in the link budget analysis.

4.2 Design Alternatives

When designing a radio system, several solutions exist with respect to the level of system integration. A system consisting of few parts may be more reliable, and use less power, than a system made up from many basic components, but it is not certain that such a fully integrated radio chip can meet the specified requirements. Power consumption and reliability must therefore be weighed against transmission performance parameters. There is no point in designing a bullet-proof radio if it can't match the application requirements. Three basic designs, based on commercially available components, were considered. Of the three, A customized design without a digital signal processor, and with different modulation schemes and data rate for the uplink and downlink, was chosen as the one best fitting the design requirements.

4.2.1 Fully Integrated Solution

The fully integrated design, shown in figure 4.1 is based upon radio-on-chip solutions where all the key functions of a transceiver are integrated into a single CMOS chip. These radio chips can be found in many normal appliances such as remote controls and short range communication devices. The question was if such a radio chip could be used as a long range, low power radio for satellite applications, if they were combined with appropriate amplifier stages for transmission and reception.

The ADF7020, ADF7020-1 and ADF7021 from Analog Devices, the CC1100 from Texas Instruments (Formerly Chipcon), and the nRF903, nRF905 and the nRF403 from Nordic Semiconductor were investigated to see if they could meet the design requirements. All of the products have very low power consumption, as they are intended for use in hand-held, battery powered applications. The radio chips usually work in the VHF to UHF bands, as higher frequencies are difficult to realize with CMOS technology. This ensures that there are several chips available with the appropriate frequencies. Most of the chips incorporate some form of programmable frequency synthesizers, but many have only a limited number of frequencies available. Modulation schemes range from different types of binary FSK, to GMSK and 4FSK. Some of the chips can also be programmed to choose between several schemes. T

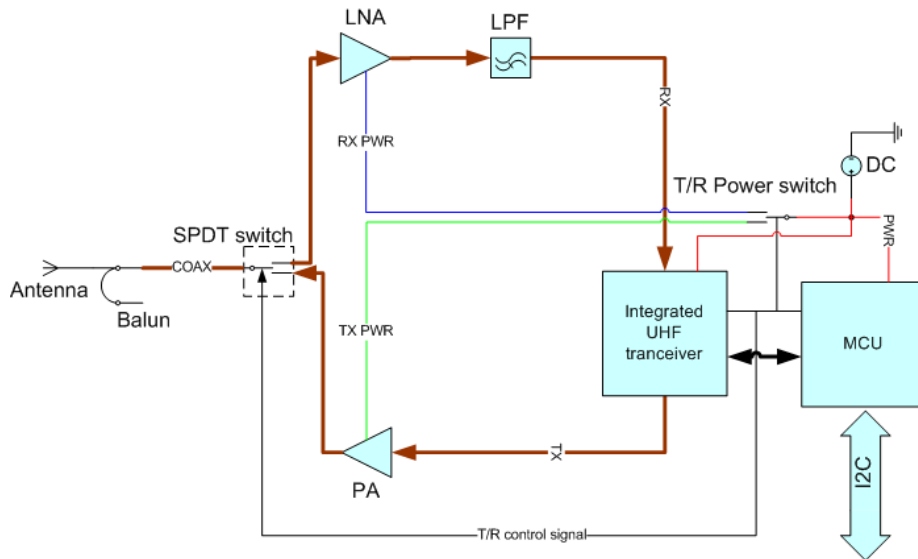


Figure 4.1: Conceptual schematic of a fully integrated transceiver.

One of the problems of CMOS integrated radios is the noise levels. With cascade noise figures approaching 10 and 11 dB, they simply generate too much noise to produce the required levels of accuracy. Very good LNA's must therefore be used to generate the required SNR. Also, as most features can be adjusted digitally, the circuits may be vulnerable to SEU's and latch-up's. In addition, none of the modulation schemes, except the GMSK ability of the CC1100, were optimum choices with regard to channel resource utilization. In all, the fully integrated design favors low power consumption and few components over transmission performance.

4.2.2 Customized DSP design

The incorporation of a DSP, short for *Digital Signal Processor*, allows full digital customization of the modulation scheme. The DSP is a processor specifically designed to perform fast signal processing. If an advanced quadrature modulation, such as $\pi/4$ -DQPSK, is used on the uplink, a DSP may be required for demodulation. Although $\pi/4$ -DQPSK can be noncoherently detected, no analog demodulation circuit for this specific modulation is known to exist.

With a high capacity uplink, software upgrades and advanced commands may be sent to the satellite. However, as most DSP's run at high clock frequencies, required for good sampling rates and resolution, they also use a lot of power. Even power-efficient DSPs, such as the TSM320VC5510 from Texas Instruments, may use over 100 mA during normal operation. If the DSP is used continuously in the receive section, such a power consumption is clearly excessive. *Received Signal Strength Indicators* may be used to wake the DSP up from sleep mode when a signal is received, thus saving power. DSPs are also completely programmable circuits, increasing the risk of communication failure due to bit-flips.

A schematic of the full DSP radio system is shown in figure 4.2. Here, a DSP is combined with the CMX980 Tetra baseband processor. This processor performs a complete transformation of transmit data into $\pi/4$ -DQPSK, but it does not demodulate receive data. Instead, the received data is sampled and filtered before being sent serially to the DSP as digital signal level information. This information then has to be interpreted by the DSP. As the sampling rate of the CMX980's receive section produces over 4 Mbit/s of signal-level data, a regular microcontroller will not be fast enough to process the received data. Because the CMX980a is used in the transmit section of the radio system, it is described in detail in section 4.3.3. It is important to note that the tasks performed by the CMX980 can be programmed into a DSP, and that regular AD and DA converters can be used to do the signal conversions.

The upconversion is performed by the AD8345 quadrature modulator, also used in the final design and described in section B, while downconversion is performed by the very versatile AD8348, a circuit containing both a temperature compensated AGC and quadrature demodulator. Because this component has a limited input frequency, the receiver section has to be a double superhet design, with an intermediate frequency stage before the AD8348. The first mixer may be the RF2418 combined LNA and mixer.

Such a design solution also requires good carrier lock, provided by the Phase Locked Loop synthesizer on the 2. IF stage. The primary synthesizer considered for this design was the PE9601 from Peregrine Semiconductors, as it is a latch-up free, radiation hardened component designed for space applications. The VCO used in the PLL has not been under closer investigation, although it is certain that very accurate oscillators will be required.

Because no DSP with sufficiently low power consumption could be found, no DSP is suggested as an alternative in the schematic. In all, the design is a possible solution if uplink performance is considered important. However, as this is currently not the case, simpler modulation schemes may be used on the uplink, making a DSP unnecessary. This is clearly an advantage considering the high power consumption and complexity of the system.

4.2.3 Semi-integrated Design Without DSP

Commercial mobile radio systems demand highly reliable, low-power integrated solutions for hand-held applications. Many specialized components, combining several analog tasks in one chip, exist on the market. The semi-integrated design benefits from this by using components that were originally designed for specific communication systems, such as GSM or TETRA. Specially designed baseband processors with hardwired modulation schemes can perform accurate modulation and demodulation with very low power consumption, and integrated IF and RF system chips can be used to create a customized design with few active components.

Another important factor demonstrated by this solution, is the use of different modulation schemes for the uplink and downlink. The need for high data capacity only applies to the downlink in this particular specification, which means that frequency modulation, such as FSK or GMSK, can be used for the uplink. This will eliminate the need for high-speed digital signal processing in the satellite receiver, with the trade-off being lower bandwidth efficiency on the uplink. The semi-integrated design will therefore be a customized solution,

where the level of application optimization is limited by the available types of communication ICs. It should be mentioned that although this solution is not really a transceiver, but a separate transmitter and receiver using the same frequency, a ground station using appurtenant equipment may regard the system as a transceiver. The term *transceiver* is therefore considered to give a sufficient description of the system.

4.3 Final Design Layout

4.3.1 General Description

After careful consideration of the different design alternatives, the semi-integrated solution, with different modulation schemes on the uplink and downlink, was the one ultimately chosen for further development. An overall schematic of the design is shown in figure 4.3. By using different modulation schemes, the radio may no longer be called a true transceiver; it is rather a separate transmitter and receiver, using the same frequency. The final circuit design uses two baseband processors; The transmitter incorporates the CMX980a, which modulates up to 36 kbit/s of raw data into a $PI/4$ -DQPSK downlink. For the uplink, the CMX909b demodulates, decodes, de-interleaves and unpacks 9600 bit/s of received MOBITEK GMSK data. Alternatively, if a custom protocol other than Mobitex is wanted, the CMX589, a GMSK demodulator without packet handling, can be used. The packet control must then be handled by the microcontroller.

All three baseband processors are made by CML Microcircuits, a company specializing in integrated circuits for communication. The baseband processors differ from DSPs in one important area, as they are hardwired to perform only one specific type of modulation scheme instead of being programmable. This should make them more robust against program anomalies caused by bit-flips, and is also the reason why they consume very little power. Unfortunately, none of the chips are available in radiation-hardened configurations. The bit rate of the downlink is essentially limited by the allocated bandwidth. The baseband processors communicate internally with an ordinary microcontroller, and as all three components draw very little current, the digital section becomes very power efficient.

The analog receiver section consists of a low noise amplifier, a combined LNA and mixer circuit, and a complete IF system-on-chip with a quadrature detector. The transmitter section uses a wideband quadrature modulator to modulate the complex baseband signal directly on the carrier, and then amplifies the output through a low-noise, linear buffer amplifier. A linear final stage amplifier, with a gain of about 24 dB, and an output power of approximately 30 dBm, does the final amplification. Note that a final design of such a power amplifier has not been done, although some testing has been performed. It is expected that further work must be done in order to present a linear PA with acceptable power efficiency that conforms with these specifications.

Bandwidth Occupation Considerations

When running the CMX980a at a default clock frequency, a baud rate of 18 kBaud is generated. Because a RRC filter with an excess bandwidth of 0.35 is

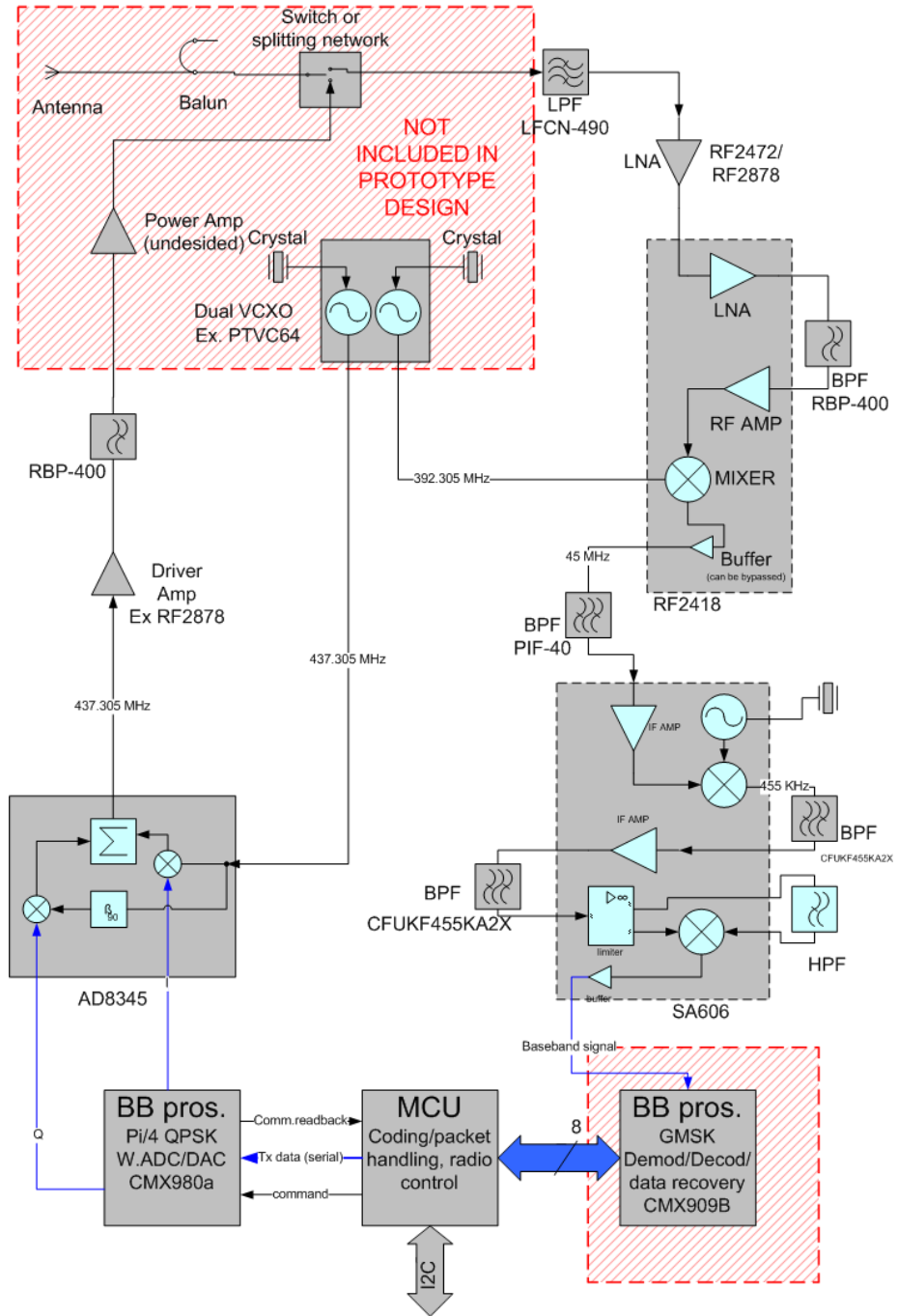


Figure 4.3: An overall schematic of the recommended system design.

used, the bandwidth consumption is 24.3 kHz, which is well within the available bandwidth of 25 kHz. However, when a Doppler shift of ± 11 kHz is introduced, the total occupied bandwidth will be 46.3 kHz. If the baud rate is reduced to 9600 baud, which can be done simply by exchanging the clock frequency crystal and rescaling the output RC filter of the CMX980, the total occupied bandwidth will be 34960 Hz, which is more acceptable. However, it is not known whether the increased bandwidth consumption caused by Doppler shift is considered when the bandwidth is allocated by the authorities. In fact, the previous NCUBE missions used a 9600 baud GMSK link on UHF frequencies, also causing an excess bandwidth occupation due to Doppler shifting.

On the uplink, the baud rate is limited by a very different problem. The ceramic resonators used as bandpass filters in the SA606 IF circuit, have a very narrow bandwidth. In fact, the widest bandwidth found on a 455 kHz resonator was only 35 kHz. Fortunately, this is adequate for the 34480 Hz bandwidth occupied by a 9600 baud signal with 0.3 excess bandwidth and ± 11 kHz Doppler shift. The reason why Doppler shift has to be considered in the receiver, is that it does not have phase locked loop tracking the carrier frequency.

Power Budget Analysis

The power budget shown in figure 4.4 gives a good indication of the power consumption of the circuit. The uncertain factor is the frequency generator circuit, which has not been investigated. Here a 40 mA current consumption is estimated, a typical value for many VCXO's. The total power consumption can be seen to conform with the demands given in [1], with a slightly higher consumption for the receiver. Of course, as the estimated value of 40 mA for the oscillator constitutes nearly half of the total receiver consumption, it is a very uncertain estimate. If the actual current consumption of the VCXO is in as high or higher than this value, the conclusion may be drawn that a frequency synthesizer is a better choice.

437 MHz transceiver Power Budget					
	Voltage	Current, mA		Power mW	
		transmit	standby	transmit	standby
Transmitter					
MCU	3	10	0	30	0
CMX980A baseband processor	3	20	0	60	0
AD8345 modulator/converter	3	65	0,07	195	0,21
VXCO	3	40	0	120	0
PA driver amp	3	11	0	33	0
Power amp with 50% DC efficiency	3	667	0,01	2001	0
PE9354 SPDT switch	3	0,02	0	0,06	0
Receiver					
		standby	receive	standby	receive
MCU	3	0	10	0	30
CMX909 modem	3	0	2,5	0	7,5
SA606	3	0	3,6	0	10,8
VXCO	3	0	40	0	120
RF2418 LNA/mixer	3	0	18	0	54
RF2472 LNA	3	0	7	0	21
PE9354 SPDT switch	3	0	0,02	0	0,06
TOTALS:	DC/DC eff	Transmit	receive	Transmit	receive
	90 %	903,3556	90,22222	2710,067	270,6333

Figure 4.4: Calculated power budget

4.3.2 Peripheral Circuitry

Microcontroller and logic circuitry

The microcontroller chosen for the prototype design is a ATMEGA128L produced by Atmel. The 8 bit RISC architecture, called AVR, was originally developed by two students at NTNU, and bought by Atmel. This resulted in an Atmel division being located in Trondheim, hence a lot of knowledge concerning these microcontrollers, and experience using them, has been built up amongst the students at NTNU. This was an important factor in deciding which controller to use, and it should be stressed that for the flight model, many other microcontrollers may be better suited than the AVR. Especially, radiation-hardened controllers may be available, and use of these will reduce the risk of failure.

The ATMEGA128L is one of the larger controllers in the AVR series, and was chosen primarily because of it's many communication features. The controller incorporates hardware two-wire(I2C) and SPI bus logic, two flexible USART connections and several 8 bit parallel ports. It also contains counters and timers, Pulse width modulators and ADCs. The architecture is based upon about 120 instructions, most of which can be executed in a single clock cycle, making the controller quite fast. The I2C bus logic is needed for communication with the satellite bus, while the SPI is used for communicating with the CMX980, together with 1 of the 16 bit counters. The interface to the CMX909 is an 8 bit parallel port with some additional signal pins. If the CMX589 is to be used, the interface will be a serial synchronized one. The MEGA128 can be serially programmed through it's *In system Programming* feature, or through the use of it's JTAG interface.

Frequency Generation Components

The circuit is designed to use a dual, voltage controlled, crystal oscillator package. The PTVC64 produced by FOQ Piezo Technik can generate the carrier frequency for the transmitter, as well as the first IF frequency of the receiver. The reason for using a dual crystal oscillator is that such high frequency oscillators tend to be very large and heavy, and the possibility of containing both oscillators in a single package is therefore a good alternative. A drawback with crystal oscillators like the PTVC64, is that they must be specifically designed for the wanted frequency, making them expensive and difficult to obtain. Despite this, crystal oscillators generally outperform frequency synthesizers, with lower complexity, higher accuracy and substantially less noise.

The major drawback of VCXO's is that they tend to have very high current consumptions. No specific value is known for the PTVC64, but a typical value may be 40 mA per oscillator. Power consumption is a critical factor, and much higher currents should not be allowed. A frequency synthesizer should therefore be considered if the current consumption cannot be lowered. The PE9601 [15] is a radiation hardened, latch-up resistant synthesizer that may be usable for this application.

Antenna Connection Network

The antenna connection network is what enables the use of a complete transceiver on the same frequency and antenna. The design incorporates a SPDT (single Pull Double Throw) RF switch for connecting either the transmitter or the receiver on the antenna connection. Unfortunately, This is not a very power efficient connection, as there is a substantial loss in such switches. The switch tested in this design is the HSWA2-30R made by Mini-Circuits. There are a number of usable RF switches on the market, but a few were singled out as good alternatives. The criteria looked for were sufficiently high compression points, a low loss, internal driver circuitry, good temperature stability and good isolation between the Tx and Rx ports. The HSWA2 meets most these requirements, with better than 32 dBm input 1dB compression point, but is not designed to be particularly robust.

A better alternative may be the PE9354DS switch by Peregrine Semiconductor. This is a radiation hardened chip optimized for space application, designed to be impervious to latch-up. Despite several inquiries directed to their Norwegian distributor Sangus Richardson AB, neither rad-hard nor engineering samples were received in time for testing. Because a rad-hardened switch would improve robustness, a dialog with Peregrine regarding the PE9354 should be established in the future. Alternatively, a well matched network may be designed without the use of switches, if the LNA input and PA output are both highly reflective in their off states. This may greatly improve PA output efficiency, as the losses in SPDT switches are substantial. Because this is very critical for the total power efficiency of the transmitter, it is advised that such a solution should be further investigated.

Power Supply

The entire circuit is designed to run on a 3V to 3.6V supply, with exception of the power amplifier stage which may use a higher voltage for better efficiency.

However, all circuits should be able to run at voltages up to 5 volts without much reconfiguration. As the voltages available from the Power Management System of the satellite has not been decided, no decision has been made as to what type of power supply should be used.

4.3.3 Transmitter Section

Baseband Processor

The CMX980A baseband processor is in essence what made the transmitter design possible. Produced by CML Microcircuits, it is a very flexible unit performing the entire conversion from digital data to a modulated baseband signal, except packet formatting and coding. The processor is primarily intended for use in the Terrestrial Trunked Radio System (TETRA), and the default modulation is therefore $\pi/4$ DQPSK with a $0.35BT$ Root-Raised Cosine filtering.

The symbol rate is fixed to $MCLK/512$, and can therefore be scaled by changing the master clock frequency. The master clock frequency can vary from 0.5MHz to 9.5MHz with a 3V supply, up to 12.5MHz with a 5V supply, enabling symbol rates ranging from 1 to 18.5 kBaud. Gray-coding is performed automatically, and transmit data is written to a 4-byte deep FIFO register. This means that byte formatted data can be written directly to the transmitter, substantially easing pre-processing. The TETRA modulation closely matches the modulation scheme wanted in the design specifications, and it is therefore assumed that the CMX980 will be used in default mode. If a different modulation scheme is wanted, the CMX980 also offers a direct write possibility, enabling the user to specify the symbol constellation and modulation. The digital filter coefficients can also be altered to change the time-bandwidth product.

Some of the most useful features of the CMX980 in respect to this design are the output gain, offset and clock phase adjustment registers. These enable precise digital adjustment of the symbol positions, making it possible to dynamically compensate irregularities in the transmit path. The processor has fully differential outputs, and the digital interface consists of three serial ports, of which two are used, based on the industrial 3-wire configuration. The serial interface was a source to a few challenges, especially since the CMX980 has to control the serial clock, and this is examined closer in the microcontroller section. The CMX980 offers many additional features not described in this report, including 4 auxiliary DA-converters and 4 AD-converters. The reader should consult the CMX980 datasheet, [16], for further information.

Quadrature Modulator

the AD8345 quadrature modulator, made by Analog Devices, is a flexible, accurate wideband modulator incorporating Gilbert Cell mixers. The wide frequency area eliminates the need for additional mixers and frequency stages, as the baseband input can be modulated directly onto the carrier wave. It boasts a good accuracy of 0.5 degree phase error and 0.2 dB amplitude balance. All inputs are differential, and the baseband inputs need 0.7V DC bias to be operational. For additional information and performance data, the AD8345 datasheet, [17] may be consulted.

Buffer Amplifier

The RF2878 LNA, used in the first stage of the receiver and described more closely in section 6.3.2, was believed to be a good alternative for a linear, low-noise PA driver because of its large dynamic range. According to its datasheet, the 1 dB compression point of the RF2878 is around 12.5 dBm measured on the output at 836 MHz. With 20 dB gain this would correspond to about -8 dB input power in that band. The AD8345 quadrature modulator delivers around -15 to -16 dBm single sideband output power when supplied with 3V, so the amplifier should be linear with these levels of input power. These levels of linearity demands higher bias currents than in the LNA case, but as the amplifier has a voltage controlled bias adjustment circuit, this can be adjusted with a minimum of external components.

Power Amplifier

The chosen power amplifier stage was the RF5110G made by RF Microdevices. This is a power amplifier capable of delivering over 32 dBm output power with 57% efficiency in the GSM band, and a gain of 32 dB with a 3.5V supply. Originally intended for use with GSM mobile systems, the amplifier can also be used at lower frequencies. The amplifier includes an analog gain control and various other features described in its datasheet[18].

At 450 MHz, the amplifier should have an efficiency of at least 45% and an output 1dB compression point of 32 dBm, according to [19]. Though not an ideal choice in efficiency or amplification, the RF5110G seemed to be one of the few commercially available amplifiers capable of meeting the requirements. However, as prototype development was started, it became clear that designing a power amplifier with sufficient linearity and power efficiency was a job requiring substantially more resources and time than what was available. Attention was therefore focused on producing a prototype transmitter that could aid such a development, rather than designing a complete system that would fail to fulfill the requirements.

4.3.4 Receiver Section

The receiver is a FSK/GMSK double superheterodyne design, containing two LNAs, two mixers, additional amplification through an IF amplifier and a hard limiter, and a quadrature detector performing the baseband downconversion. Still, the analog part of the receiver only contains three separate, active components. This is achieved through the use of two components combining several important receiver tasks in one. In addition to a LNA, the RF2418 by RF microdevices contains a mixer with a buffered output, doing the first downconversion to 45 MHz. The next stages are included in the SA606, an IF system chip made by Philips, which mixes, filters and hard-limits the signal before presenting the baseband signal through the use of a quadrature detector.

Input Low pass filter

A simple, single-chip low pass filter, the LFCN-490+ from Mini-Circuits, is suggested as an input filter. A band pass filter is considered unnecessary on the input, because of the good low frequency rejection of the antenna [1]. The filter

has a low insertion loss of about 0.5 dB at 437 MHz, and a 3 dB frequency at about 650 MHz according to the datasheet [20]. The very small size is convenient in order to keep unscreened line lengths as small as possible.

First LNA Stage

The RF2878 low noise amplifier is a RoHS-compliant version of the older RF2361 LNA by RF Microdevices. Produced using a GaAs HBT process, the R2878 has a good noise figure of 1.5 dB, considering its low current consumption. The bias current can be externally adjusted through a voltage control circuit, enabling adjustment of the amplifier gain and efficiency. A gain of 20 dB is achievable with a current consumption of 7.5 mA, according to the RF2878 datasheet [21].

Second LNA Stage and First IF Stage

The First downconversion of the received signal is performed by the RF2418 integrated LNA and mixer circuit. Produced by RF MicroDevices, the circuit incorporates both an LNA and a mixer, and was originally conceived for UHF digital and analog receivers. The mixer section has buffered inputs and output, enabling amplification and mixing with a minimum of external components. The LNA output and mixer input are accessed externally, so that appropriate filtering can be included on the mixer input. The entire circuit is said to give a cascade gain of around 20 dB, with a reasonably low cascade noise figure of 2.4 dB when an external image filter is included. The RF2418 datasheet [22], gives detailed information of its performance.

RF Band Pass Filter

For removing unwanted image frequencies before the first mixer stage, the RBP-400+ band pass filter from Mini-Circuits is suggested. The filter, described in detail in the datasheet [23] has a steep, high order response with a pass band between 292 and 490 MHz. As the insertion loss is quite high, around 1.5 dB, the filter is implemented after the RF2418 LNA. It can also be used on the transmitter output to remove intermodulation products generated by the amplifier, but should be incorporated before the last PA stage to ensure good transmitter efficiency. The filter comes in a screened SMD package.

IF Band Pass Filter

the PIF-40+ band pass filter by Mini-Circuits was used in the design to remove unwanted frequency components generated by the RF2418 mixer. The filter has a pass band ranging from about 35 to 49 MHz, appropriate for the 45 MHz IF frequency. The insertion loss is claimed to be as low as 0.31 dB for a 44.7 MHz frequency. The filter is physically large, and quite heavy, although this is mainly because of its metal shielding.

IF-to-Baseband Subsystem

The second IF stage and baseband stage are constructed through the use of a single system-on-chip circuit, the SA606 from Philips, though with certain external components. Used in a VHF receiver for the earlier NCUBE projects,

[24], [25], the SA606 first mixes the signal down to 455 kHz. The LO frequency is generated by a crystal oscillator circuit with an external crystal. The signal is then amplified and filtered through two external ceramic resonators before being hard-limited and fed to the quadrature detector. The output of the detector is low-pass filtered and amplified before being sampled by the baseband processor. Because of the excellent sensitivity of the hard-limiter, the SA606 gives an effective gain of at least 90 dB, and good phase accuracy is provided through the use of the quadrature detector.

The datasheet outlines an application circuit for the SA606, which is thought to be sufficient for the receiver design. It is important to note, however, that what seems to be a mistake, has been drawn in this application circuit. The mistake does not seem to have been discovered during the NCUBE designs, and the issue is further explained in section 6.3.6. The two external ceramic filters were chosen as the CFUKF455KA2X-R0 ceramic resonator made by Murata. These have a bandwidth of 35 kHz, and will therefore have sufficient bandwidth to include a doppler shift of up to 11 kHz.

Receiver Baseband Processor

The receiver baseband processor was not closely investigated in this design. Instead, the digital and software design of the receiver relies on the work done by Roger Birkeland in his VHF transceiver study [26], which uses an identical IF system and baud rate. The processor mainly considered was the CML MicroCircuits CMX909b, a GMSK modulator/demodulator with packet handling, FEC and interleaving. The versatility of the CMX909 relieves the microcontroller from packet handling tasks, and as the functions are hardwired in the CMX909, the possibility for SEU's or latch-up is low.

However, the CMX909 is confined to the use of a MOBITEX packet format, described in the datasheet [27]. The protocol can be somewhat customized, as the frame header is user defined, but if a completely different protocol is wanted, the CMX589, also made by CML, may be a better choice. The CMX589 has the same modulation scheme and the same $0.3 WT_b$ gaussian filter as the the CMX909, but it only relays raw received data. The CMX589 incorporates a serial synchronized digital interface, while The CMX909 communicates with the microcontroller through an 8-bit parallel port. Fortunately, none of these processors need external circuitry to communicate with a standard 8-bit microcontroller.

Chapter 5

Link Budget Analysis

This chapter describes the downlink and uplink budgets for both 400 and 800 km circular, polar orbits. The parameters have been calculated as described in the theory chapters. A minimum elevation of 10° has been chosen, based on the fact that a local ground station will probably be situated in a densely populated area. An exception is made for the worst case uplink scenario of 800 km, where a minimum elevation angle of 20° has been assumed, due to SNR demands.

As no ground station has been developed, typical values have been chosen to describe the ground station receiver noise, transmitted power and antenna gain. The ground station antenna gain of 20 dB, implies that satellite tracking is performed.

The link budgets assume the use of a directive satellite antenna, developed by the author for a double Cubesat [28] during the autumn of 2006. The radiation pattern of the antenna is given in [1], chapter 6, presenting a maximum gain of 5.77 dB. The gain will decrease to approximately 2 dB for an elevation angle of 10° , using a rather pessimistic flat earth assumption. The radiation patterns were confirmed by practical measurements during the spring of 2007. However, the antenna efficiency has not been measured or calculated, and is assumed to be equal to the relatively standard dipole efficiency of 70%.

5.1 Noise Bandwidth Calculations

The noise bandwidth of a system is usually estimated to be slightly higher than the 3dB bandwidth of the narrowest filter in the receiver. As mentioned on page 107 in [2], it is generally difficult to design bandpass filters with a bandwidth greater than 1% of the carrier frequency. Thus, superheterodyne receivers are commonly employed to ease the filter requirements, as they enable the filtering of signals at lower IF frequencies.

The goal should be to get the filter bandwidth as close to the signal bandwidth as possible. Ceramic resonators are designed with standard center frequencies to be used on IF stages, including 455 kHz and 10.7 MHz. At 455 kHz, a bandwidth of 35 kHz is achievable with such resonators. Because of the high doppler shift, and the fact that the receiver has no frequency tracking ability, the required system bandwidth will be $R_b(1 + WT_b) + 2 * \delta f = 32480 [Hz]$ for a doppler shift of ± 10 kHz. Hence, the noise bandwidth becomes larger than the

signal bandwidth.

For the downlink, the situation is less difficult. Here, when frequency tracking through the use of phase-locked loops are assumed, the noise bandwidth will be limited to the bandwidth of the RRC filters in the receiver. Since no concrete information about the ground station is available, it is assumed that the noise bandwidth will be 25 kHz, slightly more than the RRC bandwidth.

5.2 Uplink Analysis

The link budgets for the receiver section is shown in figure 5.1. Based on measurements and datasheet information, cascaded noise and gain values for the receiver section was found. This calculation, shown in figure 5.2, made the basis for the uplink budget. The noise figures of the active components have not been measured, because of the high noise floor of the unscreened test circuits. These figures have therefore been derived from the component datasheets. Passive matching networks have been given an estimated loss of 0.5 dB. This may be seen as a large value, but as the passive networks will collect noise from surrounding systems, as well as generating thermal noise, the given losses and noise contributions are assumed to be reasonable. The matching networks increase the total equivalent noise temperature with approximately 70 K.

The IF amplifier and hard limiter gain of the SA606 proved difficult to measure, because of a too high noise floor in the test circuit. The gain of 50 dB is therefore a pessimistic assumption, based on the electrical characteristics given in the SA606 datasheet. The sensitivity of the circuit could therefore not be measured either, as the hard limiter triggered continuously. However, as the noise floor was lower than -100 dBm, this suggests that the sensitivity of 0.31 μ V given in the SA606 datasheet is a probable assumption. Although the SNR of the SA606 output is the value used in the link budget, it is the sensitivity of the hard limiter that is the deciding factor in the performance of the receiver.

Link Budget for Payload Receiver					
Assuming circular orbit	800 km Orbit Height		400 km Orbit Height		
Constants	Worst Case	Best Case	Worst Case	Best Case	Unit
Carrier Frequency	4,37E+08	4,37E+08	4,37E+08	4,37E+08	[Hz]
Speed of light	3,00E+08	3,00E+08	3,00E+08	3,00E+08	[m/s]
Carrier Wavelength	0,69	0,69	0,69	0,69	[m]
Earth Radius	6378000,00	6378000,00	6378000,00	6378000,00	[m]
Pi	3,14	3,14	3,14	3,14	
Boltzmann's constant	1,38E-23	1,38E-23	1,38E-23	1,38E-23	[J/K]
Keplers Constant (GMe)	3,99E+14	3,99E+14	3,99E+14	3,99E+14	[m/s ²]
Orbit Parameters	Value	Value	Value	Value	Unit
elevation	10,00	90,00	10,00	90,00	[deg]
Orbit Height	800000,00	800000,00	400000,00	400000,00	[m]
Path Loss Margins					
Polarization Loss	3,00	3,00	3,00	3,00	[dB]
Ionospheric attenuation	0,50	0,50	0,50	0,50	[dB]
Ionospheric scintillation	6,00	6,00	6,00	6,00	[dB]
Ground Station Parameters					
Transmitter Output Power	1,00	1,00	1,00	1,00	[W]
Transmitter antenna Gain	20,00	20,00	20,00	20,00	[dB]
Satellite antenna properties					
Satellite Antenna Gain	2,00	5,77	2,00	5,77	[dB]
brightness noise temperature	290,00	290,00	290,00	290,00	[K]
antenna efficiency	0,70	0,70	0,70	0,70	
Satellite receiver properties					
Receiver noise temperature	347,77	347,77	347,77	347,77	[K]
Receiver Gain before 2. IF stage	32,23	32,23	32,23	32,23	[dB]
Receiver sensitivity on 2. IF stage	-130,00	-130,00	-130,00	-130,00	[dBW]
System Noise bandwidth	3,50E+04	3,50E+04	3,50E+04	3,50E+04	[Hz]
Modulation Parameters					
Bits per symbol	1,00	1,00	1,00	1,00	[bit/symbol]
symbol rate	9,60E+03	9,60E+03	9,60E+03	9,60E+03	[baud]
TOTALS					
Slant Range	2366866,61	800000,00	1439827,11	400000,00	[m]
Maximum Visible Time	637,14		372,56		[s]
Maximum Doppler shift	10110,70		10757,52		[Hz]
EIRP	20,00	20,00	20,00	20,00	[dB]
Free Space Loss	152,73	143,31	148,42	137,29	[dB]
Total Path Loss Margin	9,50	9,50	9,50	9,50	[dBW]
Sensitivity Margin	21,54	30,97	25,86	36,99	[dB]
Received Power	-140,69	-131,26	-136,37	-125,24	[dBW]
System Noise Power	-155,75	-155,75	-155,75	-155,75	[dBW]
Estimated SNR	15,06	24,48	19,38	30,51	[dB]
Estimated Eb/No	20,68	30,10	25,00	36,12	[dB]

Figure 5.1: Uplink Budgets for 400 and 800 km orbit heights

Receiver Gain and Noise calculation						
Component	name	Gain[dB]	NF[dB]	Noise temp[K]	Cascade	
					Gain[dB]	Noise temp[K]
Antenna connection	SMA	-0,06	0,06	4,03	-0,06	4,03
coax cable	0,25 m	-0,1	0,1	6,75	-0,16	10,88
connection	SMA	-0,06	0,06	4,03	-0,22	15,07
switch	PE9354	-0,4	0,4	27,98	-0,62	44,50
Filter	FCN490	-0,75	0,75	54,67	-1,37	107,56
Matching network	passive components	-0,5	0,5	35,39	-1,87	156,06
LNA	RF2878	21	1,5	119,64	19,13	340,08
Matching network	passive components	-0,5	0,5	35,39	18,63	340,52
2. LNA	RF2418	12,5	1,8	148,93	31,13	342,56
Matching network	passive components	-0,5	0,5	35,39	30,63	342,58
Filter	RBP_400	-1,5	1,5	119,64	29,13	342,69
Matching network	passive components	-0,5	0,5	35,39	28,63	342,73
RF.amp&mixer	RF2418	5	10	2610,00	33,63	346,31
Matching network	passive components	-0,5	0,5	35,39	33,13	346,32
Filter	PIF-40	-0,4	0,4	27,98	32,73	346,34
Matching network	passive components	-0,5	0,5	35,39	32,23	346,36
2. Mixer stage	SA606	17	6,2	918,92	49,23	346,91
Filter	CFUKF455KA2X	-4	4	438,45	45,23	346,91
IF amp	SA606	40	20	28710,00	85,23	347,77
Filter	CFUKF455KA2X	-4	4	438,45	81,23	347,77
Hard Limiter	SA606	50	20	28710,00	131,23	347,77

Figure 5.2: Gain and Noise Calculations for the Receiver Section

5.3 Downlink Analysis

The link budgets for the transmitter section is shown in figure 5.3. As one can see from the link budget in figure 5.3, in the worst case scenario of 800 km orbit height, the minimum elevation angle has been increased to 20° due to the low SNR. However, if a coding gain is included, the BER may be acceptable for a 10° degree as well. The ground station is assumed to have a noise temperature of 500 K, which should be achievable, and the brightness noise temperature is assumed to be 290 K despite the high gain, to counter for the possibility of heavy clouds or rain.

The assumed modulation is $\pi/4$ -DQPSK, with a symbol rate of 18 kBaud. The losses in the output network of the transmitter are based on measurements done on evaluation circuits, and may be a bit pessimistic. The exception is the PE9354 switch, which was not received in time for testing. Although a loss of 0.5 dB or lower is reported in it's datasheet, the matching network of the switch may be difficult to design. A matching network loss of an additional 0.5 dB is therefore added to the receiver input.

Link Budget for Payload transmitter					
Assuming Circular Orbit	800 km Orbit height		400 km Orbit Height		
Constants	Worst Case	Best Case	Worst Case	Best Case	Unit
Carrier Frequency	4,37E+08	4,37E+08	4,37E+08	4,37E+08	[Hz]
Speed of light	3,00E+08	3,00E+08	3,00E+08	3,00E+08	[m/s]
Carrier Wavelength	0,69	0,69	0,69	0,69	[m]
Earth Radius	6,38E+06	6,38E+06	6,38E+06	6,38E+06	[m]
Pi	3,14	3,14	3,14	3,14	
Boltzmann's constant	1,38E-23	1,38E-23	1,38E-23	1,38E-23	[J/K]
Keplers Constant (GMe)	3,99E+14	3,99E+14	3,99E+14	3,99E+14	
Orbit Parameters	Value	Value	Value	Value	Unit
elevation	20,00	90,00	10,00	90,00	[deg]
Orbit Height	800000,00	800000,00	400000,00	400000,00	[m]
Path Loss Margins					
Polarization Loss	3,00	3,00	3,00	3,00	[dB]
Ionospheric attenuation	0,50	0,50	0,50	0,50	[dB]
Ionospheric scintillation	6,00	6,00	6,00	6,00	[dB]
Ground Station Properties					
Receiver antenna gain	20,00	20,00	20,00	20,00	[dBW]
Noise bandwidth	2,50E+04	2,50E+04	2,50E+04	2,50E+04	[Hz]
antenna noise temperature	300,00	300,00	300,00	300,00	[K]
Receiver noise temperature	500,00	500,00	500,00	500,00	[K]
Satellite Transmitter Properties					
PA output power	0,00	0,00	0,00	0,00	[dBW]
Antenna SMA connector loss	-0,05	-0,05	-0,05	-0,05	[dB]
coax cable loss	-0,20	-0,20	-0,20	-0,20	[dB]
PCB SMA connector loss	-0,05	-0,05	-0,05	-0,05	[dB]
PE9354 switch loss	-1,00	-1,00	-1,00	-1,00	[dB]
Satellite Antenna Properties					
Antenna Efficiency	0,70	0,70	0,70	0,70	[dB]
Satellite antenna gain	2,00	5,77	2,00	5,77	[dB]
Modulation Parameters					
Bits per symbol	2,00	2,00	2,00	2,00	[bit/symbol]
symbol rate	1,80E+04	1,80E+04	1,80E+04	1,80E+04	[baud]
TOTALS					
Slant Range	1768700,02	800000,00	1439827,11	400000,00	[m]
visible time	4,50E+02	0,00E+00	3,73E+02	0,00E+00	[s]
Maximum Doppler shift	9923,10	0,00	10757,52	0,00	[Hz]
EIRP	-0,85	2,92	-0,85	2,92	[dB]
Free Space Loss	150,20	143,31	148,42	137,29	[dB]
Total Path Loss Margin	9,50	9,50	9,50	9,50	[dBW]
Received Power	-140,55	-129,89	-138,77	-123,87	[dBW]
System Noise Power	-155,59	-155,59	-155,59	-155,59	[dBW]
Estimated SNR	15,04	25,70	16,82	31,72	[dB]
Estimated Eb/No	13,45	24,11	15,24	30,13	[dB]

Figure 5.3: Downlink Budgets for 400 and 800 km orbit heights

Chapter 6

Prototype Construction, Testing and Measurements

6.1 Procedure

Because of the uncertainty in the matching qualities of the selected components, it was decided to test each component of the system individually. This meant creating an evaluation board for each of the components and matching their input and output impedances to 50 Ohm. By doing this, a working prototype could be tested at any level of completion, as the components could easily be connected or disconnected. The drawbacks of such a procedure are that the circuits will be poorly matched to each other, and that they will collect a large amount of noise because of the large unscreened circuitry. Thus it will be very difficult to carry out true performance tests of the completed prototype, but as the prime concern was to whether the circuits would work as intended or not, this kind of procedure was considered best.

The quite elaborate design method was made possible by the very good prototyping equipment available at the institute. The PCB design program "Eagle" version 4, made by Cadsoft USA, was used to design the prototype circuits, which could then be milled out on the Rapid PCB Prototyping machine owned by the Electronics and Telecommunications Institute. Impedance matching networks were designed using the development software "Advanced Design System", ADS, by Agilent. S-parameters were measured on the completed circuits using an Agilent network analyzer. The S-parameter traces were stored on file, and the unmatched and matched networks were compared in ADS. The networks shown in the PCB schematics are equal to the networks designed in ADS, unless otherwise noted. Below follows a list of the most commonly employed measurement equipment used:

<i>Instrument Type</i>	<i>Name</i>	<i>Producer</i>
Network Analyzer	PNA N5230, 0.01 to 30 GHz	Agilent
Oscilloscope	Infinium 1.5 GHz, 8 GSamples/s	Hewlett Packard
Function Generator	33120A	Hewlett Packard
Spectrum Analyzer	FSEA 3.5 GHz	Rohde & Schwarz
Signal Generator	SMU200A	Rohde & Schwarz
Signal Analyzer	FSQ40	Rohde & Schwarz
Power Meter	ML2438A	Anritsu
Multimeter	8840A (used in load-pull meas.)	Fluke
RF/IF Generator	83752A Synthesized sweeper	Hewlett Packard

Table 6.1: Instruments frequently used during prototype testing.

6.2 Transmitter Components

The transmitter circuit consists of four main components that were tested; The CMX980 baseband processor, the AD8345 quadrature modulator/upconverter, the RF2878 buffer amplifier and the RF5110G final stage amplifier. The buffer amplifier test circuit is identical to the RF2878 LNA circuit described in the receiver section, and will not be included here. It is also important to note that the RF5110G power amplifier did not deliver sufficient results, and that a replacement with higher efficiency should be designed. Filtering should be applied to remove harmonics before the final stage amplifier. The RBP-400 band-pass filter, described in section 6.3.3, should provide reasonably good characteristics for this use. Note that a general description of each component is given in section 4.3.

6.2.1 CMX980a Baseband Processor

Evaluation Board Layout

The evaluation board of the CMX980 is a fairly simple layout in terms of components. The header pins were originally thought to be connected directly to the STK500 evaluation board, and the layout was therefore made with three 10-pin headers. The serial configuration did not work as originally intended, however, and to solve the problem the pin configuration needed to be altered. The final solution includes the use of additional interface circuitry, consisting of shift registers and flip-flops, described in the section concerning the microcontroller. The circuit has separate analog and digital ground planes, connected by an AC blocking inductor.

The circuit is fairly equal to the recommended layout described in the CMX980 datasheet [16], with decoupling circuitry to each supply pin. None of the external components needs changing if the master clock frequency is changed, except the RC circuitry on the analog outputs. The datasheet suggests 1 nF capacitors and 6.2 kOhm resistors for the default operation of 18 kBaud symbol rate. Because the primary task of the RC circuit is to aid the RRC filters and remove clock noise, these values must be scaled with the symbol rate. The evaluation board gets its master clock signal from the microcontroller. The AD8345 quadrature modulator, which the CMX980 outputs were

to be connected to, needed bias voltage on its inputs. A voltage division circuit for the analogue bias section, the BIAS1 pin, was therefore added to set up a bias voltage on the Tx outputs.

Optional Output Bias Circuit

The internal bias circuitry of the CMX980 became the source of some confusion, as initial information from the CML technical support staff suggested that the BIAS1 pin of the CMX980 could not be used to set the bias of the Tx outputs. Instead, it was suggested that one should use an external, buffered bias circuitry. A buffered bias circuit was therefore designed with help from supervisor Morten Olavsbråten, using two op-amps for each output pin. Before the buffer circuit was completed, however, initial tests of the CMX980 showed that the BIAS1 pin could in fact be used to set the bias, thus making additional circuitry unnecessary. By connecting the outputs directly to the quadrature modulator, the digital offset adjustment could also be used, and this would not have been the case if the buffer circuits had been employed.

Initial Tests and Measurements

After the extensive work of making the CMX980 communicate with the microcontroller, it was confirmed that, in contradiction to the information given by the CML technical support, the bias voltage could be set using the BIAS1 pin. However, because of a voltage contribution by the internal bias circuit, designing the voltage divider circuit was not straight forward. The output bias voltage was measured on a HP Infinium oscilloscope by enabling transmission, but without sending any information. To get the desired DC voltage of between 0.6V and 0.8V on the Tx output, the 3V supply was, after some trial and error, divided with a 4.7 k Ω and a 1 k Ω resistor. This would ideally give a voltage of 0.52V, but because of the internal voltage contribution, the output bias became close to 0.76V. The oscilloscope also showed an uncompensated DC offset of 24 mV on the I channel, and -4 mV on the Q channel. These offsets were compensated by writing appropriate values to the offset correction registers. When the offset was within 2 mV, the output amplitudes were adjusted to approximately 130 mV peak to peak by writing appropriate values to the gain correction registers. This would give a differential p-p amplitude of 260 mV, well within the clipping range of the AD8345.

For transmission tests, a 4.608 MHz master clock crystal was used, resulting in the CMX980 running at half the baud rate. By doing this, one could verify that the circuit would work problem-free, even at lower clock frequencies than normal. To compensate for the FIR filter response at this frequency, the output capacitors were increased to 2.2 nF. Waveforms of the I and Q channel can be seen in figure A.4 and A.5.

One should note that the correction register values are always zero after a reset has been performed. In fact, this applies to all the registers of the CMX980 except the FIR filter coefficient registers, who are loaded with default values on reset. Amplitude and offset values must therefore always be loaded before transmission can start. Additional commands sent to the CMX980 included power down of the receive section and auxiliary circuits. A command was also sent to enable the CMX to route its symbol clock out on the IRQ pin. Thus

a reference timing signal was available for signal recovery during test. The software section has a more detailed description of the digital communication interface and the commands sent to the CMX980.

6.2.2 AD8345 Quadrature Modulator and Upconverter

Evaluation Board Layout

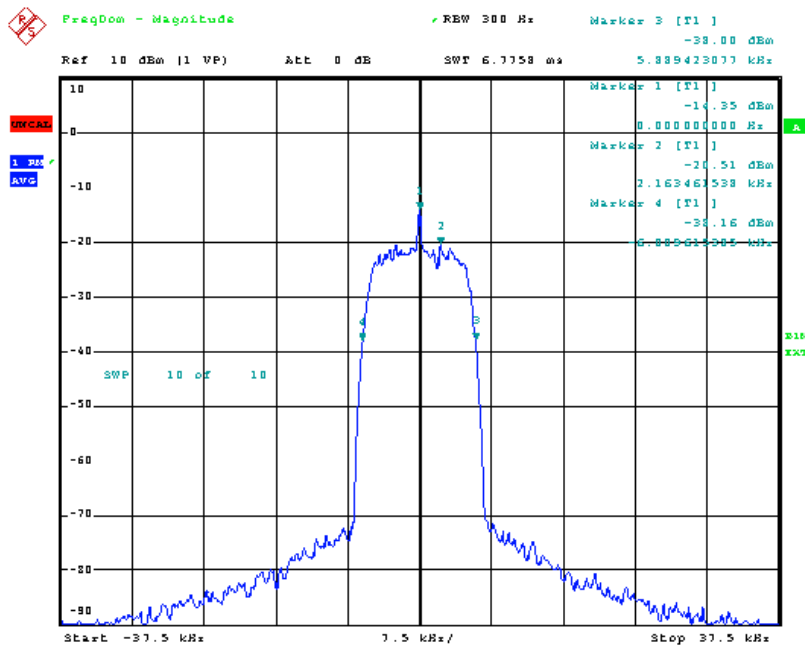
The evaluation board for the AD8345 was originally made with differential LO inputs. This made it very difficult to supply a good carrier wave, and the input was therefore made single-ended when the ETC1-1-13 balun from Mini-Circuits was received. The final layout is therefore identical to the schematic shown here, although the balun was fitted to the circuit with differential inputs, made initially. The Capacitors 2 to 5 are decoupling capacitors, while capacitor 1, 6 and 7 are DC blocking capacitors.

Initial Tests and Measurements

As no signal generator equipment with a DC bias option was available, a full test of the AD8345 had to wait until the CMX980 was available for generating input signals. However, the LO leakage could be measured by applying a 0.7 V DC bias voltage on the inputs. The leakage was approximately -43 dBm, very close to the specifications in the datasheet. Adjustment of the I and Q channel differential offsets, possible to do digitally with the CMX980, can help to reduce carrier leakage even further.

The output power of the AD8345 is severely reduced when running at a 3V supply, compared to the optimum 5V supply. The input levels have to be reduced from a differential p-p amplitude of 1.2V for a 5V supply, to 200mV for the minimum 2.7V supply to avoid clipping of the signal peaks. At 3V, the input amplitude can be increased above 200mV by a small amount. As the input amplitude can be adjusted digitally with the CMX980, an optimum input amplitude can be found by measuring the AD8345 output while changing the input amplitude values. Some clipping may be allowed, though it tends to increase signal leakage into adjacent channels and distort the output signal. the signal amplitude should therefore be adjusted with respect to received signal distortion.

When the CMX980 development work had been completed, a test of the combined circuit could be tested. The CMX980 was roughly calibrated by the use of an oscilloscope as described above. Then, an FFT measurement was done on the output of the AD8345 with the CMX980 as a baseband signal generator, using the FSQ40 signal analyser with a Chebychev window function. The result, shown in figure 6.1, shows a good signal with steep flanks, though with a substantial carrier leakage. It might be possible to reduce this leakage by tuning the CMX980 outputs even better.



CMX980 FFT spectrum; Chebychev window
 Date: 28.MAY.2007 11:32:29

Figure 6.1: Measured FFT spectrum of the AD8345 using a Chebychev window function. The CMX980 evaluation board is used to generate basband I and Q signals with a baud rate of 9600 baud.

6.2.3 RF2878 Output Buffer Amplifier

The RF2878 was thought to be a suitable linear preamplifier for the output stage. However, since no information was given in the datasheet, C, regarding performance in the 400 MHz area, power sweeps were done on the RF2878 evaluation board to see if the amplifier was usable, both as an LNA and a buffer circuit. The voltage on the VPD pin, controlling the bias current through internal circuitry on the RF2878, was also varied in order to establish the optimum bias conditions for the amplifier.

Evaluation Board Layout

As the bias current of the RF2878 can be adjusted with the voltage on the VPD pin, the same evaluation board that was used in the LNA case, shown in appendix C, was used to test the amplifier as a buffer. The only difference was that the resistor used to set the VPD voltage, was shorted, so that a variable VPD voltage could be applied. The circuit is further described in section 6.3.2.

Initial Tests and Measurements

As all external components on the evaluation board of the RF2878 are identical to the ones in the circuit described in section 6.3.2, the network analysis given in that section is valid for these measurements as well. The power measurement was done using the load-pull measurement software system Winpower, version 7.7.01.07, by Focus Microwaves. It connects to an Anritsu ML2438A power meter, measuring input and output power, and a Fluke 8840A multimeter measuring the current consumption. The system remotely controls the Rohde & Schwarz SMU200A vector signal generator, generating the input power and varying over a specified range.

The circuit was supplied with 3 volts on the supply pin at all times. The voltage on the VPD pin was varied between each sweep, thus making the amplifier run at various power levels. At first, the current consumption would not go above 11.5 mA, indicating that the amplifier was not completely on. After changing the amplifier, the total maximum current consumption with VPD current included was about 25 mA, which is in coherence with the datasheet. The relation between the VPD voltage and the average current consumptions can be seen in figure C.5.

With a higher input power, current consumption will increase somewhat, but it will fall significantly when the amplifier becomes saturated. This can be seen from the current plot for the 1dB compression point in the same figure. The current consumption can be reduced by lowering the VPD voltage as long as the linearity is kept sufficiently high. This is clearly shown in figure 6.2, where the highest 1dB compression point is in fact given at a VPD voltage of 2.4, corresponding to a drain current of approximately 14 mA. The power sweeps, some of which are shown in figure C.6, revealed that the evaluation board circuit also had a very linear response at the desired input power level of -17 to -16 dBm with this bias current. The amplification was about 21.5 dB at this input level, less than 0.5 dB, or in this case, 0.5 mW, below the maximum output.

To see how the amplifier would perform with a modulated signal at the approximate output amplitude of the AD8345, an 18 kBaud $\pi/4$ -DQPSK signal with a carrier frequency of 437.305 MHz was generated with the SMU200A

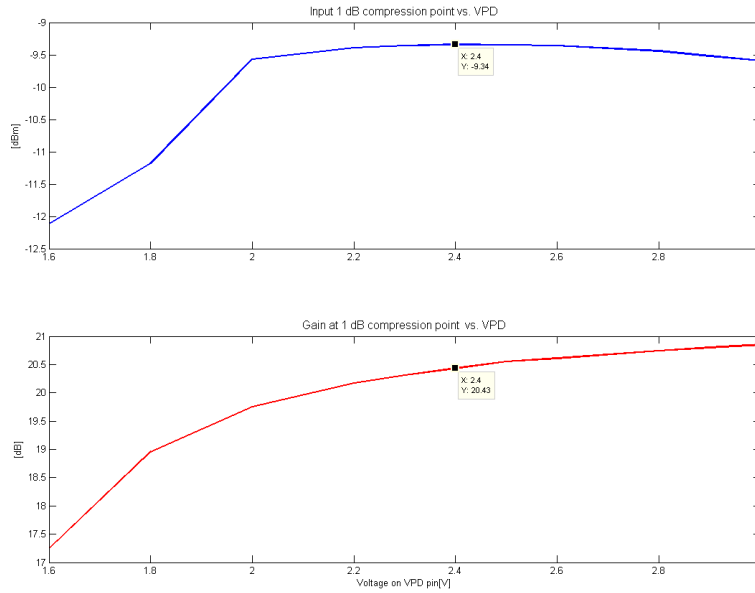


Figure 6.2: RF2878 Input 1dB compression point vs. VPD voltage

signal generator. The signal was applied to the input of the RF2878 with an amplitude of -16 dBm, and the output *Adjacent Channel Power Ratio* (ACPR) was measured with the Rohde & Schwarz FSQ40 signal analyzer. The result is shown in figure 6.3, and as one can see, the sideband power is well within acceptable levels. The in-band and sideband power measurements are given in table 6.2.3.

Parameter	Value	unit
<i>Bias Current</i>	10.52	mA
<i>Input power</i>	-16	dBm
<i>carrier frequency</i>	437.305	MHz
In-band Power	6.67	dBm
ACPR:		
Sideband	lower[dB]	upper[dB]
adjacent	-31.33	-32.42
1. alternate	-74.02	-73.98
2.alternate	83.68	84.10

Table 6.2: RF2878 ACPR measurement results

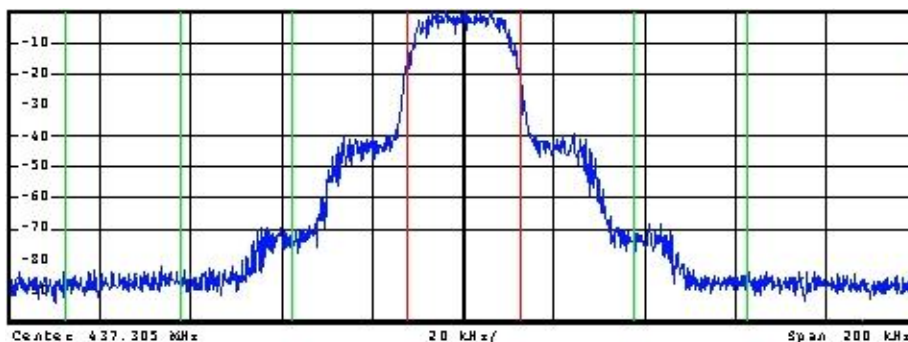


Figure 6.3: RF2878 ACPR measurement. The input is a 18 kBaud pi/4-DQPSK signal with -16 dBm power. The bias current of the RF2878 is 10.52 mA.

6.2.4 RF5110 Power Amplifier Stage

An evaluation circuit was made to test the RF5110G power amplifier, but as it was deemed possible to achieve much higher efficiencies using a custom-made design, extensive testing of output stages were abandoned. In all, the PA represents a very important part of the transmitter when it comes to efficiency. Because of the need for linearity in quadrature modulation, and the wish for high efficiency, the development of an optimized PA should be given high priority, and considerably more time than what is available in this assignment. In [29], several solutions for high efficiency TETRA transmitters are discussed.

Evaluation Board Layout

The evaluation board was designed with a basis in the 450 MHz application schematic given in the datasheet of the RF5110G. The 39 nH power inductor for the final stage supply was chosen from Coilcrafts high power range, while the rest of the components are standard types. The package of the RF5110G was a challenge to solder, with it's 16 small pads and center ground pad. Solder was first placed on the pins and center pad, and the amplifier was then pushed gently down and soldered with hot air. Through hole connections in the ground plane beneath the amplifier also had to be made to insure good heat dissipation. This type of package might cause problems when in a vacuum environment, as air and moisture may become trapped beneath the chip and break it off when freezing.

Initial Tests and Measurements

the initial tests of the RF5110g showed a rather poor match with the wanted frequency area. The match fell to low in frequency, resulting in a low 26.9 dB voltage gain for the 437 MHz area, as shown in figure 6.4. In fact, as the figure shows, an unmatched version of the circuit, where all but the bias network inductor was removed, gave a higher voltage gain than the application circuit.

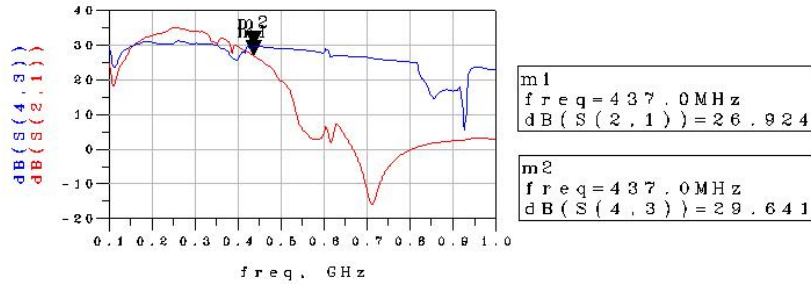


Figure 6.4: RF5110G gain. S2.1 Shows the response of the complete 450MHz application circuit, while S(4,3) shows the response of an unmatched variant with just the bias network connected.

A power sweep was performed on the amplifier, revealing saturation at amplitudes way lower than expected. Compression started at a mere 12 dBm output power, instead of the expected 30. It was assumed that the circuit was not working properly, but further work with the RF5110g was abandoned due to lack of time. the RF5110g may be a suitable amplifier, but other, customized designs will probably prove better suited.

6.3 Receiver Components

The main receiver components that were subjected to testing, are the RF2878 LNA, the RF2418 combined LNA and mixer, and the SA606 IF-to-Baseband subsystem. In addition to these components, filtering is applied in the receiver at various stages, using the LFCN-490 low pass filter, the RBP-400 carrier band pass filter and the PIF-40 IF band pass filter. These filters were also subjected to a more extensive evaluation. A general description of each component is given in section 4.3.

6.3.1 LFCN-490 Low Pass Filter

To remove unwanted high-frequency components and reduce input noise, the LFCN-490 low-pass filter was assumed to be a good choice. A band-pass filter on the input was considered unnecessary because of the high-pass frequency response of the antenna.

Evaluation Board Layout

The evaluation board for the LFCN-490 band-pass filter was made with the possibility of adding matching components. However, none were added for the initial measurements. The schematic is shown in appendix E

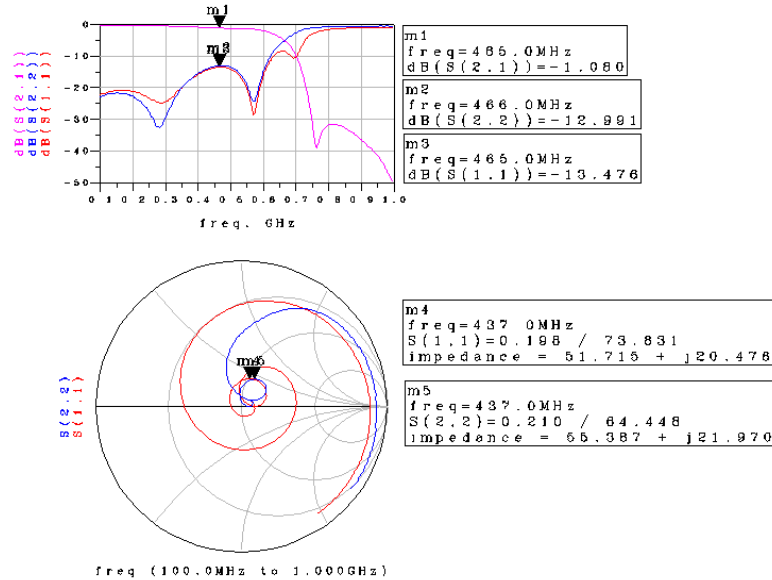


Figure 6.5: S-parameters of the LFCN-490 low pass filter.

Initial Tests And Measurements

The response of the LFCN-490 filter was as expected, with a low insertion loss in the passband. Matching networks were considered unnecessary, as the filter has input and output impedances close to 50 Ohm. The response of the filter is shown in figure 6.5.

6.3.2 RF2878 Low-Noise Amplifier stage

Because the RF2878 is the first LNA in the receiver chain, keeping the input loss low through good impedance matching is essential. Any added noise on the input of the RF2878 will be amplified through the entire receiver chain. Unfortunately, a large input matching network will also gather a substantial amount of noise if it is exposed to surrounding digital systems. A trade-off between network complexity and low loss must therefore be done. On the evaluation board, however, this was not seen to be very important, as the entire circuit would be unscreened during tests, anyway. The challenge here was to get a good impedance match to 50 Ohm. this was done using the Advanced Design System software by Agilent, usually referred to as just ADS. A rather straight forward analysis was done, using s-parameter trace files supplied by RF MicroDevices.

Evaluation Board Layout

The evaluation board is dominated by the bias and matching networks designed in ADS. In both input and output matching networks, parallel capacitors were

needed to get the impedance exactly right. The design is also DC blocked on both inputs and outputs to protect the amplifier. The output DC block, made up from capacitors C8 and C6, is necessary to block the bias current from the DC path through the L4 and L1 inductors. In addition to the matching networks, a resistor network for the VPD pin is included, making it possible to scale the bias current using only a single resistor, if one uses the current plots C.5 as guidance. Schematic and board layout is shown in appendix C.

Initial Tests and Measurements

The S-parameter sweeps, shown in figure 6.6, were done with a full bias current

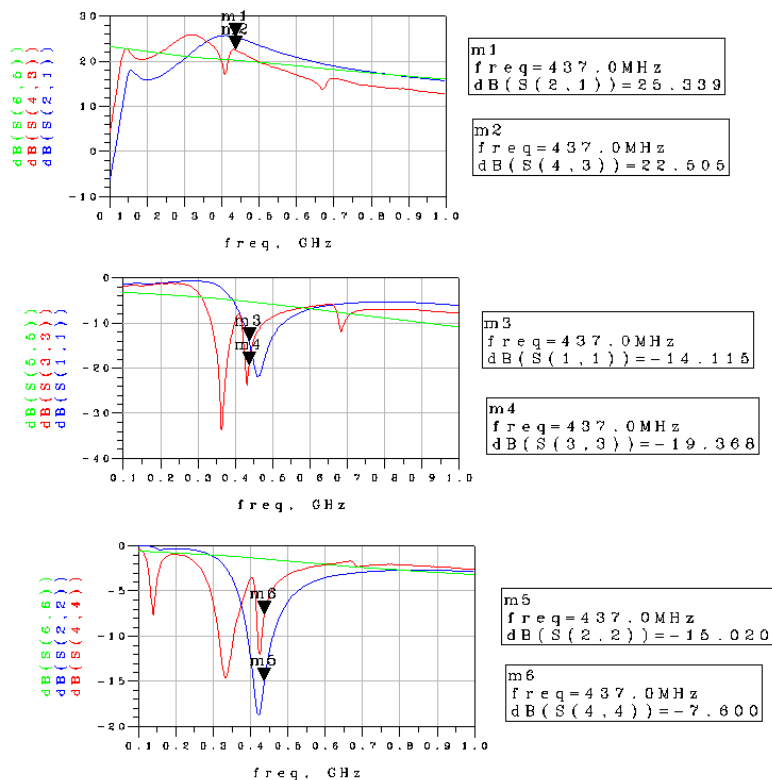


Figure 6.6: RF2878 evaluation board S-parameters. Port 1 and 2 shows the simulated response, while port 3 and 4 shows the actual measured response of the matched circuit. Port 5 and 6 shows the S-parameters of the RF2878 trace file received from RFMD.

setting, meaning that the amplifier was running at full capacity. The reason for this was that the Agilent PNA would become unbalanced at an output power lower than -25 dBm, so to get an unsaturated response the amplifier had to

run at full power. As seen the 22.5 dB gain is about 3 dB lower than the ideal matched response, but this is still completely acceptable and better than what was hoped for. Although a small deviation between the simulated and matched results occurred, the match was good enough for testing. An output spectrum measurement was also done, using the FSQ40 signal analyzer, for a -100 dBm carrier frequency at 437 MHz. The measurement, shown in figure C.4, indicated an acceptable gain of about 21 dB for small scale signals.

6.3.3 Carrier Band pass Filter

Evaluation Board Layout

The evaluation board for the RBP-400 is shown in appendix D. The circuit board was designed with spaces for optional matching networks. The initial measurements were done without any additional components, and it was found that the response of the filter could be further enhanced by a matching network. Input and output LC matching networks were therefore designed and simulated in ADS, with the initial measurements as a reference. The component values are shown in the schematic of figure D.1 in the appendix.

Initial Tests and Measurements

Figure 6.7 shows simulated and measured s-parameters of the filter. As can be seen, only about 0.3 dB is gained in the pass band by matching the circuit. However, this is for a 50 Ohm match, which is what the filter was designed for, so not much improvement was expected. However, it can be assumed that the initial measurement is a good basis for designing matching networks for other impedances.

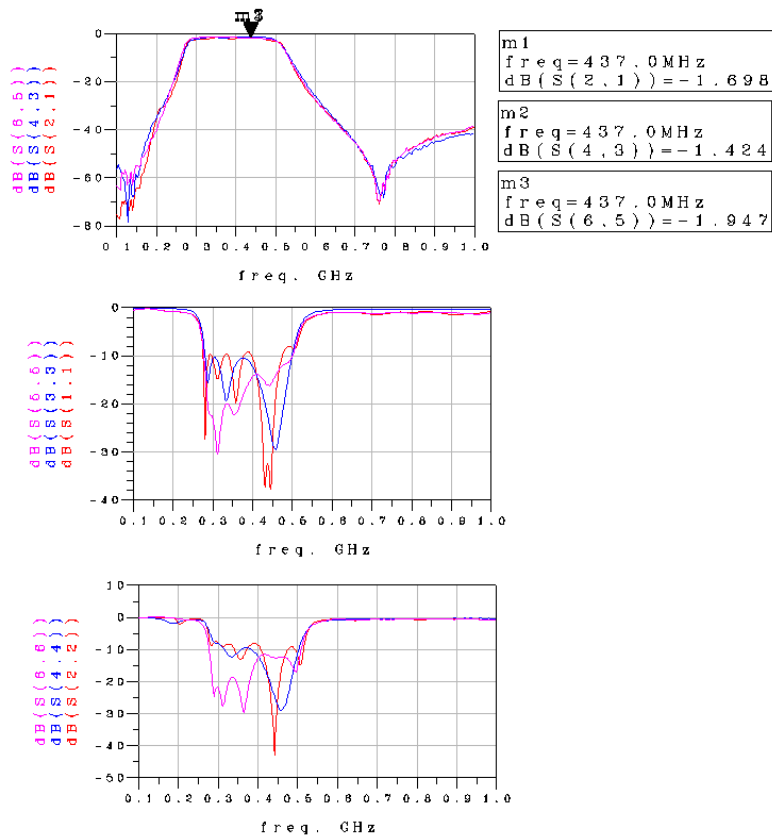


Figure 6.7: S-parameters of the RBP-400 band-pass filter. Ports 1 and 2 show the measured response, while Port 3 and 4 shows the simulated response, of the matched circuit. Port 5 and 6 show the measured, unmatched response of the filter.

6.3.4 RF2418 LNA and IF stage

As the RF2418 includes both a LNA and a mixer section, it was decided to investigate the two main components separately. This was also done because a band pass filter, the RBP-400, had to be inserted between the LNA and mixer. RFMD supplied S-parameter trace-files for the LNA, the RF input and IF output, but not for the LO mixer input.

Evaluation Board Layout

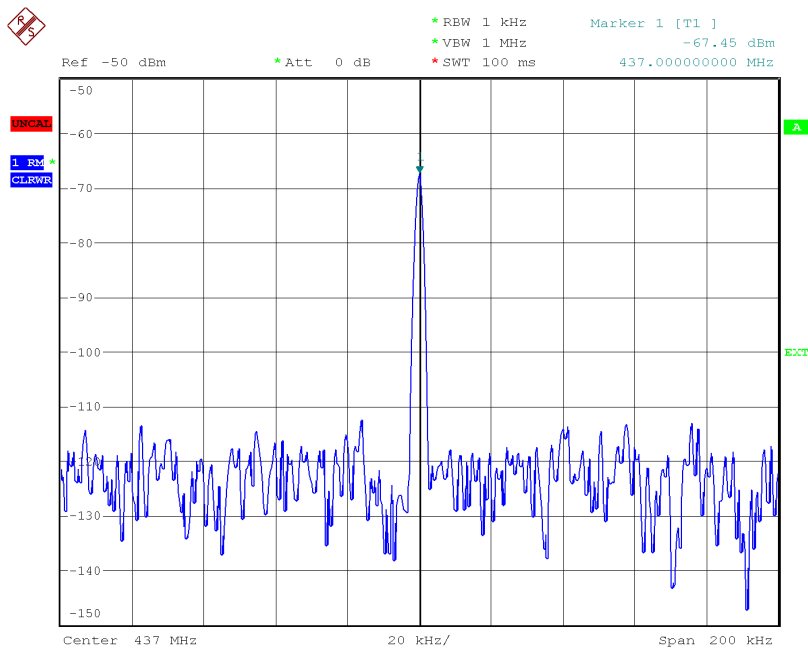
The evaluation board, shown in appendix F.1 consists mainly of impedance matching components. The RF2418 is quite self-sustained, with close to 50 Ohm inputs and outputs, but some additional matching circuitry was believed necessary to get an optimum performance. The Resistors R1 and R2 set the bias current for the output buffer amplifier, while the L3 inductor is scaled to resonate with an internal capacitance, as described in the datasheet [22]. the LNA output is internally DC blocked, so an output capacitor was not necessary.

Initial Tests and Measurements

It proved quite easy to get an acceptable impedance match for the LNA of the RF2418, as it has a good reverse isolation of nearly 40 dB. Still, the measured result was situated to low in frequency, and the matching network was therefore scaled with frequency using ADS, as can be seen from the s-parameter plots in figure F.4, to provide a correct response. A computer optimization for a 490 MHz frequency proved to give a good match at 437 MHz. This deviation is probably due to parasitic capacitances generated between the circuit transmission lines and ground, and the matching network should therefore be considered to belong to the evaluation board exclusively.

The LNA gave an acceptable gain of 11.5 dB at the -17 dBm input power of the Agilent PNA. For a better analysis of the small signal performance of the LNA, a spectrum measurement, shown in figure 6.8, was done with the FSQ40 signal analyzer. Here, a -80 dBm, 437 MHz carrier was applied to the output, and as seen in the plot, a gain of about 12.5 dB was achieved. The current consumption for the entire chip during this test was measured to less than 19 mA.

The RF and LO inputs of the RF2418 proved more difficult to work with. A rather high reflection, shown in figure F.6 and F.7, had to be accepted, as the matching networks did not respond as well as the simulations indicated. However, as these are buffered inputs, the reflection coefficient does not say how well the buffer amplifier works with the input network. As there is no way of measuring this on the RF2418, because the connections between the RF buffers and mixer are internal, it is recommended that a frequency scaling of the 850 MHz buffered application circuit shown in the datasheet, [22], is used. Alternatively, the LO input may be matched with a resistor suitable for the chosen oscillator. This also applies to the IF output, where a rather complicated network was designed on the basis of ADS simulations. As shown in the reflection coefficient plot of figure F.8, the measured response was much lower in frequency than what had been simulated, indicating large parasitic capacitances in the circuit.



RF2418_3V_Itot=19mA_-80dBmIN
 Date: 25.JUN.2007 15:32:46

Figure 6.8: Output spectrum of the RF2418 LNA, where a -80dBm, 437 MHz carrier frequency is applied to the input.

The low power gain of the mixer section was measured in a similar way as the LNA, by applying a 437 MHz carrier to the input and measuring the output on a high resolution spectrum analyzer. A 392 MHz frequency was generated with a HP 83752A synthesized sweeper and applied to the LO input at a power of 0 dBm, thus producing a 45 MHz IF frequency on the output. The mixer gain was measured to 5 dBm as shown in figure F.9, which is in correspondence with the RF2418 datasheet [22]. By using a LO frequency of 482 MHz, producing the same 45 MHz component on the output, it seemed that a slightly higher mixer gain was achieved. Despite the fact that the mixer gain was acceptable, the IF output network should be redesigned, preferably simplified, to give a better frequency match, or at least a more uniform frequency response.

6.3.5 PIF-40 IF Band Pass Filter

The PIF-40 band pass filter was believed to be a suitable IF filter for removing unwanted frequency components generated by the RF2418 mixer.

Evaluation Board Layout

The evaluation board for the PIF-40, shown in appendix G is a rather straight forward design, with pads ready made for impedance matching. Initial measurements showed that the filter had a near 50 Ohm characteristic, making the implementation of matching circuitry unnecessary. Because of the size of the filter, the package was mounted on the solder side of the circuit board, together with the SMA connectors. The component footprint of the PIF-40 shown in figure G.2 is therefore mirrored.

Initial Tests and Measurements

The initial test of the PIF-40 revealed an acceptable filter response, with less than 0.5 dB loss in the pass band, and in accordance with the datasheet, [30]. The only downside to the filter is therefore it's sheer size and weight, but a filter designed from standard components with similar characteristics would probably use more space, generate more noise and be less robust. The Frequency response is shown in figure 6.9.

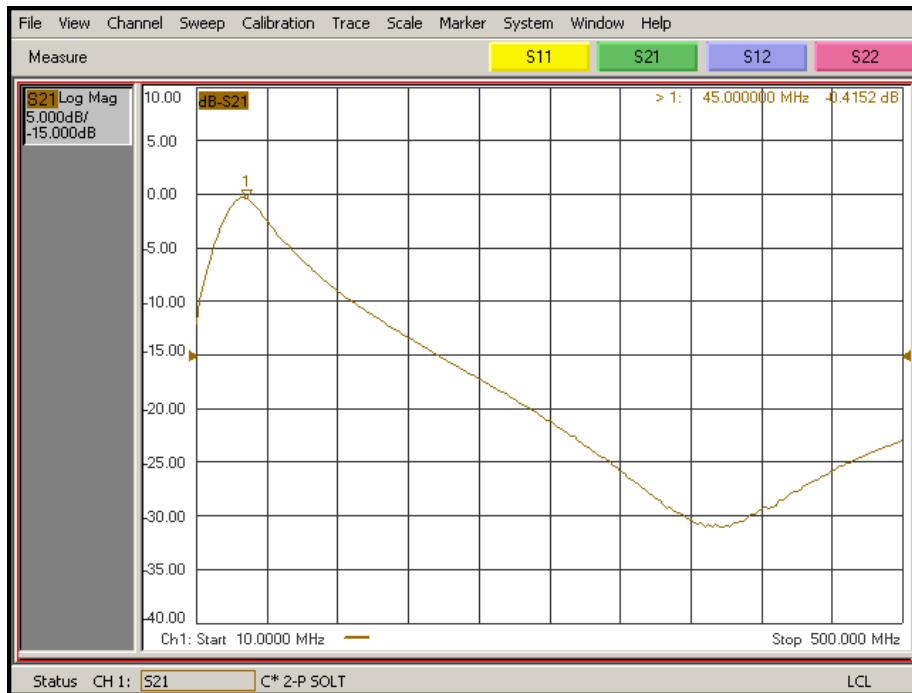


Figure 6.9: The frequency response of the PIF-40 IF band pass filter.

6.3.6 SA606 IF-to-Baseband section

Evaluation Board Layout

The SA606 evaluation board, made by Roger Birkeland for his VHF receiver [26], was originally a copy of the 45 MHz application circuit described in the datasheet [31]. It was assumed that the circuit, shown in figure H.1, would function properly, as identical circuits had been used in the previous NCUBE missions, according to [25] and [24]. However, for reasons described below, the application circuit needed to be altered in a crucial point in order for it to give a proper output signal.

The final circuit schematic with appurtenant layout is shown in figure H.2 and H.3. As seen here, the capacitor C27 has been placed in parallel with the R10 resistor, instead of in series as suggested in the application circuit. An extra AC coupling has been added in the form of the capacitor C4. The RF input has also been changed, incorporating the ETC1-1-13M wideband transformer [32] to generate the differential input instead of the inductor circuit proposed in the application schematic. Capacitors C1 and C2 have been installed as DC blocking capacitors for the inputs, as these are not internally DC blocked. Finally, an extra capacitor, C3, was installed in parallel with the variable capacitor C6, in order to get the oscillator circuit working.

The 455 kHz ceramic resonators used in the evaluation board, the SFU 455A by Murata, are not the ones that should be used in a UHF radio. Although their bandwidth may be sufficient for VHF Doppler shifts, and for test purposes, they will be too narrow for the ± 11 kHz shift at UHF frequencies. The filters

that should be used are the CFUKF455KA2X-R0 resonators from Murata.

Initial Tests and Measurements

All measurements on the SA606 were done with a HP Infinium 8 Gsamples/s oscilloscope. As mentioned, measurements done on the original application circuit revealed some problems. The mixer section of the SA606 did not seem to work properly, as no signal was detected on the output. The problem was eventually tracked down to the crystal oscillator. The crystal used, a 44.545 MHz SMD crystal from CTS Communications Components, was supposed to have a 13 pF load capacitance in order to function correctly. Unfortunately, the extensive oscillator network of the application circuit made it difficult to assess the parallel capacitance, and it was expected that the variable capacitor would have a sufficient range to tune the circuit into oscillation. The oscillator seemed to work fine when measured, but a signal could not be detected on the mixer output. After some debate to what might cause the problem, it was discovered that the extra capacitance added by the probe used to measure the circuit, was enough to start the oscillation. When the probe was removed, the oscillation stopped, as the initial capacitance had not been sufficient. The solution was to add the parallel capacitor C3, with a capacitance of 10 pF, equal to the probe.

During this process, an alteration of the input network was also performed. By using the ETC1-1-13 transformer to generate differential inputs, a marginally better input signal level was achieved. The use of the transformer may complicate matching, but as it will be connected to the PIF-40 band pass filter, with impedance close to 50 Ohm, it is not believed to cause difficulties.

The final, and most important modification of the application circuit was made on the audio output. Although a recognizable baseband signal could be distinguished in the envelope of the output signal, the amplitude was very low, only a few mV, and the IF frequency very prominent. The SA606 has a buffer amplifier on the audio output, with a feedback path accessible at pin 7. The application schematic suggests that a series RC section, consisting of capacitor C27 and resistor R10, is connected to this output. This actually creates a high-pass response in the output buffer, attenuating the baseband envelope and amplifying the IF carrier frequency. A quick calculation revealed that the C27 capacitor and R10 resistor was probably meant to be in parallel, rather than a series configuration, probably a mishap in the design of the schematic. When the RC section was changed into a parallel configuration, the output signal was greatly improved, with at least 2.5 V p-p amplitude.

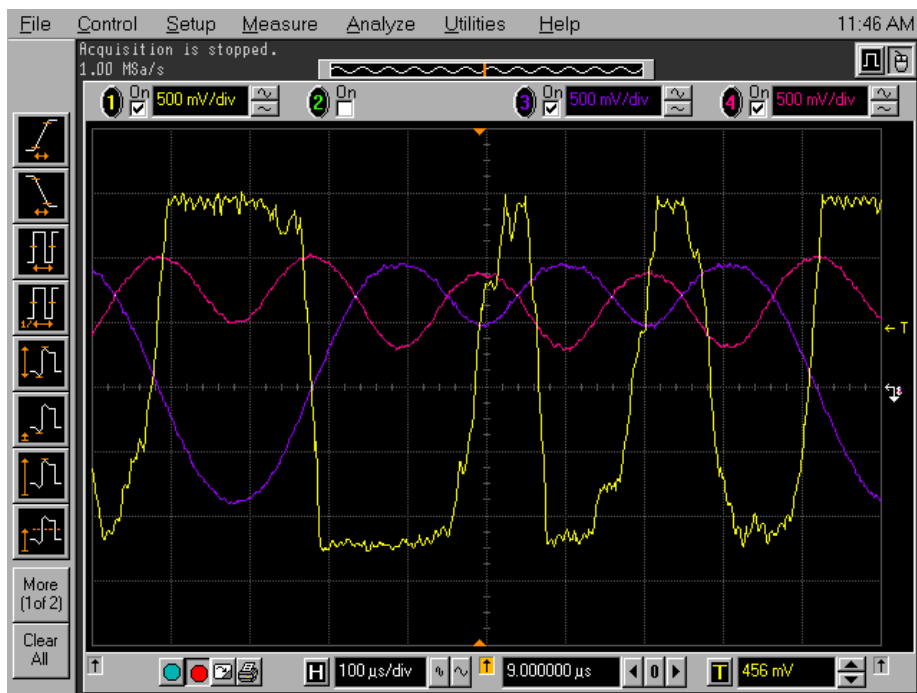


Figure 6.10: The baseband output signal of the SA606, measured on channel 1, for a -70 dBm IF input signal. Channel 3 and 4 show the I and Q channels generating the 9600 baud GMSK signal, where the bit sequence is 11001010.

Because a small IF frequency was still observable, though not nearly as prominent as it had been, an extra parallel capacitor, C4, was added to the output just in front of the SMA connector. This removed even more of the 455 kHz leakage. In the test, a 9600 baud GMSK signal on a 45 MHz carrier was generated using the SMU200A vector signal generator, and applied to the SA606 input network. During noisy test conditions, the circuit gave a readable output for input levels as low as -93 dBm, as can be seen in figure 6.10. AWGN noise corresponding to $E_b/N_0 = 12dB$ was also added to the -93 dB carrier, with no visible degradation of the output signal. The current consumption of the circuit was measured to less than 4 mA. Additional waveform measurements done on the SA606 can be seen in appendix H.2. According to a subsequent test described in [26], the output signal was successfully detected by the CMX909 processor.

6.3.7 GMSK Baseband Processor

Because no decision has been made to which receiver baseband processor should be used, neither the CMX909 nor the CMX589 have been tested in this prototype development. Readers should consult the thesis by Roger Birkeland, [26], where extensive work concerning the CMX909 has been performed. It is assumed that the data output signal of the SA606 can be directly interpreted by both baseband processors, with only minor adjustments.

6.4 Additional Circuitry and Components

In addition to the transmit and receive section components, a transmit/receive SPDT switch was tested. A microcontroller with some additional logic circuits was also evaluated.

6.4.1 HSWA2-30R Transmit/Receive Switch

Evaluation Board Layout

The evaluation board for the HSWA2-30R was made by Roger Birkeland for his VHF radio. None of the external components were mounted during initial testing, as they were only intended for impedance matching. The chip package, though small and with built-in pads, proved relatively easy to solder using hot air. However, one might question the durability of such packages in space conditions, as gas residues or vapor may be trapped under the chip and break it off when freezing. Long-term vacuum testing may reveal potential problems.

Initial Tests and Measurements

The initial S-parameter measurements showed a very unstable circuit, with irregular fluctuations over the entire band. The reason was swiftly tracked down to the large, unconnected topside copper plane of the evaluation board. When this plane was connected to ground, the circuit instantly became stable. Unfortunately, initial performance were not as good as one could have hoped for, with an insertion loss of nearly 1.5 dB for both channels. This means that the PA must produce an additional dB of power compared to what was estimated

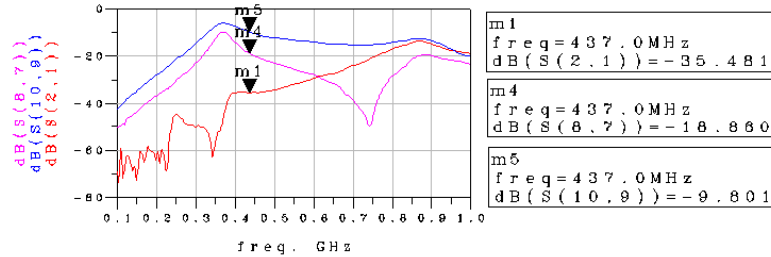


Figure 6.11: Isolation measurements for the HSWA2-30R switch. $S(2,1)$ shows the leakage from channel 1 to 2. $S(8,7)$ is the leakage from a closed channel 1, and $S(10,9)$ from a closed channel 2, to the output. Note that the unconnected port in each measurement is always an open circuit.

in the link budget, in order to maintain the SNR. A reduction in output power from 31 to 29.5 dBm is equivalent to 370 mW of power, and it is clear that this would severely degrade the overall efficiency of the transmitter.

Key measurements can be seen in figures 6.11 and 6.12. It's important to note that the measurements were done on a 2-port PNA, and that the port not measured was kept unconnected at all times. This may have degraded the circuit somewhat in terms of isolation, but it should not have affected the insertion loss of the circuit very much. It is believed that the evaluation board did not function properly, as the measured performance was quite poor compared to what was reported in the HSWA2's datasheet [33]. This illustrates the sensitivity of the circuit to nonideal parasitic effects, and the difficulty of getting it to work properly. That more time should be spent designing the output network is therefore recommendable.

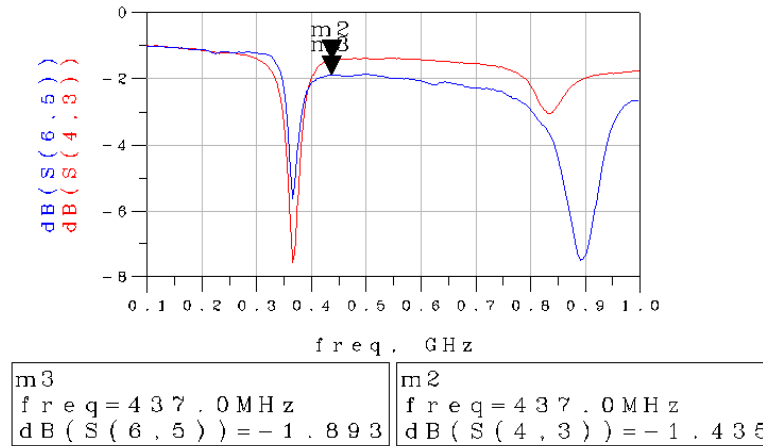


Figure 6.12: Throughput measurements of the HSWA2-30R. S(4,3) is channel 1, S(6,5) channel 2. Note that the unconnected port in each measurement is always an open circuit.

6.4.2 Microcontroller and Interface Logic

The ATmega128L microcontroller was only used to control the CMX980 base-band processor in this design, but it has the capability of controlling both transmitter and receiver logic as well as performing packet handling.

Microcontroller Development Board

The microcontroller development board used, was a commercial product called STK500, available from Atmel. For use with the ATmega128, an additional expansion module for the STK500, called STK501, was necessary. The entire board can be seen connected to the CMX980 and external circuitry in figure K.6. The port configuration of the development board decided the interface layout to the other digital circuits in the evaluation design. The development board has a crystal driven clock generator that was used to clock both the CMX980 and the microcontroller, and RS232 line drivers for communication with an ordinary computer.

External Logic Circuitry for the CMX90 Serial Interface

Because complications with the CMX980 serial port arose, additional external circuitry had to be designed. It was initially believed that the ATmega128 would be fast enough to communicate with the CMX980's three-wire interface. However this was not the case, and the 8-bit Serial Peripheral Interface of the microcontroller did not have the ability to load its output register sufficiently fast to generate a continuous 16 bit data word.

The solution was to make an external 16 bit shift register out of two 8-bit 74LVD165D shift registers. The shift registers are parallel-loadable, and can therefore be loaded one at a time while the serial clock is held by additional circuitry. A standard 74-series dual flip-flop also had to be incorporated in the frame synchronization and clock enable signals, to ensure that the bit timing would be correct. The two circuits are shown in appendix K.1. The complete interface between the digital circuits can be seen in figure K.5. This is a schematic only, and as one can see, the dual flip-flop package has been split into two separate units.

Initial Tests and Measurements

As the test and development of the transmitter logic was mainly a software issue, it is described in detail in the software development chapter.

Chapter 7

Serial Interface and Software Development

This chapter describes the development of the serial communication interface for the ATmega128 microcontroller and the CMX980a baseband processor. The software was developed in C using the AVR LIBC open source C library. It was compiled with GCC, short for *GNU Compiler Collection*, which is an open source C compiler. The programming and debugging interface for the ATmega128 microcontroller was the AVR Studio 4, a development software supplied by Atmel that utilizes the GNU compiler as a plugin. In addition to the STK500 development board, a JTAG unit was used for debugging. The timing of the serial port functions was measured using a HP Logic Analyzer. The timing diagrams are included together with the software functions in appendix K.3. It is advised that the CMX980 and ATmega128 datasheets, [16] and [34], are consulted to gain a complete knowledge of the baseband processor and microcontroller functions.

7.1 CMX980 Serial Interface

7.1.1 overview

The CMX980 uses three serial ports to communicate with microcontrollers or DSPs. One port receives commands and transmit data, while another returns register values and status data. A third port relays level data from the receive section, but this port is not considered in this design as the processor is only being used for transmission. Each serial port has a *Frame synchronization Pin*, which is set high for 1 bit period prior to the first bit of a packet. The command and transmit synchronization pin will from here on be called CMDDFS, while the readback synchronization pin will be called CMDRDFS.

CMDDFS is controlled by the microcontroller, while CMDRDFS is controlled by the CMX980. The serial clock is fixed to a frequency equal to either 1/2 or 1/4 times the master clock. As the baud rate clock of the transmit section is always equal to 1/512 times the master clock, this means a quite high bit rate on the serial bus. For the default 18 kBaud operation, the master clock will be 9.216 MHz, and the serial clock will be 2.304 MHz minimum. It is recommended that the microcontroller and CMX980 uses the same master clock. Not only will

this aid synchronization, but it will also save space, weight and power.

7.1.2 Serial Packet Formats

The command data packets, described in detail in [16], consist of 1 read/write bit, 7 register address bits, and 8 data bits, creating a 16 bit package with the read/write bit as MSB. Before transmission, the CMDFS pin must be set high for 1 bit period. Transmit data packets are somewhat different. The transmit FIFO register is mapped over 4 address locations, because the 2 LSB address bits are used to give information about signal ramping and packet format.

When reading from the CMX980, a read command first has to be sent. This is done by transmitting a command with the read/write bit low, followed by the 7 bit address. After receiving the address, The CMX980 will delay 1 bit period, set the Command Read Frame sync pin for another bit period, then transmit back 16 bits. The first 8 bits are invalid data, while the next 8 are the value of the read register. The CMX980 is always the *master* entity of the serial bus because it controls the serial clock.

During transmission, a mode is available that stops the serial clock temporarily if the transmit FIFO register, which is 4 words deep, becomes full. This relieves the microcontroller from the task of continuously checking the status of the FIFO register.

7.2 External Circuitry

7.2.1 External Shift Register Circuit

Because of the high clock frequency of the CMX980 serial interface, an external shift register circuit had to be made in order for the microcontroller to write to, and read from, the CMX980 memory registers. It was first attempted to make the circuit work without any additional circuitry through the use of the SPI serial interface of the microcontroller. However, because the SPI uses an 8 bit shift register, which is single buffered in the transmit direction, the shift register had to be loaded with a new word in the middle of each data packet. With a serial clock rate at one quarter the master clock frequency, this simply was not possible, as such an operation took way more than four CPU clock cycles to perform.

It was therefore decided to use external shift registers, effectively building a new, customized serial interface. Two 74LV165D shift registers, described in [35], were cascaded to form a 16 bit shift register, as shown in the schematic of figure K.1. The 74LV165D is parallel loadable, thus enabling the microcontroller to load a complete word in a single operation. The parallel ports of the shift registers were connected together, and the load/shift pin of each was used to decide which register should be loaded. The clock inhibit pin was used to initiate transmission at the correct moment.

7.2.2 External Flip-Flop Synchronization Circuit

The ATmega128 has four built in timer/counters, one of which was used to sample the serial clock of the CMX980. When the external shift register circuit was made, it was hoped that this timer could be used to synchronize the serial

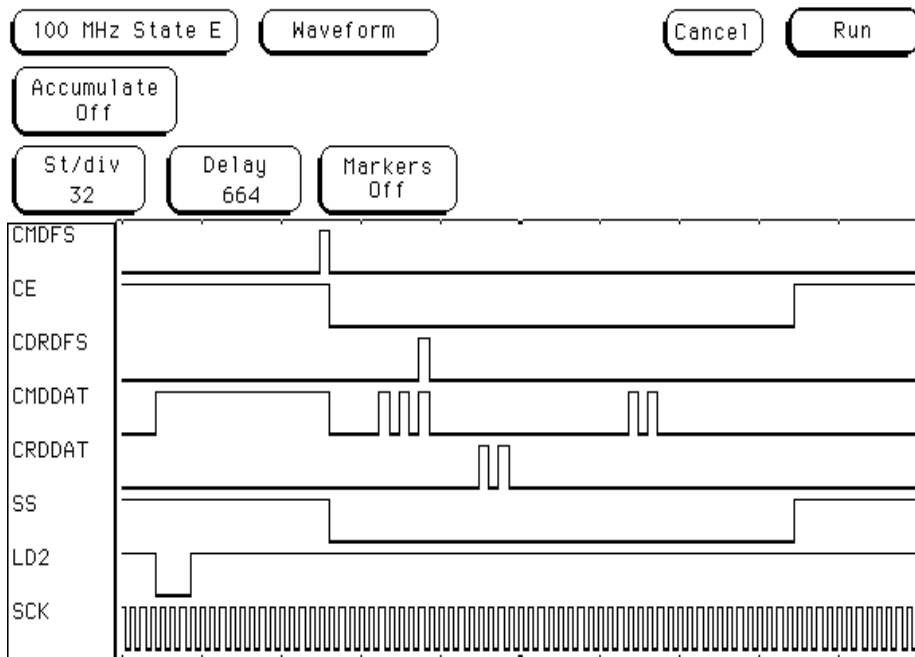


Figure 7.1: Measured timing diagram of a failed CMX980 write operation. Because of timing inaccuracy, the operation is interpreted by the CMX980 as a read request.

ports sufficiently. Unfortunately, this was not completely successful. The lack of synchronization meant that packages would sometimes be shifted by an entire bit. The timing diagram of figure 7.1 is a measurement capturing what happens when such an incident occurs. As seen, the CMDRDFS pin goes high after the first 8 bits have been sent, indicating that the packet has been interpreted as a read command. The write function of the software was altered to utilize this, detecting faulty timing by checking if the CMDRDFS pin had gone high during transmission. However, this was not an acceptable solution, because it could not guarantee the constant flow of data necessary for correct downlink transmission.

The final solution was to add a standard 74x dual flip-flop, where one flip-flop controls the CMDFS signal, and the other controls the clock inhibit signals of the shift registers. Triggered by the serial clock, the flip-flops guarantee correct write commands. An interface circuit was designed and produced for the dual flip-flop, that also contained headers for easier connection of the CMX980 and shift register circuits to the microcontrollers STK500 evaluation board.

7.3 Software Functions

The software functions and their task is listed in table 7.3. The complete code is given in appendix K.3, where it is also comprehensively commented. It is important to note that the port definitions and functions apply to the ATmega128 only.

Function Name	task
<i>Setup Functions</i>	
Directions	Setting the initial data direction registers.
InterruptSetup	Enabling and setting external interrupts 2 and 3.
CMX980RST	CMX980 reset function.
BitCounterSetup	Sets up 16 bit counter 1.
CMX980InitialSetup	Sets the startup register values in the CMX980.
CMX980AdjustmentSetup	Programs the gain and offset adjustment.
<i>Write and Read Functions</i>	
WriteToCMX980	Writes data to the specified address in the CMX980.
ReadFromCMX980	Returning the value of the specified CMX980 register.
<i>Higher Level Functions</i>	
SetRegister	Setting register values on the CMX980 and confirming.
Transmit	Writing 4 transmit words, while checking FIFOstatus.
HandshakeTransmit	Transmits only one word, while in handshake mode.

Table 7.1: Overview of the functions in the CMX980 control interface

Chapter 8

Development and Demonstration Circuit Designs

Based on the experiences done with the evaluation boards, two complete development circuits, one receiver circuit and one transmitter circuit, were designed. Unfortunately, one was not able to produce the circuits due to lack of time. However, as the layouts have been completed, the circuits can easily be produced and soldered at the institute. Components for the circuits have also been purchased.

8.1 PI/4-DQPSK Transmitter Development Circuit

The Transmitter demonstration circuit, shown in figure 8.1 contains an ATmega128 microcontroller, a CMX980a baseband processor, an AD8345 quadrature modulator, an RF2878 buffer amplifier and an RBP-400 band-pass filter. New matching networks for the RF2878 were designed in ADS to match it directly to the RBP-400 band pass filter, and the AD8345 output is assumed to be close to 50 Ohms, as stated in it's datasheet [17]. The simulation network and results are shown in appendix L.

The circuit is primarily intended for use in the development of a power amplifier and controller software. The circuit can also be used to develop software for the receiver baseband processor, as two 8-bit ports on the ATmega128 have been made available through pin headers. This means that the circuit can be connected directly to the CMX909 development board described in [26]. Important features of the circuit includes:

- JTAG and ISP pin headers, enabling programming and debugging of the microcontroller.
- USART connection available through the ISP header, enabling RS232 communication.

- I2C connection for satellite bus communication.
- Two full 8-bit ports for connection with the receiver baseband processor.
- SMA connection for the IRQ pin of the CMX980a, giving access to the symbol clock.
- 50 Ohm SMA output for power amplifier connection.
- 50 Ohm SMA connection for the carrier frequency oscillator.
- internal 3.3V power supply with a jumper, enabling current measurements.
- AC blocked analog and digital supply rails.

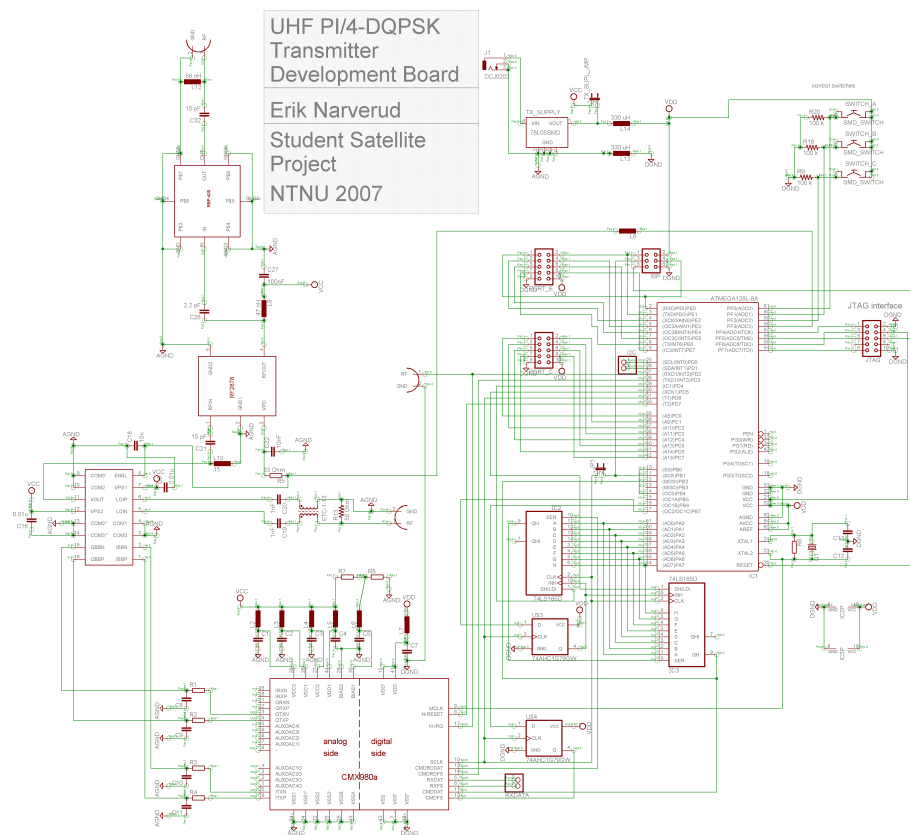


Figure 8.1: Schematic of the transmitter demonstration circuit.

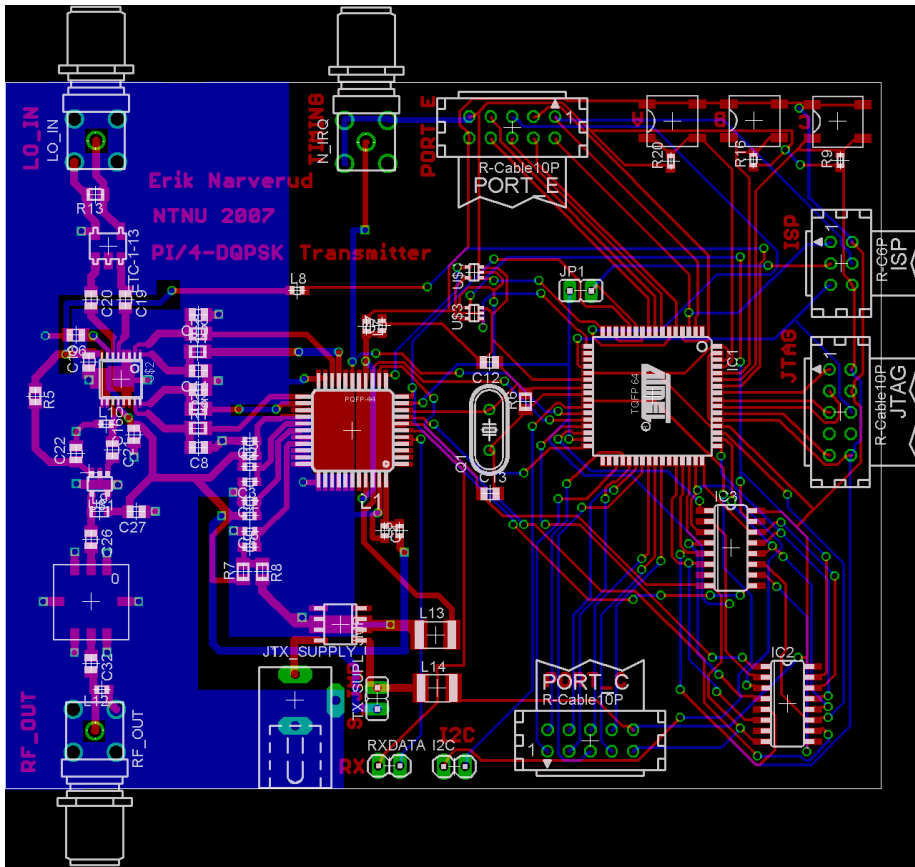


Figure 8.2: Layout of the transmitter development circuit.

8.2 GMSK Receiver Development Circuit

Unlike the transmitter circuit, the receiver, shown in figure 8.3, is purely analog, converting a UHF GMSK signal into a baseband GMSK signal. It consists of a LFCN-490 low pass input filter, an RF2878 LNA, the RF2418 LNA and mixer and the SA606 IF system. The RBP-400 band pass filter is inserted before the RF2418 mixer, and the PIF-40 band pass filter is inserted behind it, to ensure a clean signal for the next IF stage.

The first stage was simulated in ADS to construct an optimized matching network. The simulated network and key results are shown in appendix M. The matching network does not take into account the parasitic capacitances that may be formed in the transmission lines. There is no guarantee that the actual network will have a response equal to the simulated version. To compensate for this, transmission lines have been made as short as possible, as can be seen from the circuit layout in figure 8.4. This has the added positive effect that noise collected in the networks will be reduced to a minimum.

Apart from the matching networks, the circuits are quite similar to the evaluation board designs. This is also true for the second IF stage, essentially equal to the SA606 evaluation board. The same ceramic resonators have been used, meaning that the development board will not have sufficient bandwidth for the 11 kHz doppler shift. However, as the circuit has not been made, it is possible to exchange these filters prior to production. The RF and LO inputs are 50 Ohm SMA connections, as are the data and RSSI outputs. The circuit can be connected directly to the CMX909 development board made by Roger Birkeland [26] with 50 Ohm coax cables.

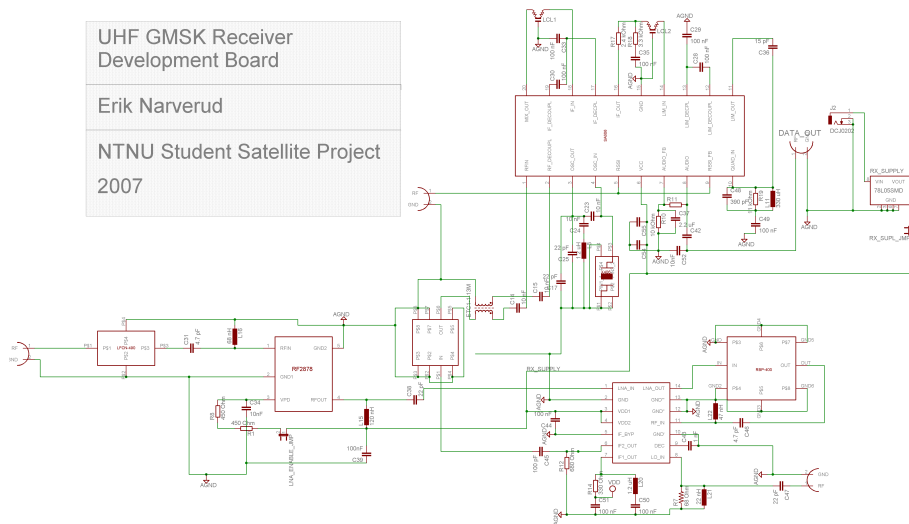


Figure 8.3: Schematic of the receiver development circuit.

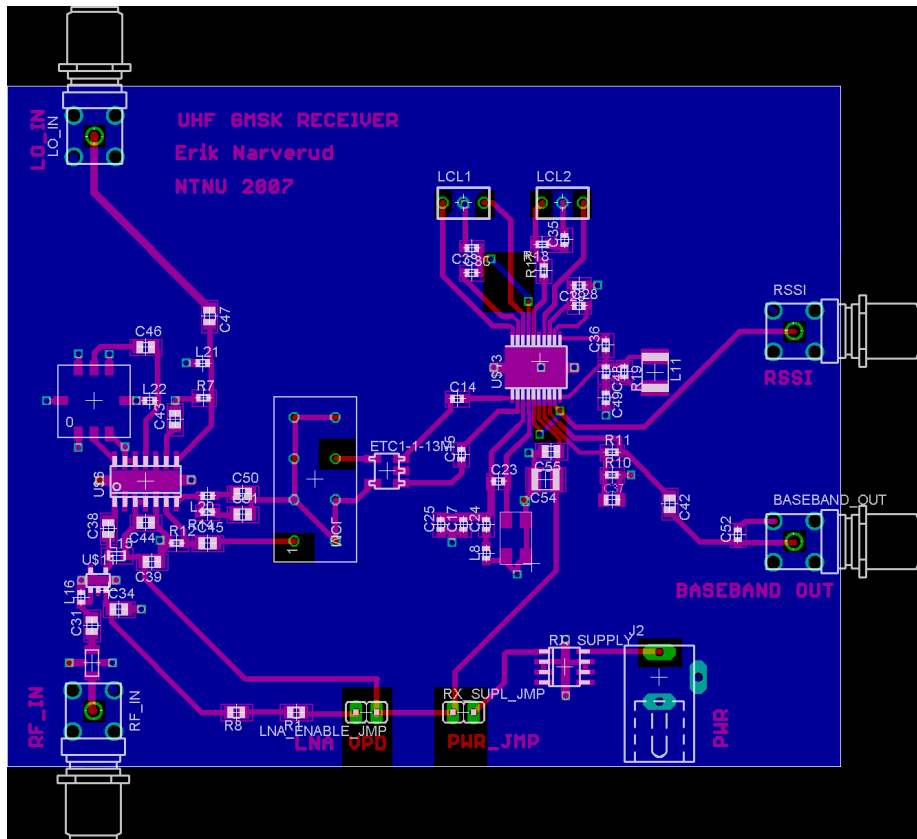


Figure 8.4: Layout of the receiver development circuit.

Chapter 9

Discussion

In this chapter, the design choices and prototype development will be further discussed. Key points from the design chapter and development and test chapter will be discussed.

9.1 Design Choices

As the final design choice is a highly customized design, although based on relatively few physical components, it cannot be directly compared to the other two solutions discussed in the design chapter. What is certain, is that today's modern DSP's consume too much power to be a realizable choice for a satellite as small as 10x10 cm.

A solution that may be further investigated is the use of a fully integrated radio system, with baseband modem, oscillators, upconverters and signal processing capabilities embedded in a single chip. Although it will probably be inferior to a customized design in terms of data rate and SNR, such a system, if realizable, will have a great advantage in power consumption and reliability, provided that important parameters can be hard-coded into the system. Unfortunately, these system chips usually incorporate some form of FSK modulation, not giving the required bandwidth efficiency needed to get a VGA image down to earth in a single pass. When frame formatting and cyclic redundancy checks are added to the bit stream, binary modulation schemes such as GMSK may not even be sufficient for the grayscale image. If a color image is considered, with its 25600 bit/s data rate requirement, the only option will be to use a multisymbol phase modulation scheme, because of the 25 kHz bandwidth limitation. At the moment, it seems that no radio-on-chip can deliver quadrature modulation, and designs like the final, customized solution is therefore the only viable option.

It should be made clear, as mentioned earlier, that this solution is not a real transceiver, as it cannot communicate with a similar unit. Of course, this functionality has never been a requirement for the radio system. Whether the radio system should be called a transceiver or not, is therefore nonessential to its use, or function, and will be considered a trivial matter of definition. The market is continuously presenting new products that can be used, and news of an even more flexible GMSK communication chip, the CMX990 by CML

microcircuits [36], was received by mail as late as may 25. Being an integrated RF transceiver with data rates as high as 16 kbit/s, this chip can be used in a fully integrated design to transmit a grayscale image in a single pass, but the color image is still out of reach for the GMSK chips. Of course, onboard image processing can be performed to reduce the data rate demand.

9.2 Transmitter section

The developed transmitter section is, in essence, a finished $\pi/4 - DQPSK$ transmitter, although it lacks a carrier oscillator and sufficient output power. Of course, many elements of the design can be debated, and probably changed to the better. The output band pass filter has quite a large insertion loss, and more linear, power efficient buffer amplifiers are probably available. On the other hand, the function of the baseband processor and quadrature modulator can be deemed quite good. Although the offset and gain adjustments can be further adjusted, this is a trivial matter, easily done through a signal analyzation. The baseband channels can even be adjusted during transmission.

Indeed, the CMX980 can be said to form the core of the downlink design, being almost tailor-made for the purpose. With a default bit rate of 36 kbit/s, it will be able to transmit a color image in a single overhead pass. If it is found that the 25 kHz bandwidth occupied at this bit rate is too much, the baud rate can easily be changed by simply exchanging the clock crystal and rescaling the output RC sections. If the baseband processor and microcontroller use the same crystal, as is intended in the development circuit, additional software may need to be adapted to the new frequency. The serial interface software should function properly without much change, although the bit counter constants may need to be adjusted.

In all, the entire transmitter circuit performs its intended tasks well, although a proper SNR measurement could not be done. The factor defining the overall success of the transmitter will be the power amplifier, and it is unfortunate that it could not be further investigated. It does, however, form an excellent design study for future students. The RF5110G has the required specifications, and although proper function was not achieved during the measurements done in this thesis, it may serve as the core of a well designed power stage. The small, legless package should however be the cause of some concern, in terms of connection durability.

9.3 receiver section

The receiver section, in comparison to the transmitter, is a quite traditional design. The use of the RF2418 combined LNA and mixer is an excellent way of keeping the number of components low, while not sacrificing performance. What can be debated, is the need for the RF2878 LNA. Seeing from the link budget that the minimum received power will be approximately -110 dB, less than 20 dB of gain will be necessary to reach the required sensitivity level of the SA606. This might be achieved through the use of the RF2418 only. However, the noise performance of the circuit will be substantially reduced, and additional signal margins will be nonexistent. As the RF2878 can be tuned to consume less than

8 mA of power, one may rather question the 18 mA drawn by the RF2418.

The SA606 IF system must be said to perform sufficiently well, and it is an excellent choice for such a low-power application. NXP has introduced newer FM IF systems, the SA606 dating back as early as 1993, but the modifications are usually made to production technology, not to functionality. Indeed, even the rather grave error in their application schematic, with the series RC section forming an output high pass filter, instead of the desired low pass characteristic, seems to withstand the test of time, being present in similar circuit applications all the way up to the SA58640 datasheet [37], dating back as late as 2005. It can of course be claimed that the application schematic is correct, but this seems strange, as the circuit undoubtedly performed much better when the RC section was configured in parallel.

The receiver baseband processor was not closely investigated in this design. As mentioned, Roger Birkeland did a rather extensive development work on the CMX909b processor [26], and the receiver section is assumed to be able to communicate with this processor without much additional circuitry. The choice of baseband processor is, as mentioned, dependent on the selected packet format and coding, and could therefore not be further assessed in this thesis.

9.4 Logic section and software

The sole purpose of the logic circuits designed in this thesis, has been to enable programming and testing of the CMX980. It must be emphasised that the microcontroller used was chosen primarily for its familiar architecture, making it easier to program. The extensive software tools available for the AVR RISC family have also been used prior to this assignment, making the development process less time consuming.

The AVR architecture cannot be said to do a sufficient task, as several external logic circuits are needed to establish a link between it and the CMX980 baseband processor. Although these extra circuits are strictly passive, each one represents a *Single Point of Failure*, and will increase the likelihood of failure, as the transmission function relies directly on the serial interface. A microcontroller with a faster serial port, or at least, a 16 bit three wire port, being able to communicate directly with the CMX980, will be preferable. It should also be noted that an even simpler interface design can be achieved, by using only one 8-bit register in conjunction with the AVR's SPI. Unfortunately, this design could not be tested due to lack of time.

However, there are advantages of the ATmega128 other than ease of development. The number of input/output ports is just what is needed for communication with both the CMX980 and CMX909, for example. This has been taken into account when designing the development circuit. The power consumption of the chip is also relatively low, although smaller AVR's with even lower power consumption exist. And last, having the AVR design center located in Trondheim should not be underrated as a valuable resource during the design phase.

Chapter 10

Conclusion

The conclusion of this thesis is that the presented radio system is a feasible solution for UHF communication in a small student satellite, operating at altitudes up to 800 km. Particularly, the downlink fulfills the requirement of being able to transmit an entire color image in one pass, provided that sufficient bandwidth is available to include the doppler shift. However, because of the very small assigned bandwidth, one should investigate the possibility of on board image processing.

The receiver performs better than anticipated, as the anticipated sensitivity will be at least 10 dB lower than the minimum received power. As work could not be completed on the design, there are important parts of the design that have not yet been tested, and continued development of these parts is crucial for the success of the system. Two development circuits are therefore presented as an aid to a continued development.

If work is continued on the system, the following design areas should be prioritized:

- Design of a customized output power amplifier with high linearity and efficiency.
- Design of a low loss antenna connection network, possibly with a diplexer or RF switch.
- Design of frequency generation circuits for the transmit carrier wave and 1. IF receiver stage.
- Develop protocols, coding and software for both uplink, downlink and control logic.
- Perform a FMECA (*Failure Mode, Effects, and Criticality Analysis*) and re-design the circuit for enhanced robustness and reliability.

All information concerning the system will be made available to other students through the project database, should they choose to pursue the completion of the radio system.

Part II

Student Satellite Project

Chapter 11

background

During the spring of 2006, Professor Odd Gutteberg launched a proposal for a 9th semester assignment regarding a pre-study of a new student satellite project at NTNU. Three students were assigned to this task, together with a doctorate student. The project started with the goal of investigating the possibility of a student satellite project at NTNU, but quite soon evolved into a large project with a much wider scope, including a complete specification document for a satellite concept.

At the same time, the Norwegian Centre for Space-related Education, NAROM, indicated that they would launch a proposal contest for Norwegian universities and university colleges, to design and build a total of four new student satellites. NAROM launched their contest during October of 2006, and the student group handed in an application in December. This proposal received the highest technical and overall evaluation score from the expert group assigned to select the contest winner. Despite this, the NTNU project was not awarded the launch.

During spring 2007, two students from Engineering Cybernetics (ITK) and one exchange student from Spain got involved in the project. The ITK students have produced master theses concerning the Attitude Determination and Control System, while the exchange student has worked with the antenna systems and commenced on a study of a ground station.

Chapter 12

Project Work

Two students, Roger Birkeland and the author, have done most of the project management related work during the spring of 2007. A project manager, doctorate student Lars Løge, was appointed during 2006, but as he had a semester abroad in the spring of 2007, he could not undertake the administration of the project. The work included weekly technical interchange meetings, developing and carrying out presentations for future students and developing and administering a database and Internet site for the project. Half-way through the semester, a system review meeting was planning and arranged, with participants from leading space industry in Norway. The work has been extensive, but very interesting and inspiring for further studying and work. The management work has given the students relevant experience regarding system engineering and project work, in a degree not usually gained through a master thesis. Figure

Week	Main Focus During Week
2	Review and "clean-up" from project. Establishment of Technical Interchange meetings
3	Project database development, study of previous projects
4	Official Start Date. Study of similar student projects
5	Link and Power Budget investigation
6	
7	Overall Design investigation, component search, specification match controlling
8	
9	Choice of final design, component search, system design review preparations
10	Final design development, System Design Review preparations
11	System Design Review 13. March, meeting and after work
12	Student Presentations – Prototype Design
13	Prototype Design
14	Easter
15	Easter
16	Prototyping and measurements – power amplifier, quadrature modulator
17	Prototyping and measurements – LNA
18	Prototyping and measurements – LNA/mixer stage
19	Prototyping and measurements – Baseband processor, Software development
20	Prototyping and measurements – Baseband processor, Software development
21	Prototyping and measurements – IF-to-Baseband subsystem
22	Prototyping and measurements – buffer amplifier
23	Report
24	Course at Andøya – Space Technology II
25	Report
26	Finalize report
	Work concerning overall project management
	No work done

Figure 12.1: Estimated workload distribution.

12.1 shows a rough estimate of the work distribution throughout the semester.

As seen, about 4 weeks have been used for project management.

12.1 Project Assignments and Master Theses Development

Suggestions for student assignments and master theses have been worked out, based on important design factors in the overall satellite design. These tasks can be found in appendix N. The assignments are multi-discipline, crossing the fields of radio, cybernetics, embedded systems and mechanical construction. In relation to these assignments, the project and assignments were presented for students in the 3rd and 4th year. By the time of writing, it is not known if any of the assignments have been chosen. The tasks generated by a possible continuance of this thesis have not been included in the list, but many are equally important.

12.2 Student Presentations

Student presentations were made in an attempt to secure a continuity in the project, and to present the future assignments for the students. The presentations were held by Roger Birkeland and the author for third and fourth grade students at the Institute For Electronics and Telecommunications at NTNU.

12.3 System Design Review Arrangement

Because the students working on the project wanted a contemporary evaluation of the satellite concept, a full-day System Design Review was planned and carried out. Representatives from other groups at NTNU, The University of Oslo, Norspace, Sintef and Conax were invited to the meeting, which was held during the midst of the semester. The review gave vital information and advice to the students, as many of the attendants had substantial knowledge of space engineering. The agenda, presentations and account from the meeting can be found in appendix N.

12.4 Technical Interchange Meetings

In the planning phase of the project work, before prototyping work commenced, weekly meetings between all students involved in the project were held. These meetings made it possible to interchange important information between the students at an early stage of the design. Important decisions, such as data bus and power distribution solutions, were discussed, giving a more solid foundation for further work.

Chapter 13

Project Database Development

Bitter lessons from earlier satellite project has unveiled the lack of information control as the biggest problem for student satellite projects. The "project staff" is continuously being replaced, and it is very difficult to keep a sustained level of knowledge within the project. To counteract this problem, the project group saw the need for a database that could store theses, reports, schematics and datasheets and make them available for future students. The hierarchical concept was based upon a classification of the satellite systems, with subsystems, units and components as the principal entities. The database was given a web interface with user limited access. A public web portal was also developed, linked to the protected database. The database development was primarily done by Roger Birkeland, as he has extensive experience in database development, with some inspirational aid from the author.

Chapter 14

Conclusion

The conclusion of the project work cannot be anything but binary. On one hand, it has been both educational and inspiring to administer such a multidisciplinary and advanced development project. On the other hand, it would not be recommendable to give this responsibility to students while they are doing project assignments or master theses, as the extent of the work is substantial and time consuming. An administrative person should therefore be responsible for project management and supervision at all times.

Although many lecturers have been positively committed to the project, it proved somewhat difficult to gain commitment from all. Participation from the lecturers is crucial, especially when considering that they are the ones assigning tasks to future students. As long as there is no special commitment from the university to undertake such a project, it will be very difficult to complete. This is partially due to the fact that students from all needed disciplines must be made aware of the project. Lecturers who can contribute to the project with knowledge of a particular discipline, must inform and include the students in the project. Although a support group of lecturers was established by the students of this year's project staff, this group is not responsible for taking any initiative concerning further development. It is merely a contact list for students to use when in need of technical support.

The NAROM launch contest must be deemed as a slight failure. Not only did it fail to award the launch to the winning project, it also failed to attract the attention of any institution that was not already undertaking a student satellite project. To schedule the first contested launch as early as 2008, resulting in a mere year of system development, can at best be interpreted as highly optimistic. This is unless NAROM was aware that development had already been undertaken by all the relevant competitors. The belief that there were several Norwegian institutions with the means, or interest, to undertake such a project must also be considered highly questionable.

The students' opinion is that NAROM should support collaboration between institutes, with close follow-up and administration of the project. Such a project will need a full-time *technical* administrator. Alternatively, NAROM should provide finance to single institutions and employ local supervisors, but the joint space community at Norwegian universities and colleges, is probably not of a size capable of running several satellite projects simultaneously.

A solution for NTNU can be to engage in cooperation with foreign univer-

sites, so that students involved in space technology studies can have the possibility for an exchange semester or year. Student assignments can also be given this way. Another possibility is engagement in ESA student projects. Presumably, such projects will be easier to carry out than a self-driven project with limited resources. Such student assignments might also be of a higher professional level, and might be more useful from a scientific point of view.

Bibliography

- [1] R. Birkeland, E.K. Blom, and E. Narverud. Small student satellite. Master's thesis, Norwegian University of Science and Technology, 2006.
- [2] T. Pratt, C. Bostian, and J. Allnutt. *Satellite Communications*. John Wiley & Sons, second edition, 1986. ISBN 0-471-37007-X.
- [3] ITU-R. Propagation data and prediction methods required for the design of earth-space telecommunication systems, 1999.
- [4] Gunnar Stette. Radiokommunikasjon, forelesninger i fag ttt4145 radiokommunikasjon, 2004.
- [5] David M. Pozar. *Microwave and RF Wireless Systems*. John Wiley & Sons, 2001. ISBN 0-471-32282-2.
- [6] D. G. Messerschmitt J. R. Barry, E. A. Lee. *Digital Communication*. Kluwer Academic Publishers, third edition, 2004. ISBN 0-7923-7548-3.
- [7] E. Kreyszig. *Advanced Engineering Mathematics*. John Wiley & Sons, eight edition, 1999. ISBN 0-471-15496-2.
- [8] Simon Haykin. *Communications Systems*. John Wiley & Sons, fourth edition, 2001. ISBN 0-471-17869-1.
- [9] L.E. Miller and J.S Lee. Ber expressions for differentially detected pi/4 dqpsk modulation. *IEEE Transactions on Communications, Volume 46 Number 1*, page 71, January 1998.
- [10] M. Scarpa, J. Vogel, J. Stonick, and S. Kiaei. Ber of differentially detected pi/4-dqpsk in the prescence of quadrature gain imbalance. *Wireless Communications and Networking Conference, 1999. WCNC. 1999 IEEE*, pages 201 – 205 vol.1, 21-24 Sept. 1999.
- [11] S. Huang and J.T Stonick. Effect of dc offset on performance of differentially detected p/4 dqpsk. *Circuits and Systems, 2000. Proceedings. ISCAS 2000 Geneva. The 2000 IEEE International Symposium on*, pages 757 – 760 vol.4, 28-31 May 2000.
- [12] M. Scarpa, J. Vogel, J. Stonick, and S. Kiaei. Performance of differentially detected pi/4 dqpsk in the presence of iq phase imbalance. *Circuits and Systems, 2000. Proceedings. ISCAS 2000 Geneva. The 2000 IEEE International Symposium on*, pages 645 – 648 vol.4, 28-31 May 2000.

- [13] Peter B. Kenington. *High-Linearity RF Amplifier Design*. Artech House, 2000. ISBN 1-58053-143-1.
- [14] Peter Berlin. *Satellite Platform Design*. Dept. of Space Science, Universities of Luleå and Umeå, Kiruna, Sweden, fourth edition, 2005. ISBN 91-631-4917-6.
- [15] Peregrine Semiconductors. *PE9601 Product Specification. 2200 MHz UltraCMOS Integer-N PLL for Rad Hard Applications*, 2005. URL <http://www.peregrine-semi.com/pdf/datasheets/pe9601ds.pdf>.
- [16] Mini-Circuits. *CMX980A TETRA Baseband Processor*, 2005. URL <http://www.cmlmicro.com/techregister/log.asp?fname=/products/datasheets/Docs/cm980ads.pdf>.
- [17] Analog Devices. *AD8345 140 MHz to 1000 MHz Quadrature Modulator*, 2005. URL http://www.analog.com/UploadedFiles/Data_Sheets/AD8345.pdf.
- [18] RF MicroDevices. *RF5110g 3V GSM Power Amplifier*, 2006. URL <http://www.rfmd.com/pdfs/5110G.pdf>.
- [19] RF MicroDevices. Infrastructure product selection guide. URL <http://www.rfmd.com/adocs/bf/Infrastructure-Product-Specs.pdf>.
- [20] Mini-Circuits. *LFCN-490+ Ceramic Low Pass Filter*, 2006. URL <http://www.mini-circuits.com/pdfs/LFCN-490.pdf>.
- [21] RF MicroDevices. *RF2878 3V Low Noise Amplifier/3V PA Driver Amplifier*, 2006. URL <http://www.rfmd.com/pdfs/2878.pdf>.
- [22] RF MicroDevices. *RF2418 Low Current LNA/Mixer*, 2006. URL <http://www.rfmd.com/pdfs/2418.pdf>.
- [23] Mini-Circuits. *RBP-400+ Surface Mount Band Pass Filter*, 2006. URL <http://www.mini-circuits.com/pdfs/RBP-400+.pdf>.
- [24] Stein Joacim Log. Konstruksjon av vhf-mottaker for studentsatelliten ncube. Master's thesis, NTNU, 2004.
- [25] Per Erik Furebotten. Ais nyttelast for ncube satellitten. Master's thesis, NTNU, 2003.
- [26] R. Birkeland. Study of a 145 mhz tranceiver. Master's thesis, Norwegian University of Science and Technology, 2007.
- [27] Mini-Circuits. *CMX909B TETRA Baseband Processor*, 2005. URL <http://www.cmlmicro.com/techregister/log.asp?fname=/products/datasheets/Docs/cm909bd.pdf>.
- [28] CDS. Cubesat design specification, revision 9, 2005. URL <http://cubesat.atl.calpoly.edu/media/Documents/Developers/CDS%20R9.pdf>.

- [29] S. Mann, M. Beach, P. Warr, and J. McGeehan. Increasing talk-time with efficient linear pas. *Tetra Market and Technology Developments(Ref. No. 2000/007)*, *IEE Seminar*, pages 6/1 – 6/22, 10 Feb. 2000.
- [30] Mini-Circuits. *PIF-40 Plug-In Band Pass Filter*, 2007. URL <http://www.mini-circuits.com/pdfs/LFCN-490.pdf>.
- [31] Philips Semiconductors. *SA606 Low-voltage high performance mixer FM IF system*, 1997. URL <http://www.nxp.com/acrobat/datasheets/SA606.pdf>.
- [32] Mini-Circuits. *TC1-1-13M+ Surface Mount RF Transformer*, 2006. URL <http://www.mini-circuits.com/pdfs/TC1-1-13M+.pdf>.
- [33] Mini-Circuits. *HSWA2-30R + SPDT RF Switch*, 2006. URL <http://www.mini-circuits.com/pdfs/HSWA2-30DR+.pdf>.
- [34] Atmel Corp. *8-bit AVR Microcontroller with 128K Bytes In-System Programmable Flash*, 2007. URL http://www.atmel.com/dyn/resources/prod_documents/doc2467.pdf.
- [35] Philips Semiconductors. *74LV165 8-bit parallel-in/serial-out shift register*, 1998. URL http://www.nxp.com/acrobat/datasheets/74LV165_3.pdf.
- [36] CML MicroCircuits. *CMX990 GMSK Packet Data Modem and RF Transceiver*, 2007. URL <http://www.cmlmicro.com/products/datasheets/Docs/cm990ds.pdf>.
- [37] NXP Semiconductors. *SA58640 Low-voltage mixer FM IF system*, 2005. URL http://www.nxp.com/acrobat_download/datasheets/SA58640_1.pdf.

Part III
Appendices

Appendix A

CMX980a Circuit Diagrams and Measurement Results

A.1 Circuit Diagrams

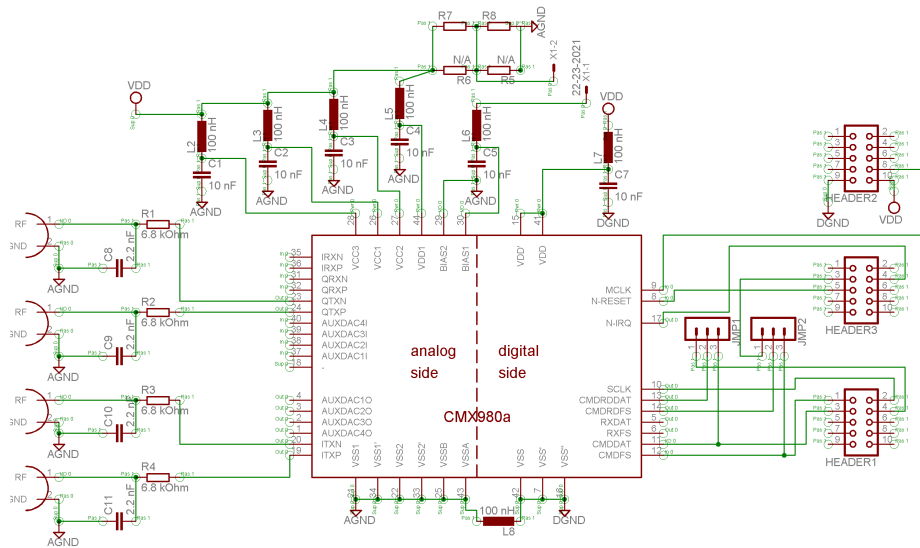


Figure A.1: CMX980a Evaluation Board Schematic.

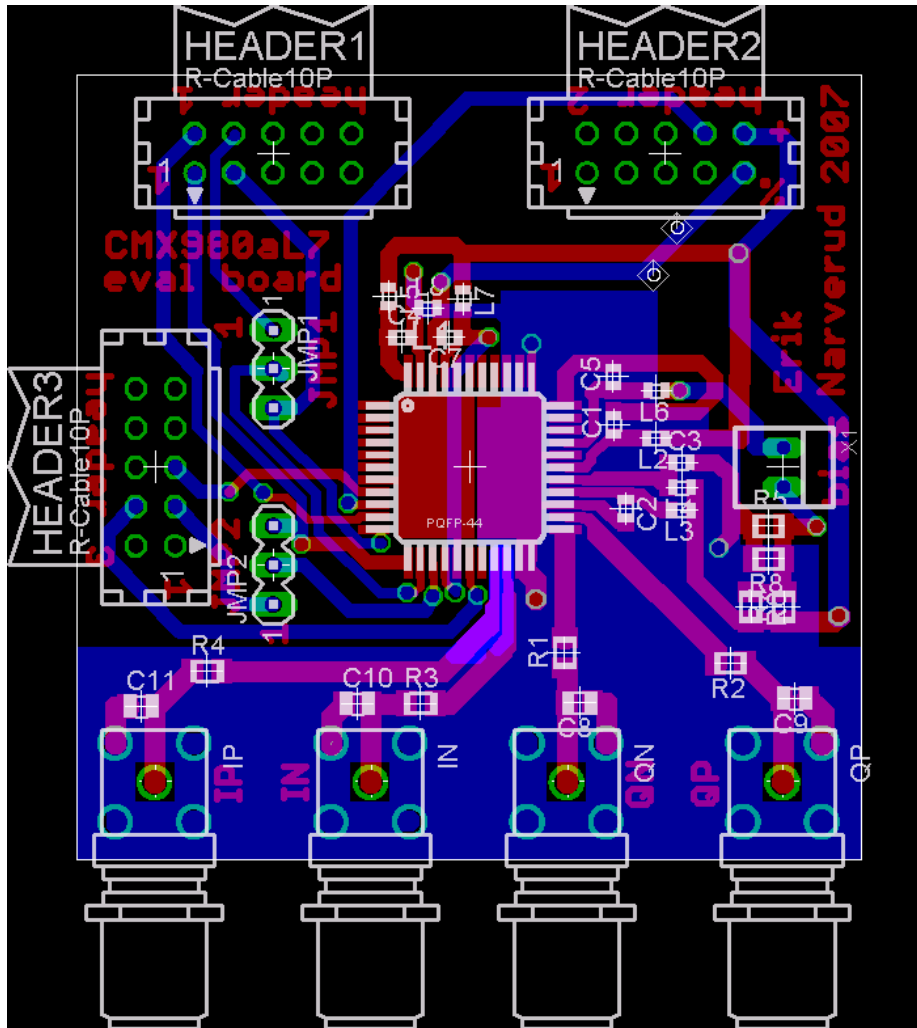


Figure A.2: CMX980a Evaluation Board Layout.

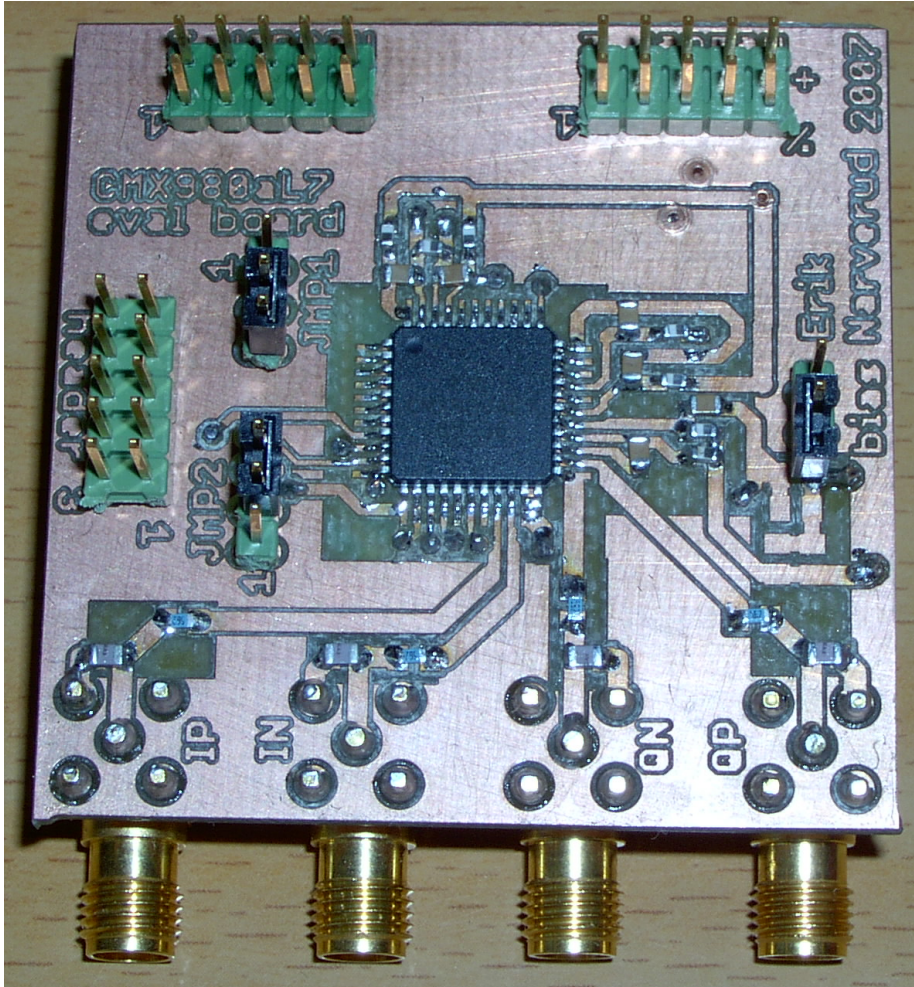


Figure A.3: An image of the CMX980 Evaluation Board schematic.

A.2 Measurement Results

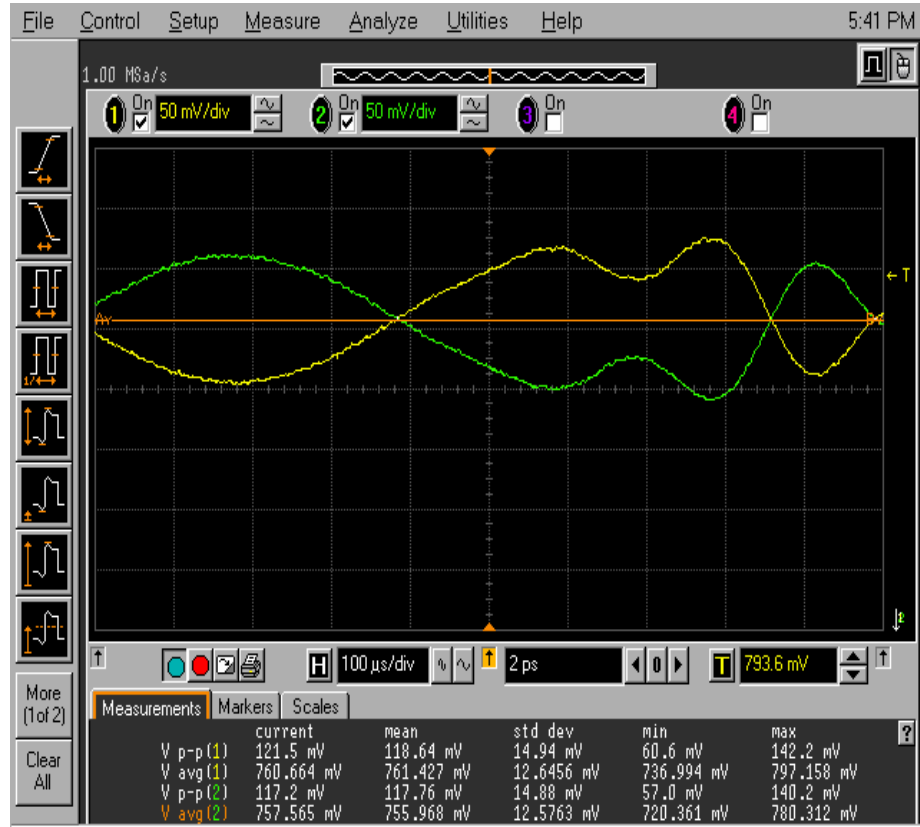


Figure A.4: Measured waveform on the I channel of the CMX980 after gain and offset adjustment.

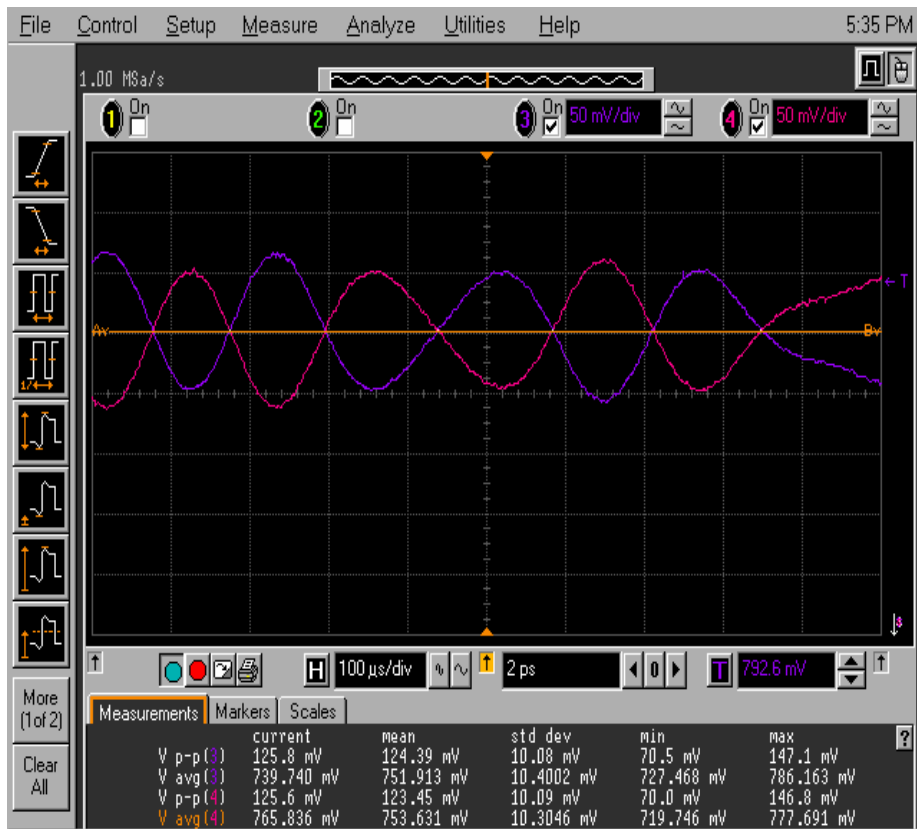


Figure A.5: Measured waveforms on the Q channel of the CMX980 after gain and offset adjustment.

Appendix B

AD8345 Circuit Diagrams

B.1 Circuit Diagrams

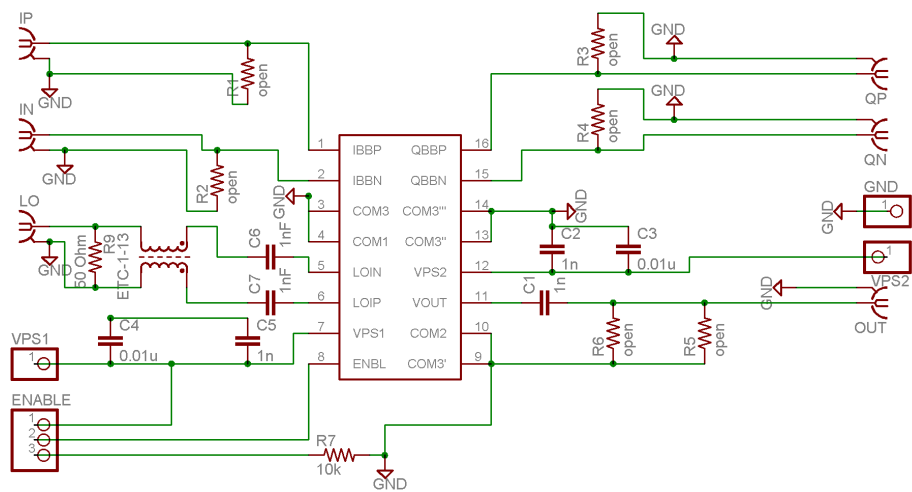


Figure B.1: AD8345 Evaluation Board Schematic.

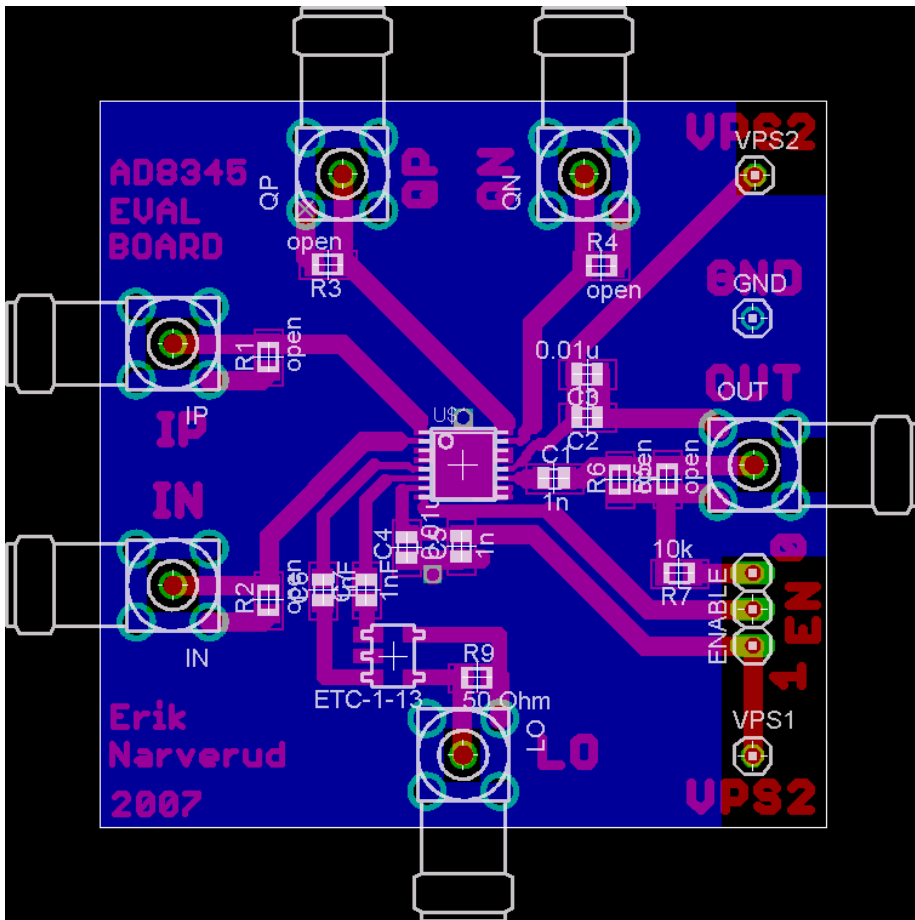


Figure B.2: AD8345 Evaluation Board Layout.

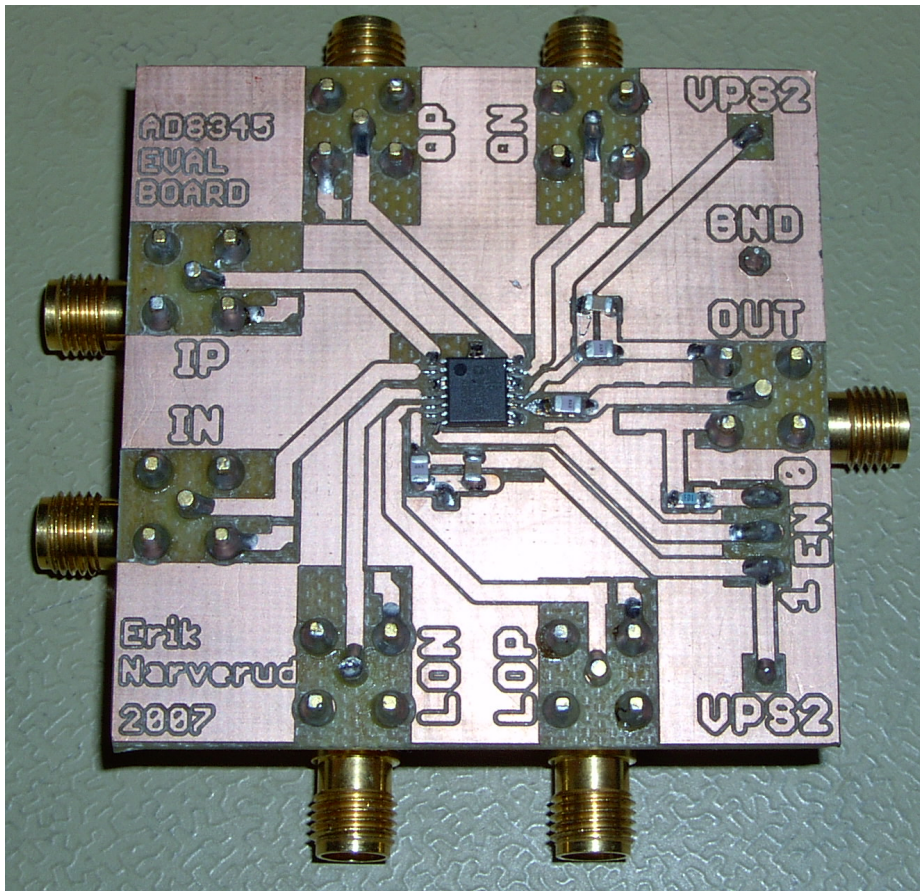


Figure B.3: An image of the AD8345 evaluation board.

Appendix C

RF2878 Circuit Diagrams and Measurement Results

C.1 Circuit Diagrams

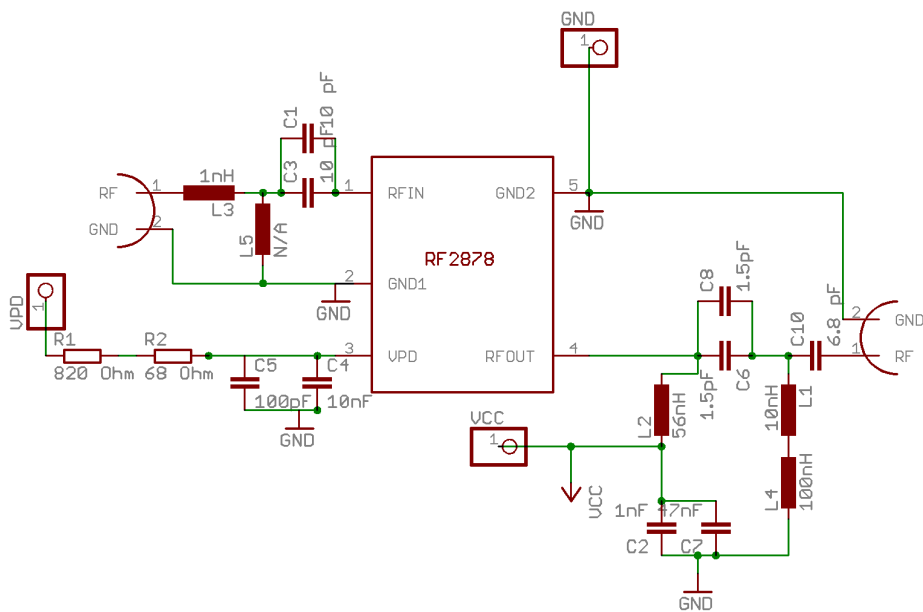


Figure C.1: RF2878 Evaluation Board Schematic.

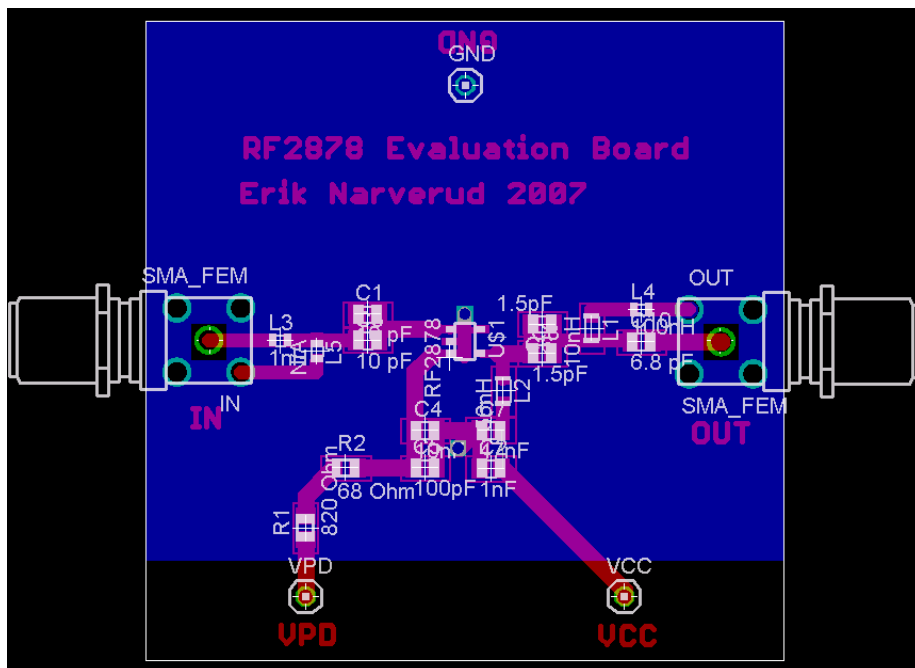


Figure C.2: RF2878 Evaluation Board Layout.

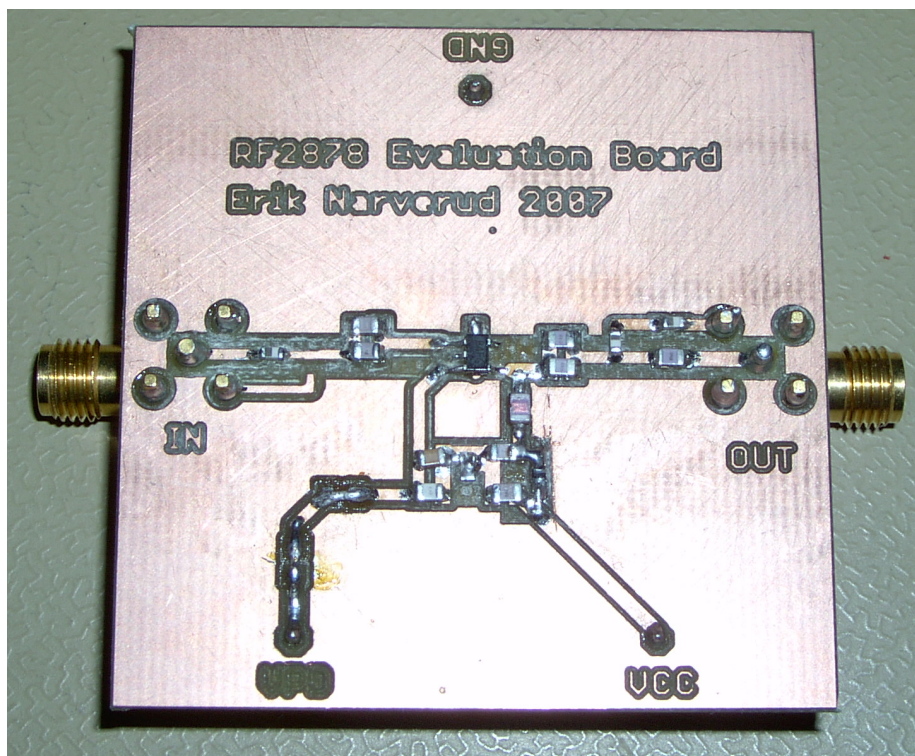
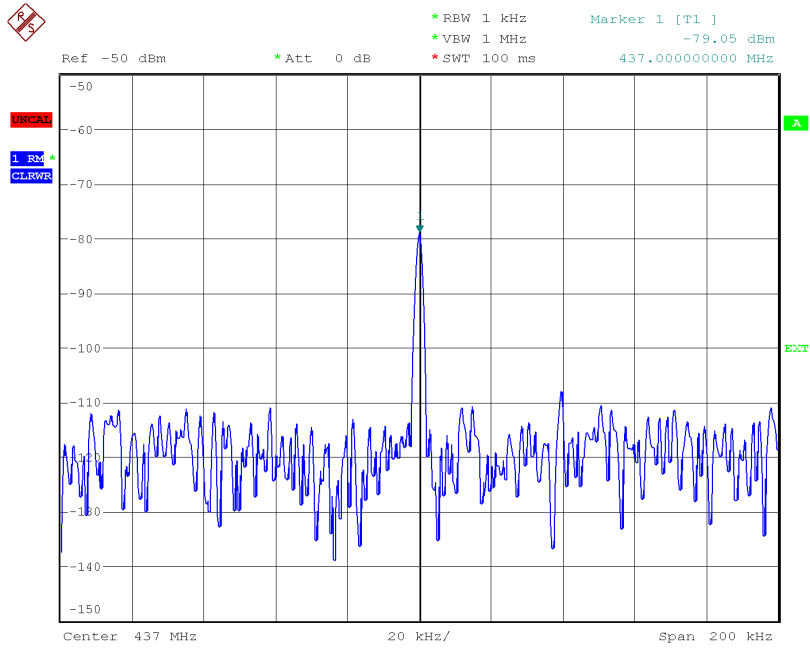


Figure C.3: A picture of the RF2878 evaluation board.

C.2 Measurement Results



RF2878_3V_VPD=2V_Itot=8mA_-100dBmIN
Date: 25.JUN.2007 15:26:13

Figure C.4: RF2878 LNA gain with VPD=2V, giving a total current consumption of less than 9 mA.

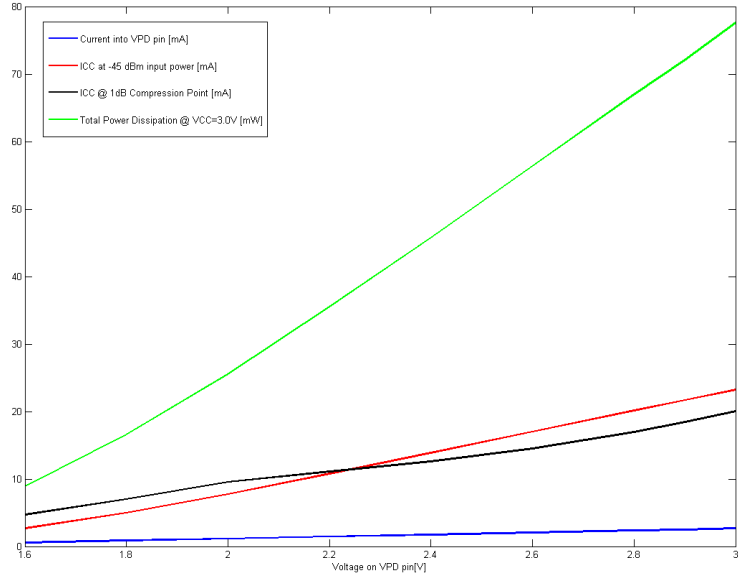


Figure C.5: RF2878 Current consumption for different bias settings.

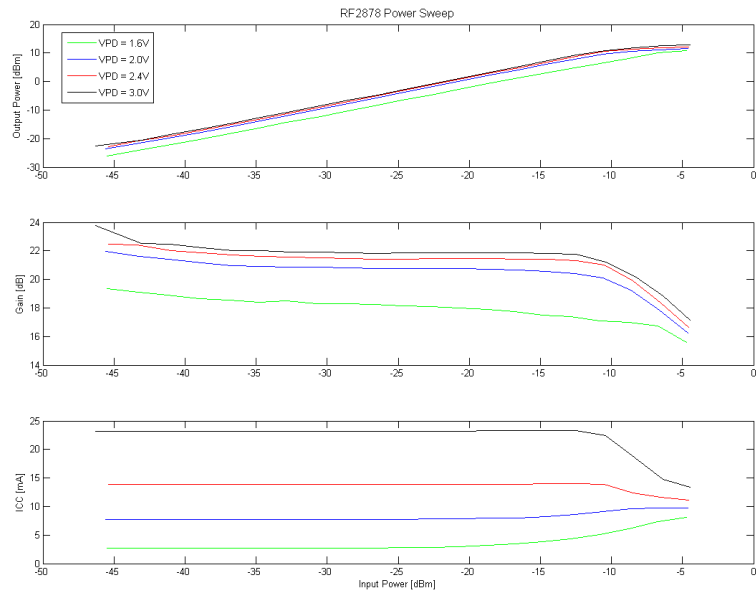


Figure C.6: RF2878 Power Sweeps for different bias current settings.

Appendix D

RBP-400 Circuit Diagrams

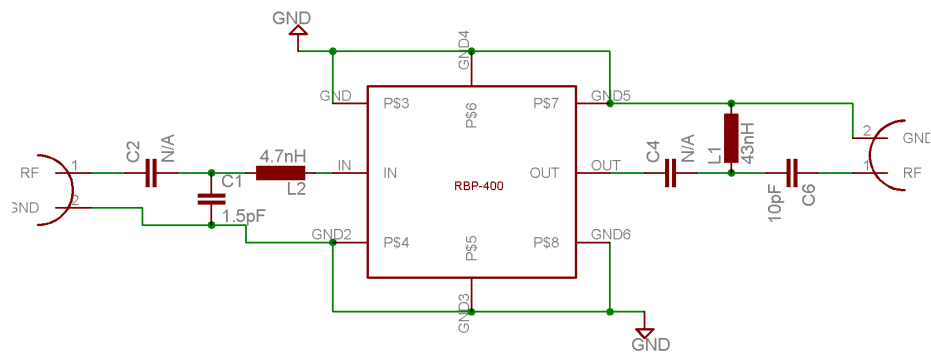


Figure D.1: RBP-400 Evaluation Board Schematic.

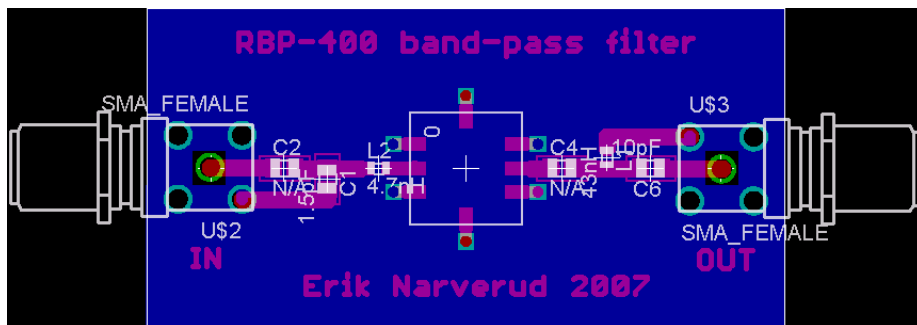


Figure D.2: RBP-400 Evaluation Board Layout.

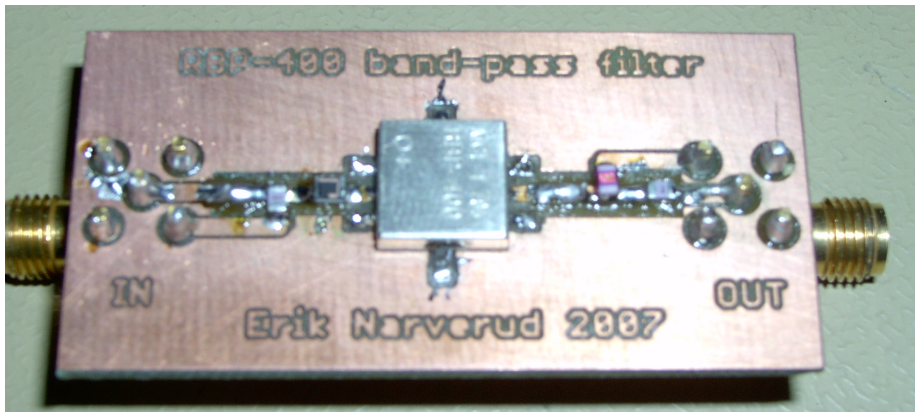


Figure D.3: A picture of the RBP-400 evaluation board.

Appendix E

LFCN490 Circuit Diagrams

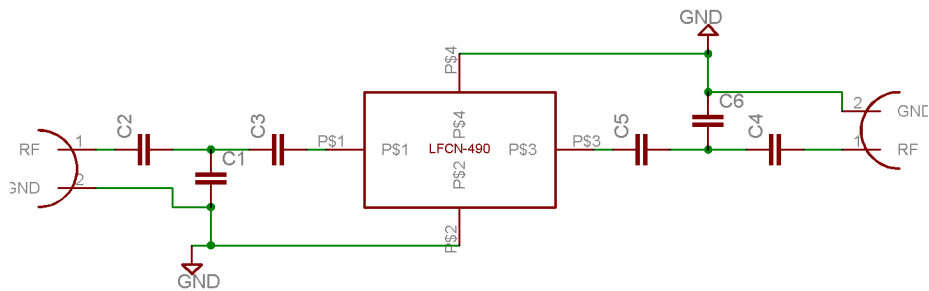


Figure E.1: LFCN490 Evaluation Board Schematic.



Figure E.2: LFCN490 Evaluation Board Layout.



Figure E.3: A picture of the LFCN-490 evaluation board.

Appendix F

RF2418 Circuit Diagrams and Measurement Results

F.1 Circuit Diagrams

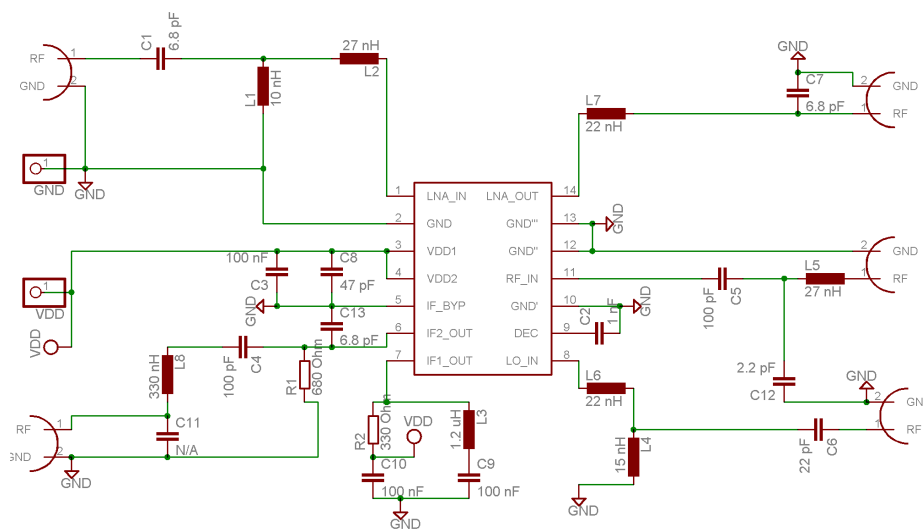


Figure F.1: RF2418 Evaluation Board Schematic.

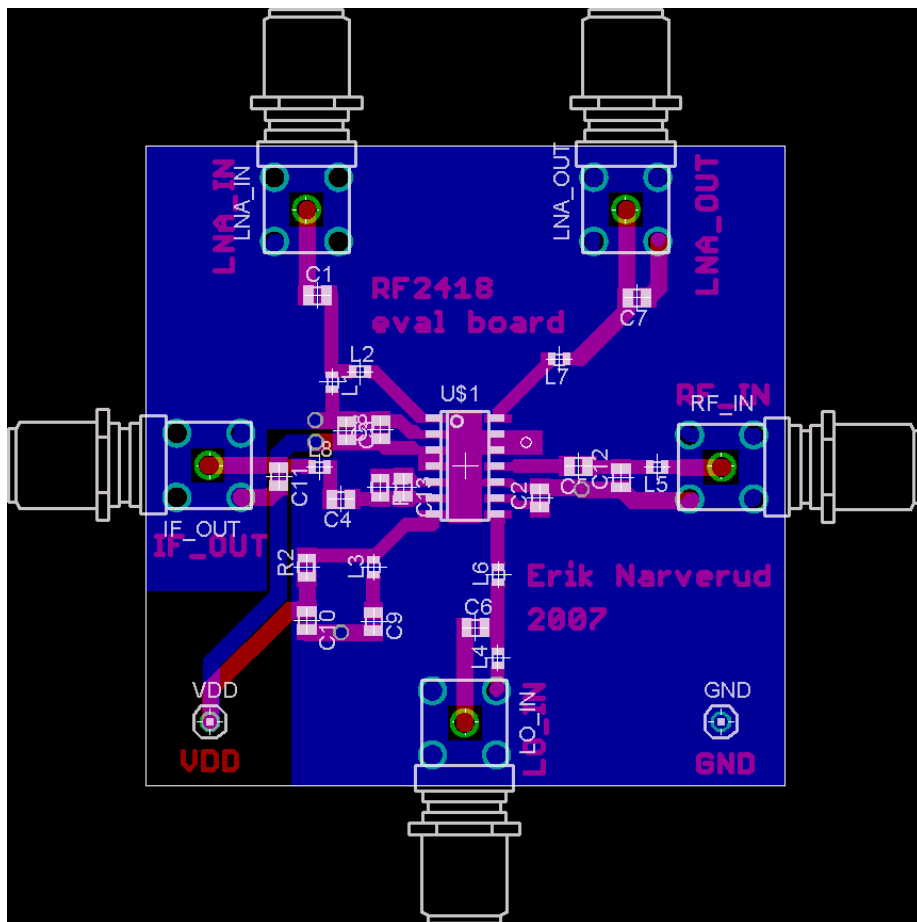


Figure F.2: RF2418 Evaluation Board Layout.

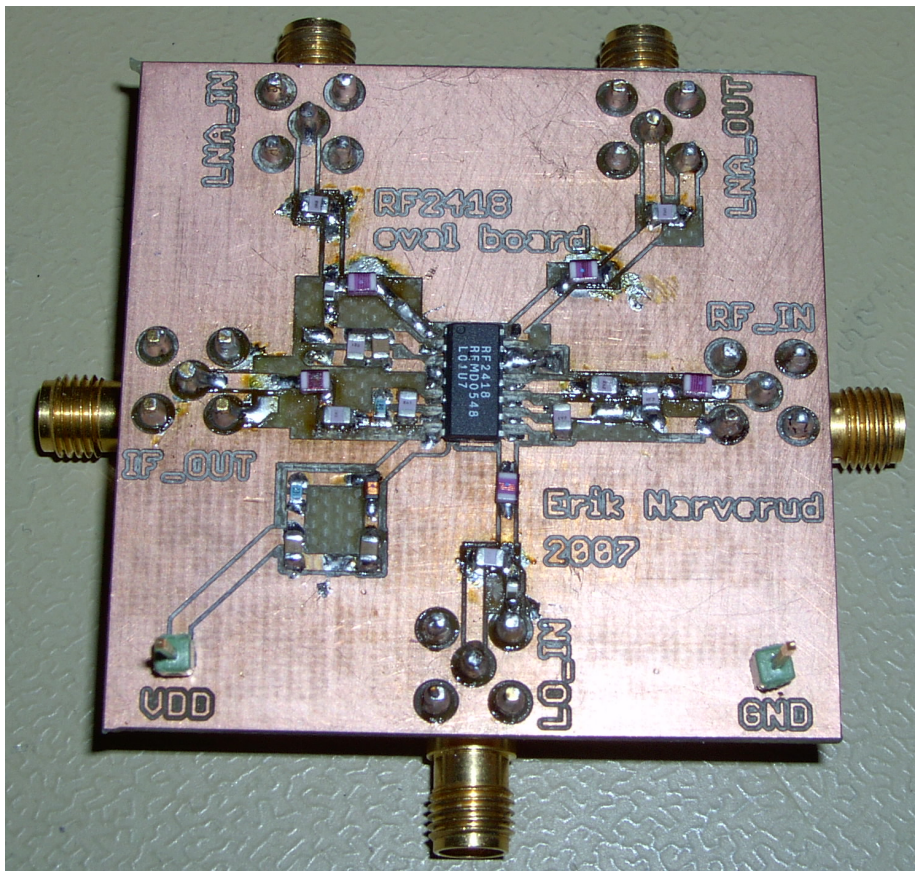


Figure F.3: A picture of the RF2418 evaluation board.

F.2 Measurement Results, LNA section

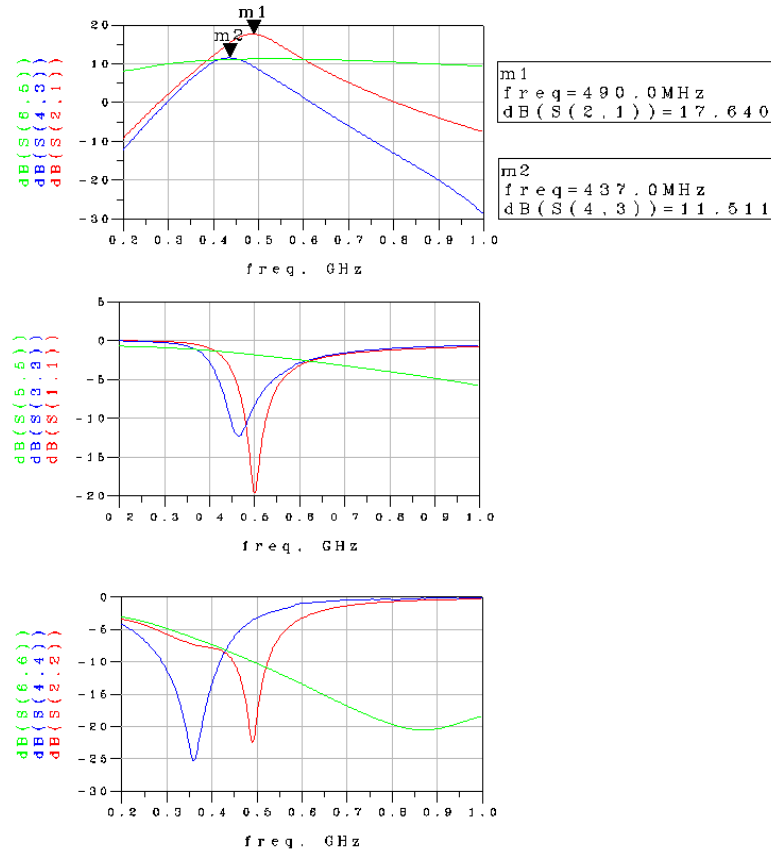


Figure F.4: S-parameters for the RF2418 LNA section. Port 1 and 2 shows the simulated network response, while port 3 and 4 shows the actual measured response. Port 5 and 6 shows the LNA response without any network, based on the trace-file received from RFMD.

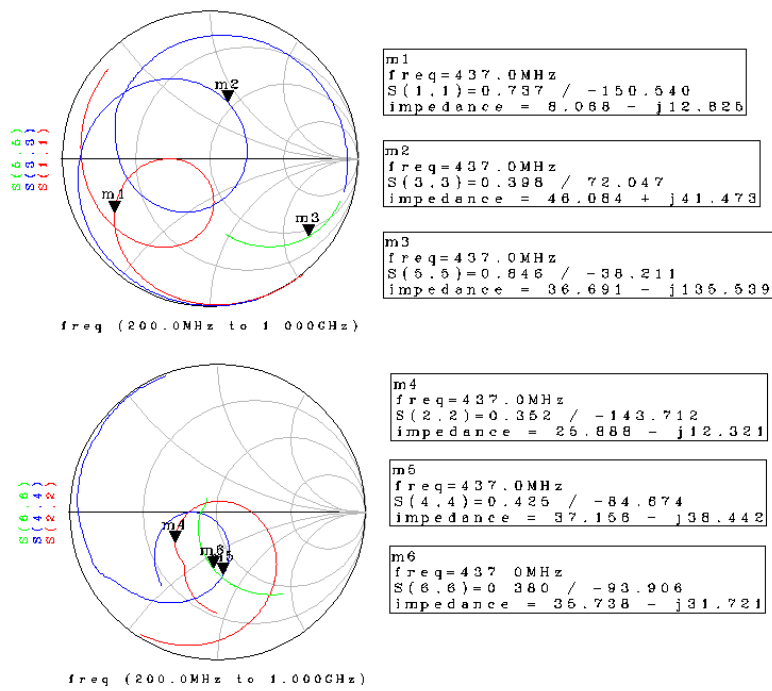


Figure F.5: Input and output impedance of the RF2418 LNA section. Port 1 and 2 shows the simulated network impedance, while port 3 and 4 shows the actual measured response. Port 5 and 6 shows the LNA impedance without any network, based on the trace-file received from RFMD.

F.3 Measurement Results, mixer section

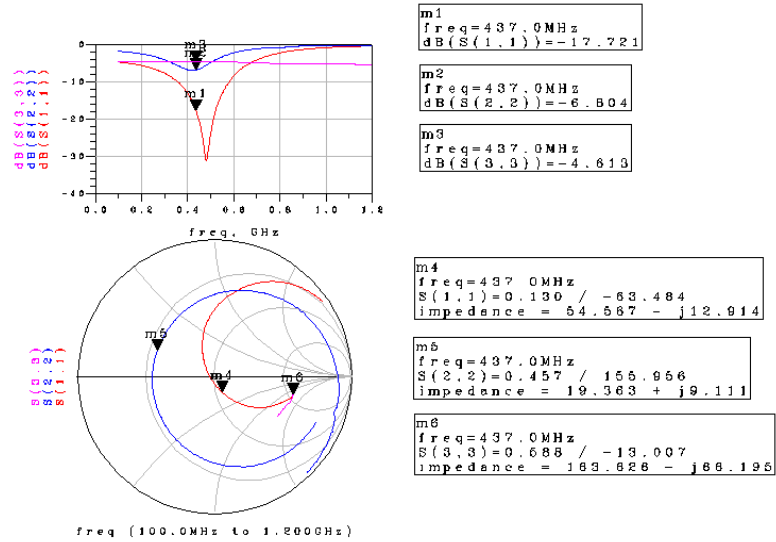


Figure F.6: Reflection Coefficient of the RF input on the RF2418 mixer section. Port 1 shows the simulated result, and port 2 the measured response. Port 3 shows the raw data from the RFMD trace file.

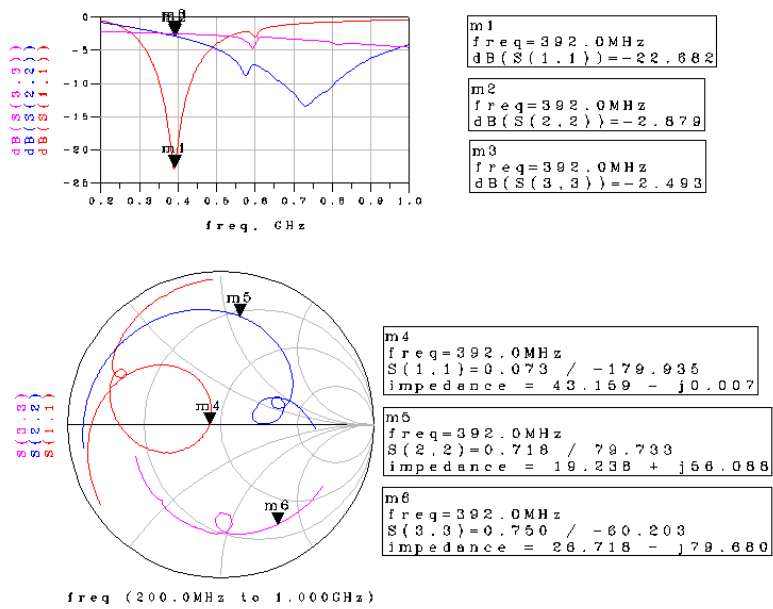


Figure F.7: Reflection Coefficient of the LO input on the RF2418 mixer section. Port 1 shows the simulated result, and port 2 the measured response. Port 3 shows the raw data from the RFMD trace file.

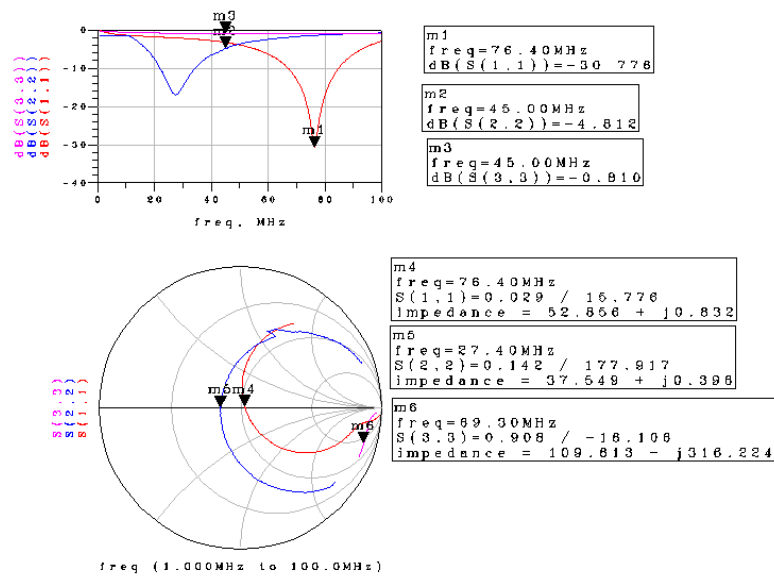
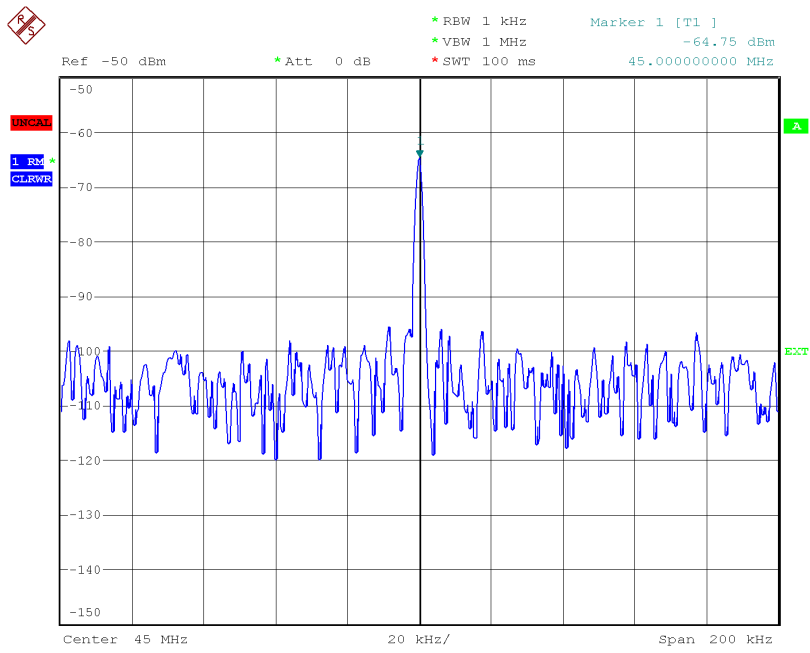


Figure F.8: Reflection Coefficient of the RF2418 IF output. Port 1 shows the simulated network response, while port 2 shows the actual measured reflection. Port 3 shows the s-parameter trace supplied by RFMD for the IF output.



RF2418IFOUT_3V_Itot=19mA_-70dBmRFIN_0dBmLOIN
 Date: 25.JUN.2007 15:36:30

Figure F.9: Narrowband Output spectrum of the RF2418 mixer. A 437 MHz RF frequency of -70 dBm, and a 392 MHz LO frequency of 0 dBm, was applied to the inputs.

Appendix G

PIF-40 Circuit Diagrams

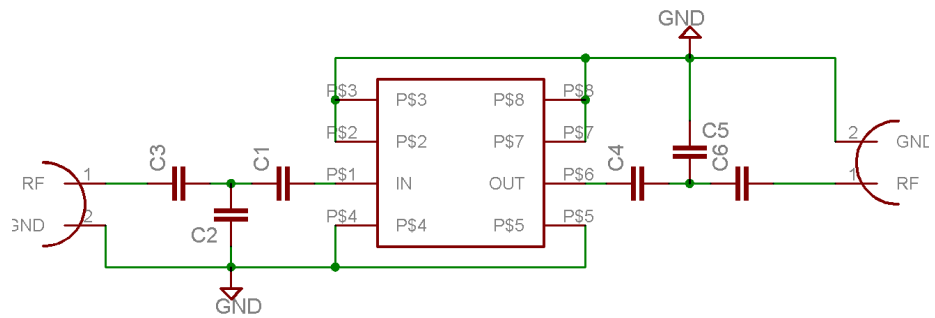


Figure G.1: PIF-40 Evaluation Board Schematic.

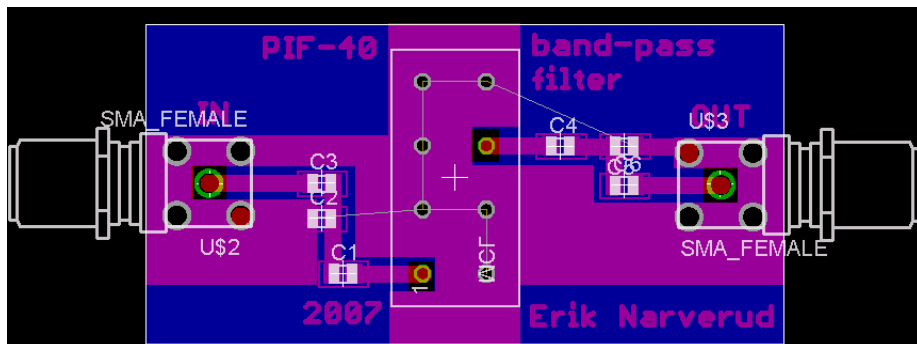


Figure G.2: PIF-40 Evaluation Board Layout.

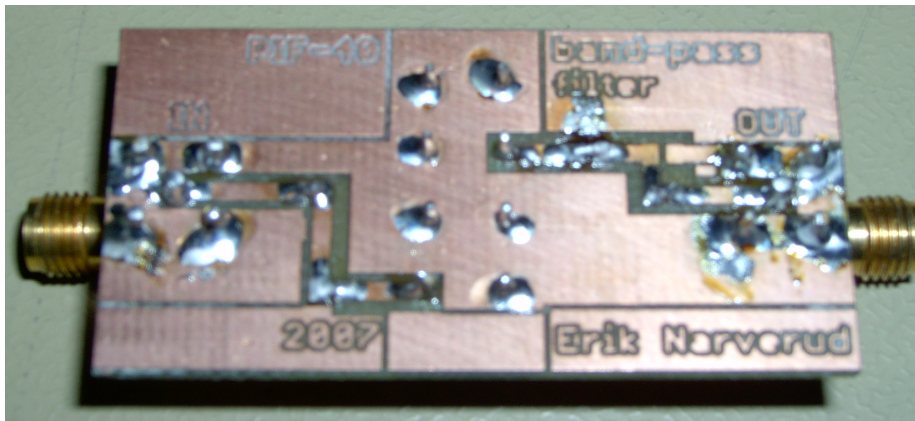


Figure G.3: A picture of the PIF-40 evaluation board.

Appendix H

SA606 Circuit Diagrams and Measurement Results

H.1 Circuit Diagrams

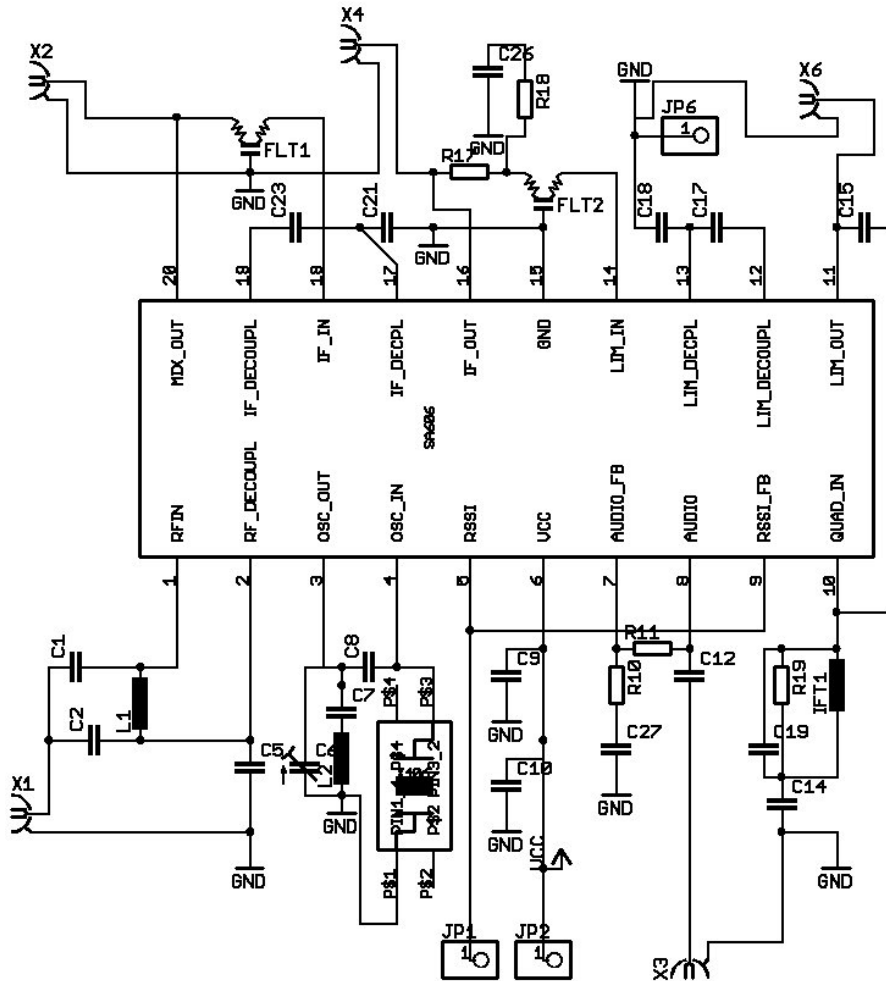


Figure H.1: Faulty SA606 evaluation board schematic, derived from datasheet application circuit.

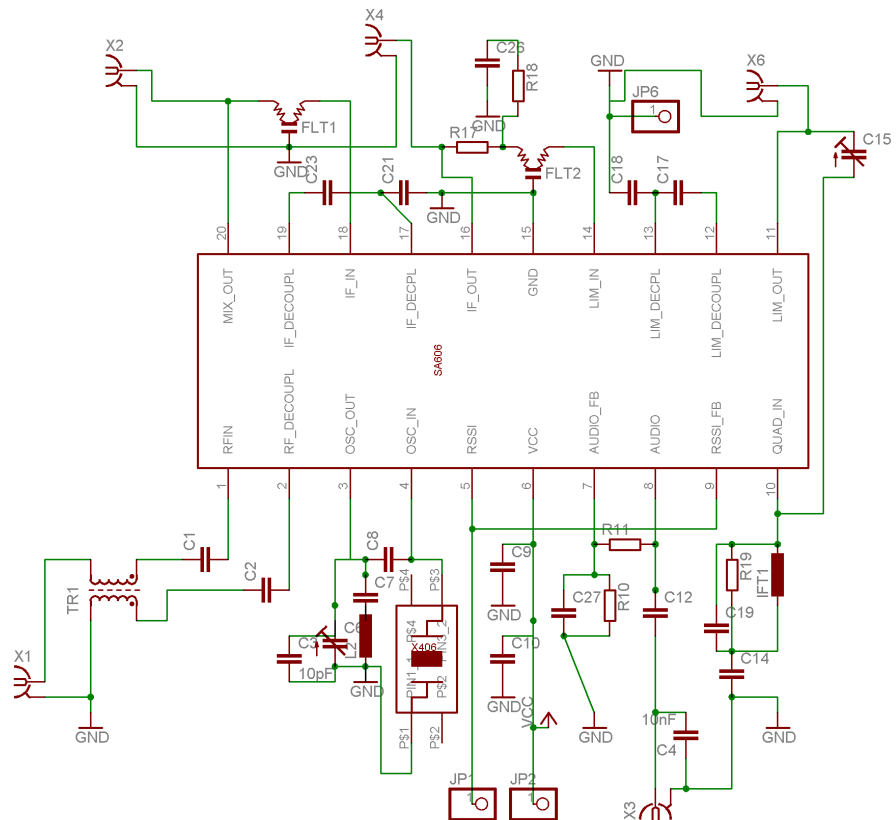


Figure H.2: Final SA606 Evaluation Board Schematic with altered input network and output filter.

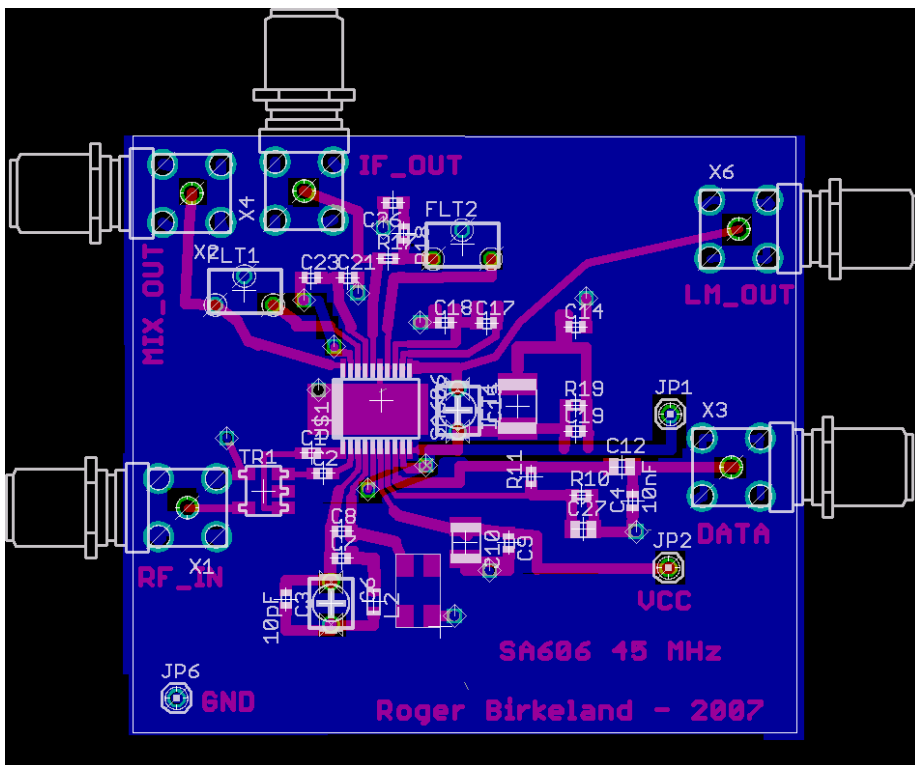


Figure H.3: Final SA606 Evaluation Board Layout.

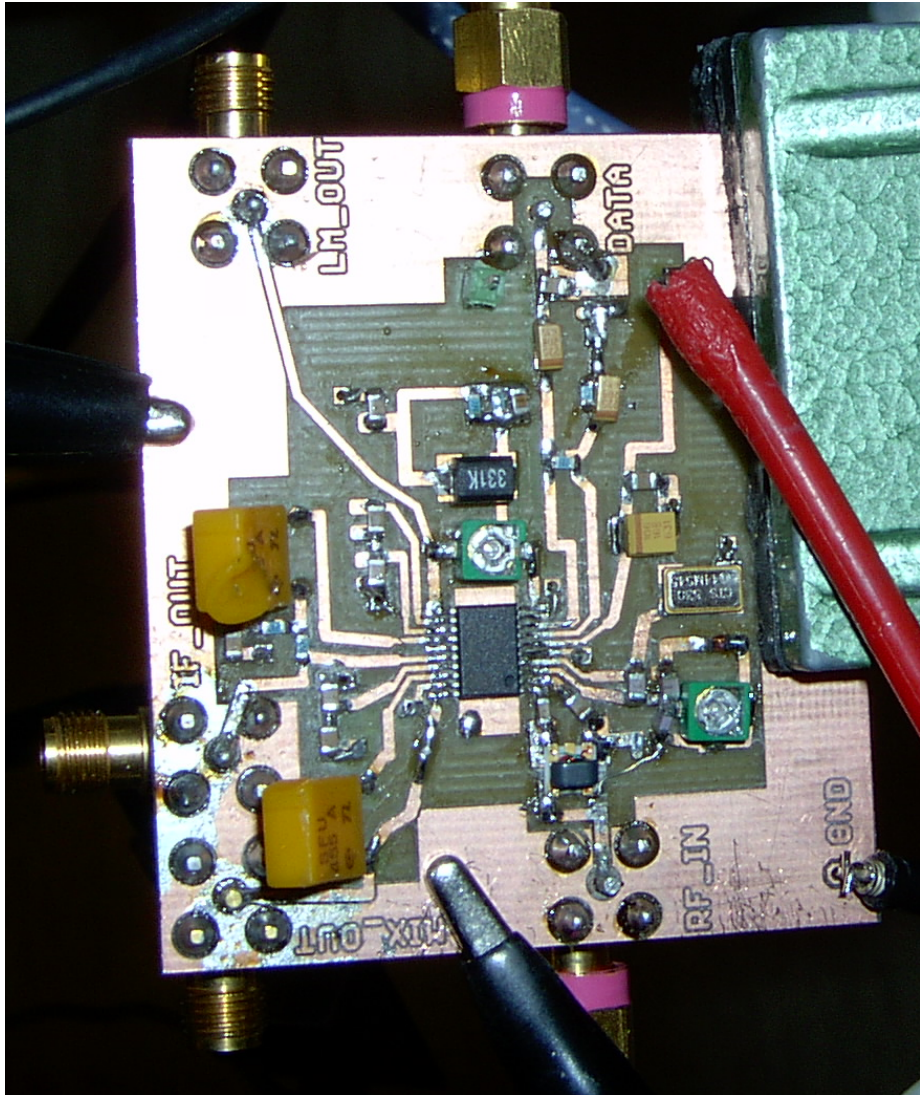


Figure H.4: A picture of the SA606 evaluation board during test.

H.2 Measurement Results

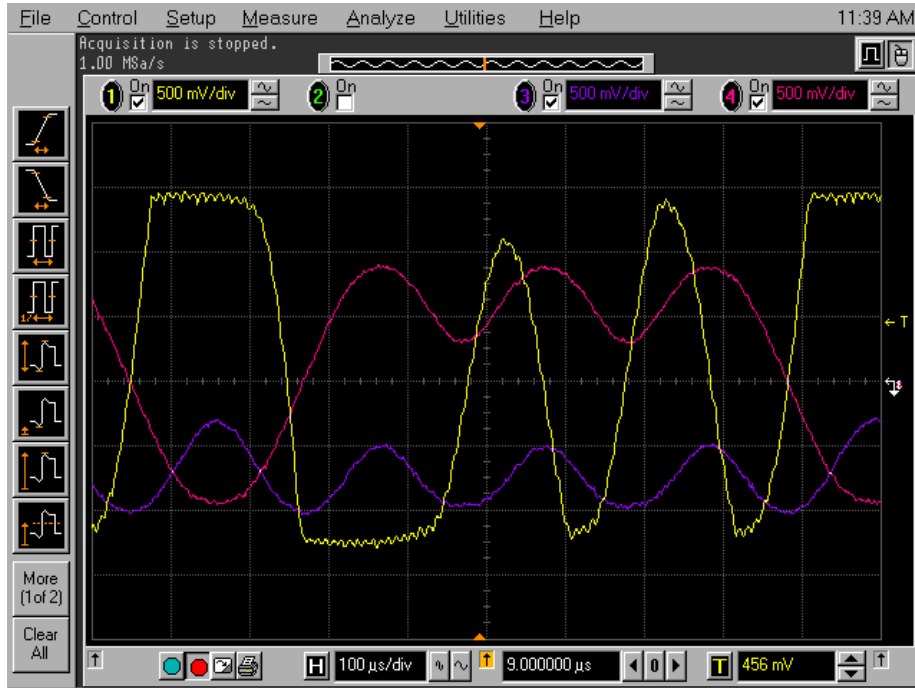


Figure H.5: The baseband output signal of the SA606, measured on channel 1, for a -70 dBm IF input signal. Channel 3 and 4 show the I and Q channels generating the 9600 baud GMSK signal, where the bit sequence is 11001010.

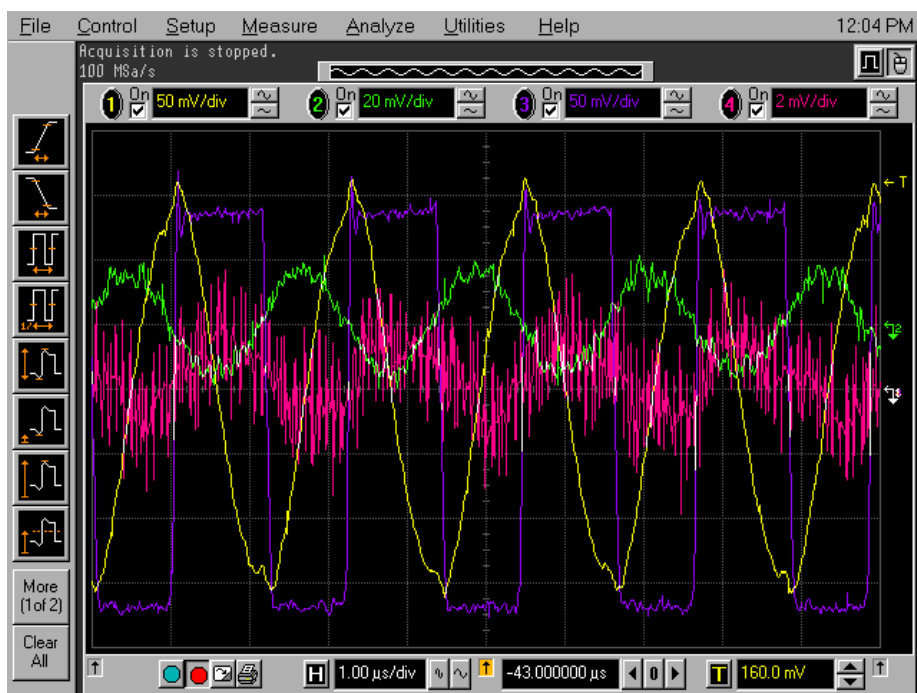


Figure H.6: Internal signals of the SA606 circuit with a -70 dBm input signal. Channel 4 shows the output signal of the mixer circuit. Channel 2 shows the input signal of the limiter, while channel 3 shows the output of the limiter. Channel 4 shows the input signal of the quadrature detector.

Appendix I

HSWA2-30R Circuit Diagrams

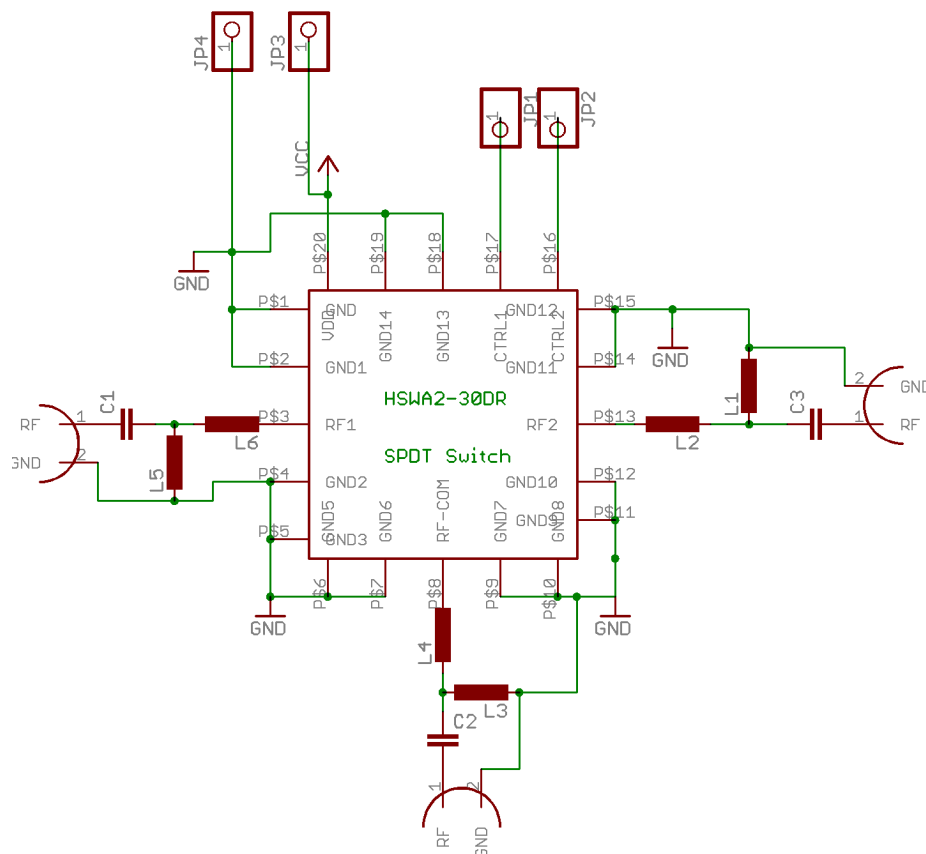


Figure I.1: HSWA2-30R Evaluation Board Schematic.

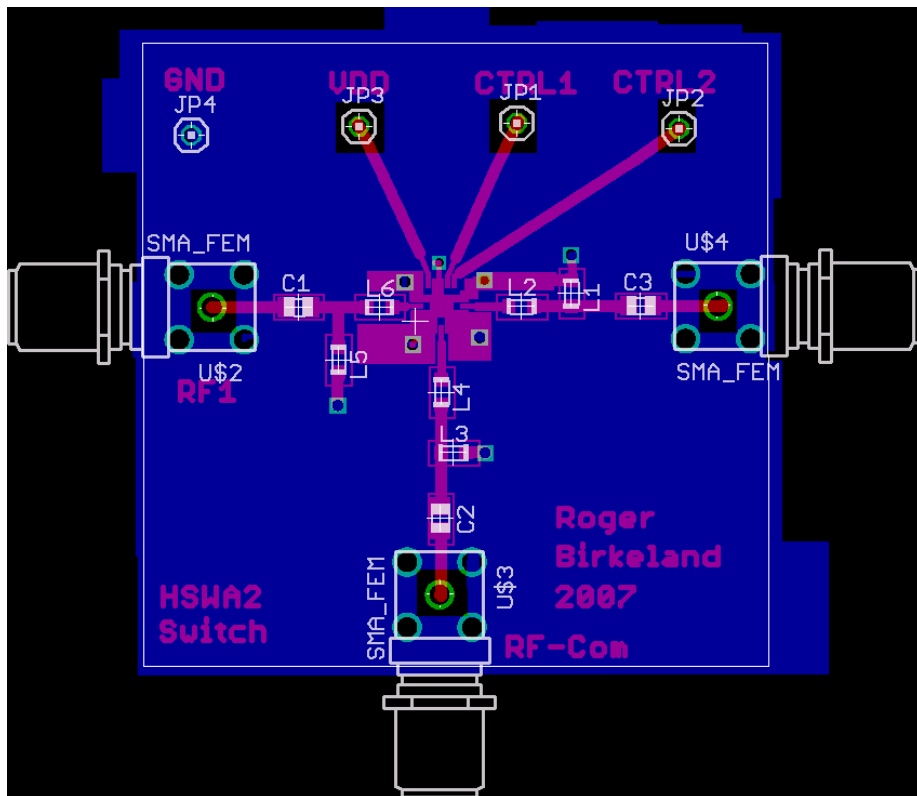


Figure I.2: HSWA2-30R Evaluation Board Layout.

Appendix J

RF5110g Circuit Diagrams

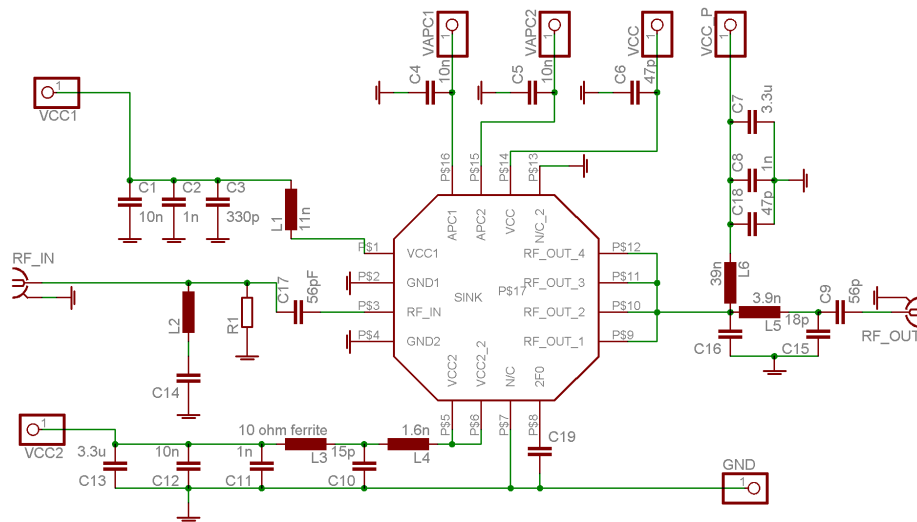


Figure J.1: RF5110g Evaluation Board Schematic.

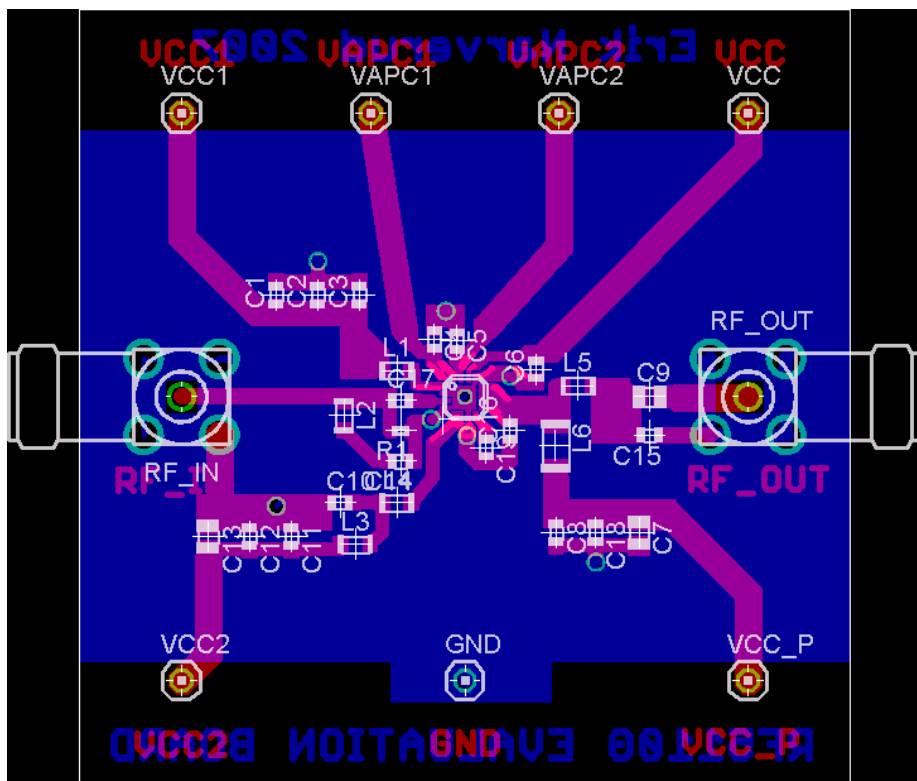


Figure J.2: RF5110g Evaluation Board Layout.

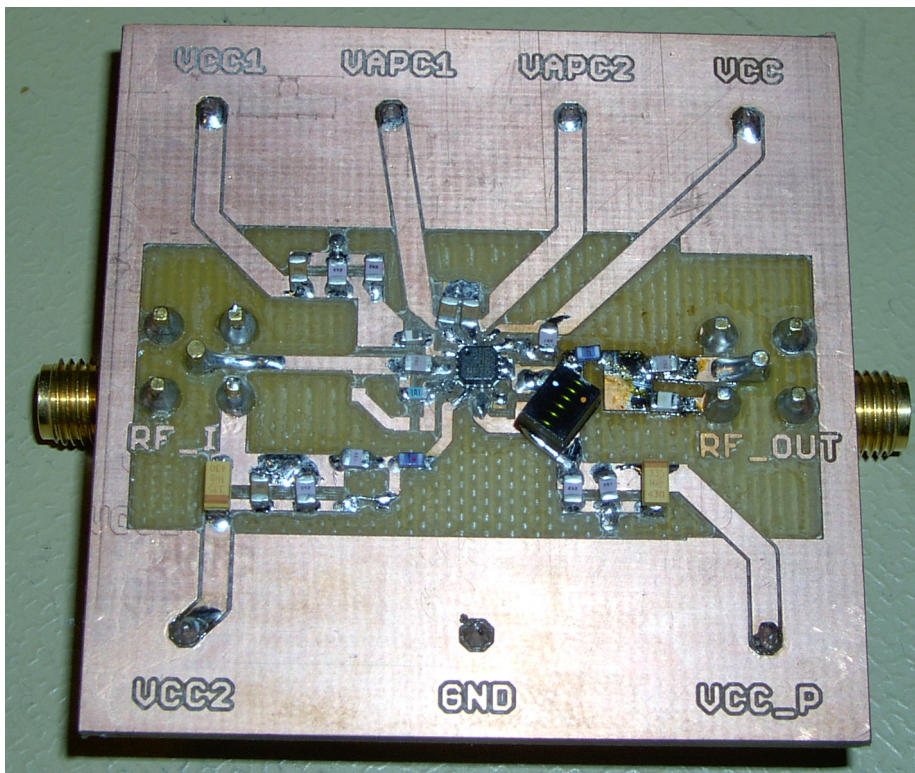


Figure J.3: A picture of the RF5110g evaluation board.

Appendix K

CMX980 serial Interface; Circuit diagrams, software and timing measurements

K.1 External logic Circuit Diagrams

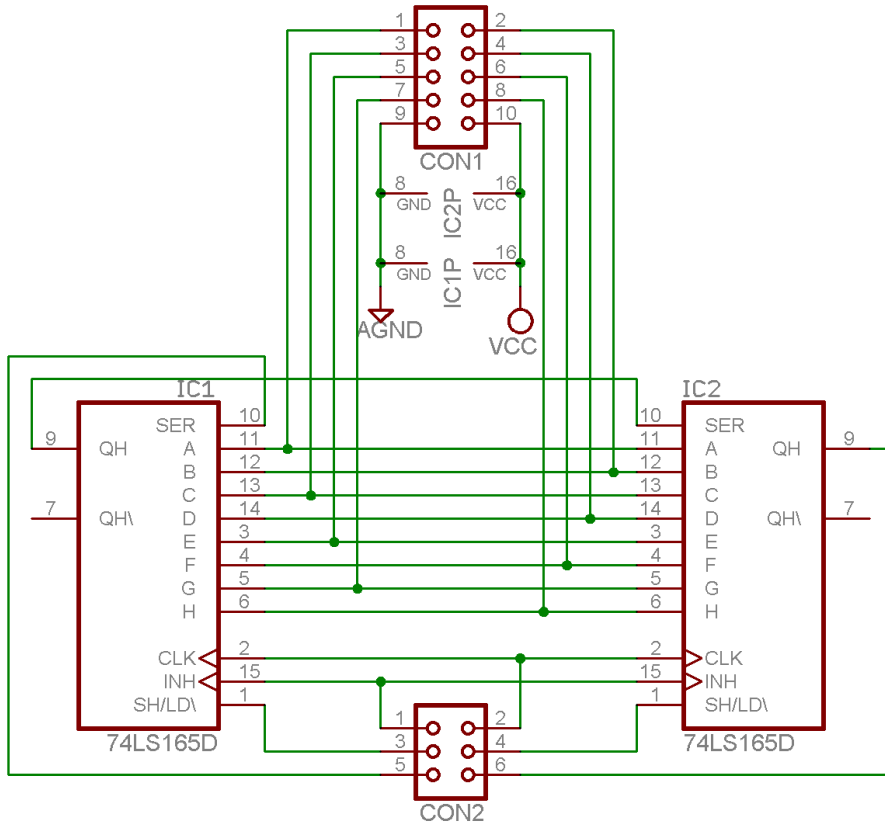


Figure K.1: Schematic of the 16-bit parallel loadable shift register circuit.

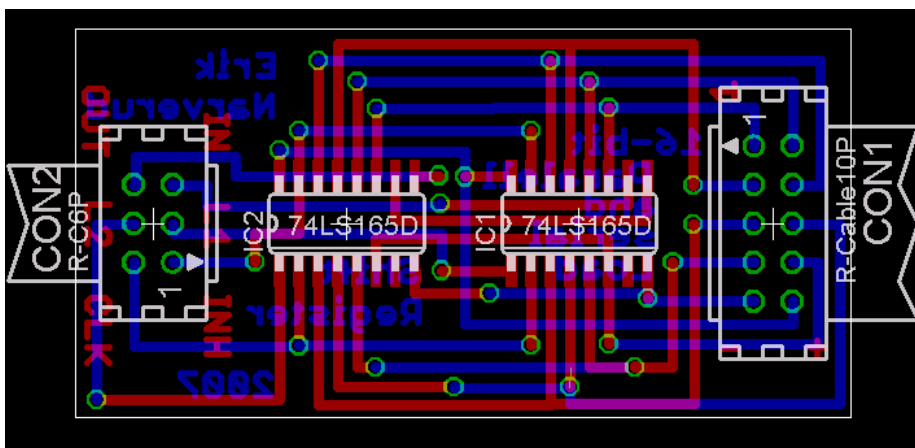


Figure K.2: Layout of the 16-bit parallel-loadable shift register circuit

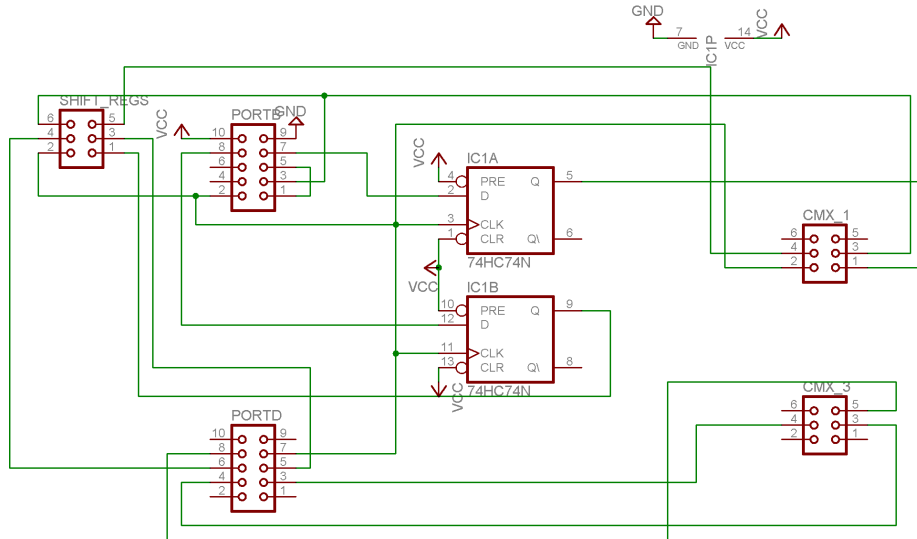


Figure K.3: Schematic of the dual flip-flop and header interface circuit

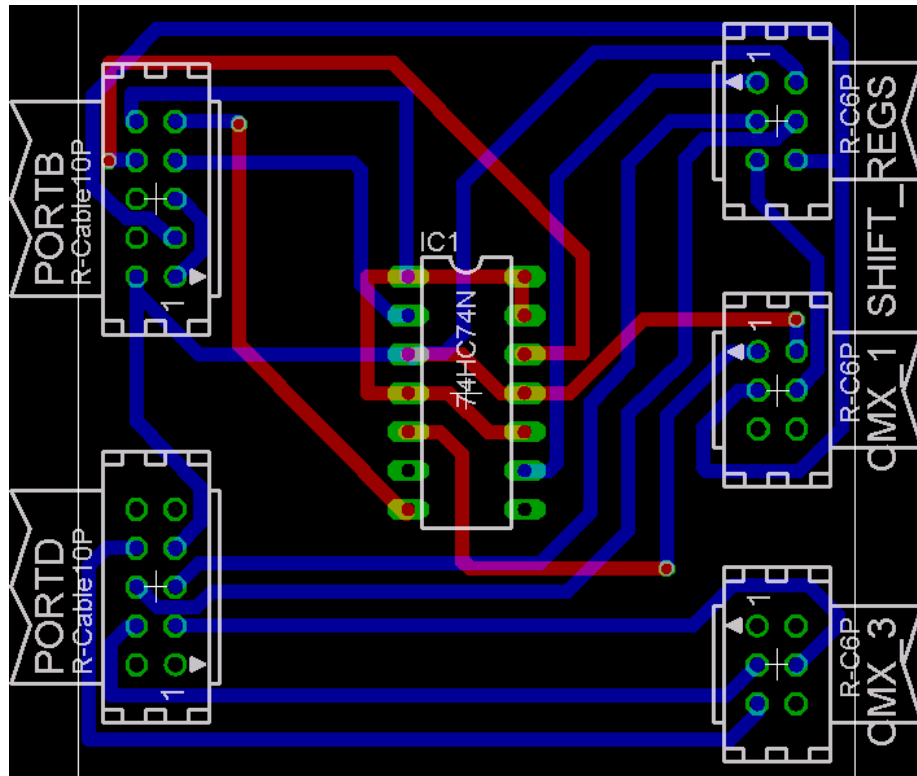


Figure K.4: Layout of the dual flip-flop and header interface circuit

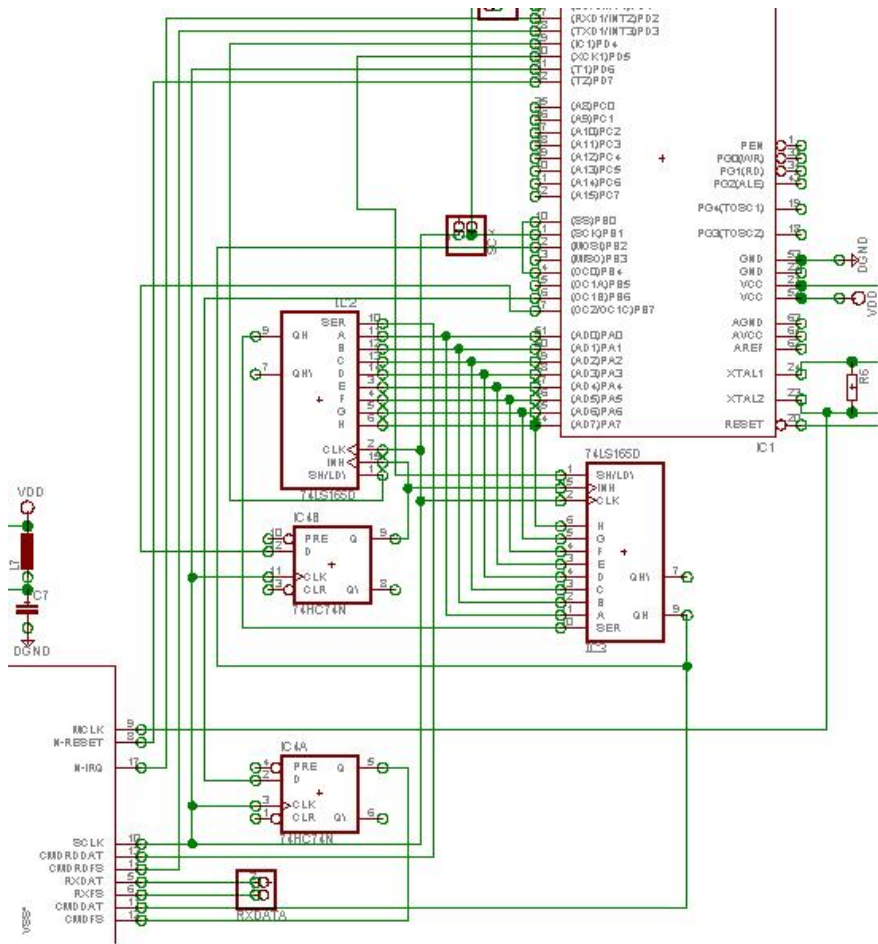


Figure K.5: Digital interface between the ATmega128 microcontroller and the CMX980 baseband processor.

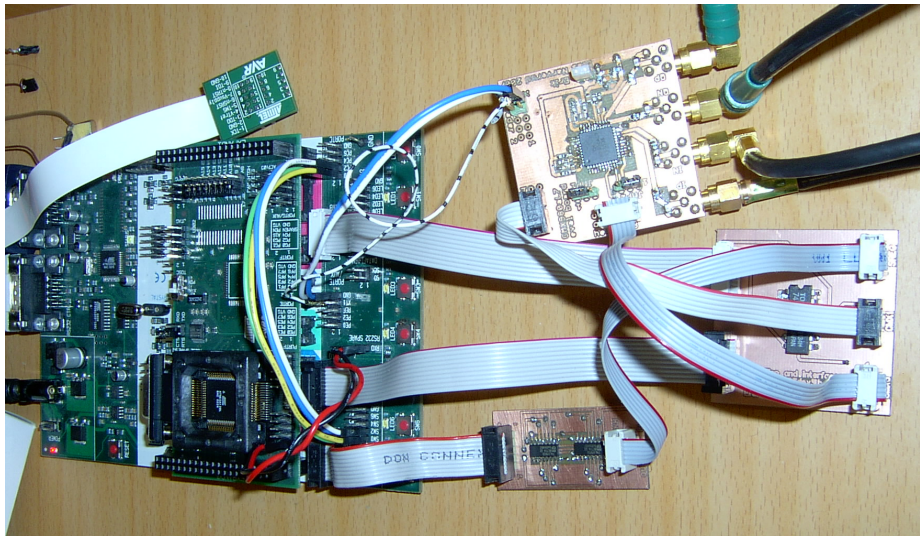


Figure K.6: A picture showing the STK-500 development board connected to the CMX980 evaluation board and the external logic circuits.

K.2 Measured timing Diagrams

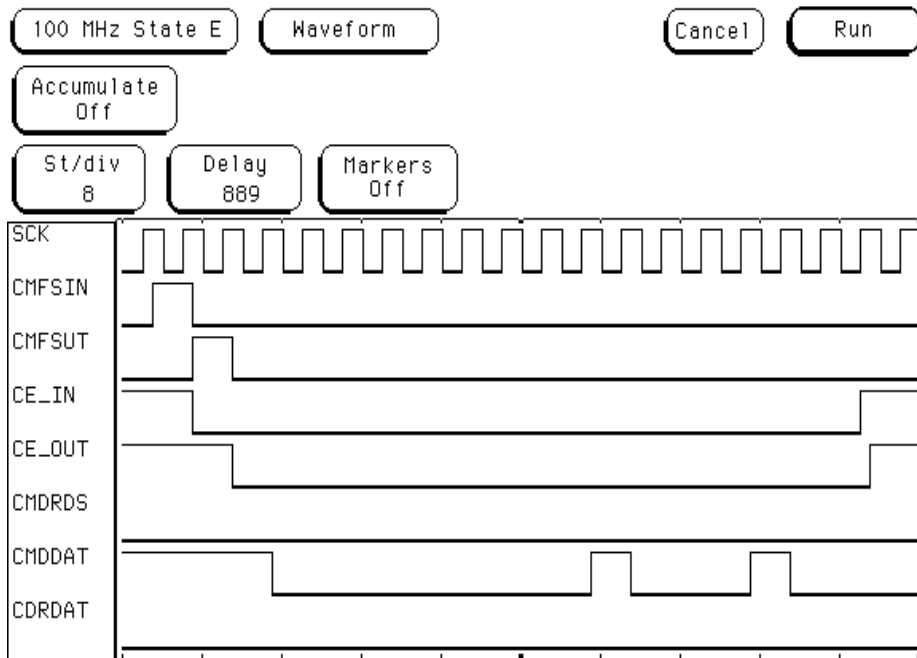


Figure K.7: Measured timing diagram of a CMX980 write operation, with the inputs and outputs of the flip-flops shown.

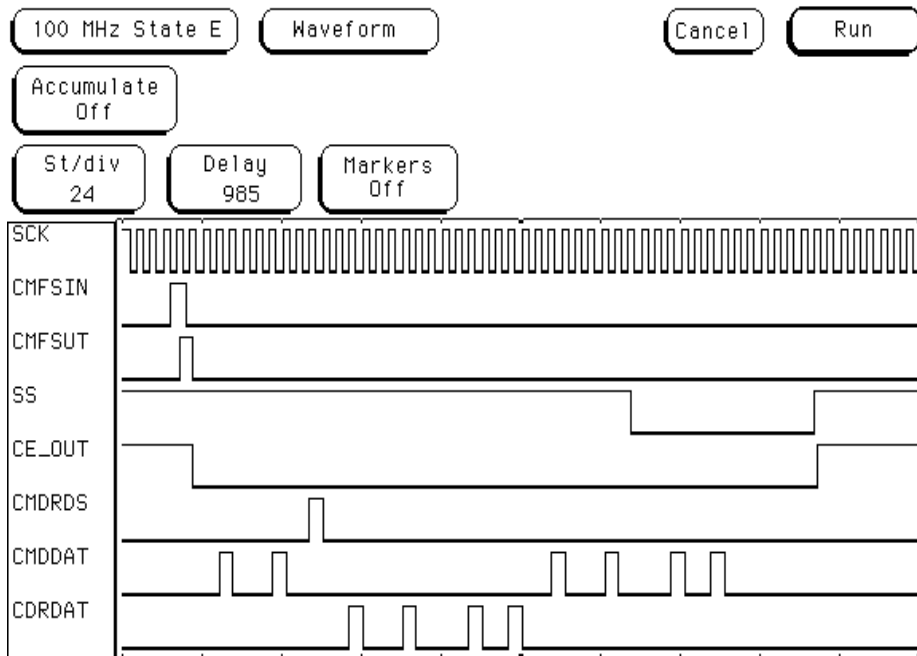


Figure K.8: Measured timing diagram of a CMX980 read operation, with the inputs and outputs of the flip-flops shown.

K.3 Microcontroller Software

Listing K.1: ATmega128 Code for CMX980a interface - *CMX980.h*

```

1  /*Register addresses, commands words and functions for\
   communication between
   the CML Microcircuits CMX980a baseband processor and \
   the Atmel ATmega128.
3
4  Erik Narverud - 2007
5
6  The circuit uses two 8-bit shift registers to \
   communicate with the 16-bit serial
7  interface on the CMX980. The CMX supplies the serial \
   clock, but the AVR controls the rest.
   Therefore, the serial clock is supplied to a counter \
   which counts the number of bits
9  transferred. This is important if the TxHandshakeEn \
   bit in the ConfigCtrl1 register of the
   CMX is set, as this will halt the serial clock during\
   transmission if the Tx FIFO register
11 is written to while full.
12
13 The CMX980 has a variety of other registers and \
   functions that are not used here.
   Consult the datasheet for a full listing
15
16 The CMX980 uses a paging system in order to expand \
   the 7-bit adress area.
17 The page idetification bits are ConfigCtrl2(7:6). \
   Reset defaults to page 0.*/
18
19 /*Registers accessable in all pages*/
   char ConfigCtrl1 = 0x00;
21 char ConfigCtrl2 = 0x01;
22
23
24
25 /*Page 0 register addresses*/
   char PowerDownCtrl = 0x02;      // Power control \
   Register
27
   char TxSetup = 0x03;           // Transmit path \
   control register
29
   char TxDataHi = 0x07;         // Transmit data \
   register.
31 char TxDataLo = 0x05;
   /*This register is mapped over 4 \
   locations, 0x04-0x07,

```

```

33         as the two LSBs are data. The |
           addresses given here will
           write Tx words with MultiSymbol=1|
           and TxRampUp=1(H1) or 0(L0).
35     */

37     char LoopBackCtrl = 0x0D;      /* LoopBack Control |
           register. The CMX980 features loopback
           connections, making it possible |
           to read both digital and
39     analogue Transmit data on the Rx |
           port by tapping into
           the Tx path.*/

41     char TxErrorStatus = 0x0E;     /* Transmit Error |
           Status Register. Resets when read.
43     char TxErrStatMask = 0x0F;     /* Tx Error Status |
           interrupt mask register
           char RxErrorStatus = 0x20; /* Receive Error |
           status register.
45     char RxErrorStatMask = 0x21;   /* Receive Error |
           Status interrupt mask register
           char TxFIFOStatus = 0x22;  /* Transmit Data |
           FIFO status register
47     char TxFIFOStatMask = 0x23;    /* Transmit data |
           FIFO status interrupt mask register
           char ClkStopCtrl = 0x3C;   /* Clock-Stop |
           Control Register

49     /*TxIQGainMult registers. These registers set the |
           output gain, which is given by the register value
51     divided by 2^11. Thus only the 4 LSBs of the MSB |
           register are valid. The values are 2s complement. |
           */
           char TxIGainLSB = 0x42;    /* I channel LSB |
           gain register
53     char TxIGainMSB = 0x43;        /* I channel MSB |
           gain register
           char TxQGainLSB = 0x48;    /* Q channel LSB |
           gain register
55     char TxQGainMSB = 0x49;        /* Q channel MSB |
           gain register

57     /*TxIQOffset registers. These registers set the |
           output offset, which is given by the register |
           value
           divided by 2^11. Thus only the 4 LSBs of the MSB |
           register are valid. The values are 2s complement. |
           */

```

```
59 char TxIOffsetLSB = 0x44;          // I channel LSB \
    offset register
char TxIOffsetMSB = 0x45;          // I channel MSB \
    offset register
61 char TxQOffsetLSB = 0x4A;        // Q channel LSB \
    offset register
char TxQOffsetMSB = 0x4B;        // Q channel MSB \
    offset register
63
65
67 /*Control words for the CMX980, used to set it up in \
    default Tx mode*/
69 char CFG1Word = (1<<6)|(1<<2);    /* Applies \
    to ConfigCtrl1, disables Rx serial port, enables \
    // handshake configuration.
71 //char CFG1Word = (1<<2);        /* Applies to \
    ConfigCtrl1.Disables Rx Serial Port.*/
73 char CFG2Word = 0x00;            // Applies to \
    ConfigCtrl2. This entire register should be low.
75 char PDCWord = (1<<7)|(1<<5);    /* Applies to \
    PowerDownCtrl. Turns on analogue Bias Chain, and
    Powers down aux. units.*/
77
char TxErrStatWord = (1<<3);        /*This word applies \
    to the TxErrStatMask register, and brings the \
    symbol clock
79                                out on the N_IRQ pin. Used for \
    system testing.*/
81 char TxSWord = 0x04;            // Applies to TxSetup. \
    Enables Tx data path.
83
85
87 /*Definitions of the connections between the CMX980 \
    and the Mega128*/
#define TXRST PORTD7
89 #define SCK PIND6
#define PL1 PORTD5
91 #define PLO PORTD4
#define TXIRQ PORTD2
93 #define CMDRDFS PORTD3
#define CE PORTB7
```

```

95 #define SS PORTB4
96 #define CMDFS PORTB6
97
98
99
101 /*setup functions*/
102
103 void Directions(void) //Setting the initial data \
    direction registers
    {
105     DDRA = 0xFF; //PORTA is a parallell 8bit output
106     DDRD = (1<<PLO)|(1<<PL1)|(1<<TXRST); //pin 7 is \
        controlling the CMX980 reset, pin 6 samples SCK
107     DDRB = (1<<CMDFS)|(1<<CE)|(1<<SS); //set specifically\
        for the CMX980 interface
108     printf("\nData_Direction_registers_set:\nDDRA=");
109     printf("%d", DDRA);
110     printf("\nDDRBB=");
111     printf("%d", DDRB);
112     printf("\nDDRDD=");
113     printf("%d", DDRD);
114     }
115
116
117 void InterruptSetup(void) //enabling and setting \
    external interrupts 2 and 3
    {
119     EICRA |= (1<<ISC31)|(1<<ISC30)|(1<<ISC21)|(1<<ISC20);
120     sei();
121     printf("\n...Global_interrupts_enabled\nEICRA=_");
122     printf("%d", EICRA);
123     }
124
125
126
127 /*CMX980 Communication functions*/
128
129 void CMX98ORST(int X) // CMX980 reset function
    {
131     if (X)
132     PORTD |= (1<<TXRST); // pulling the CMX reset \
        high and waiting a bit)
133     else
134     PORTD &= !(1<<TXRST);
135
136     _delay_loop_1(100);
137     printf("\nCMX980_RESET=");
138     printf("%d", X);

```

```
139 EIMSK |= (1<<INT2);          // Enabling the CMX980 \
    interrupt routine;
printf("\nEXT_INT2 enabled, EIMSK=");
141 printf("%d", EIMSK);
    }
143
145
147
149 void BitCounterSetup(void)    /* Sets up 16 bit \
    counter 1 to count the number of serial
    bits shifted.*/
151 {
    TCCR1B = 0x00;              // Resetting counter \
    functions
153 TCCR1B |= (1<<CS12)|(1<<CS11)|(1<<CS10); /* Sets \
    counter in CTC mode with clock to external pin,
    triggered on rising edge*/
155 OCR1A = 11;                  // Totals 17 periods in \
    write function
    OCR1B = 5;                  // The counter value for \
    compare match B
157 OCR1C = 9;                  // The counter value for \
    compare match C

159 SFIOR |= (1<<TSM)|(1<<PSR321); // holding \
    counter

161 TCNT1 = 0x00;                // Resetting counter \
    register
```

Appendix L

Transmitter Development Circuit Simulation Results

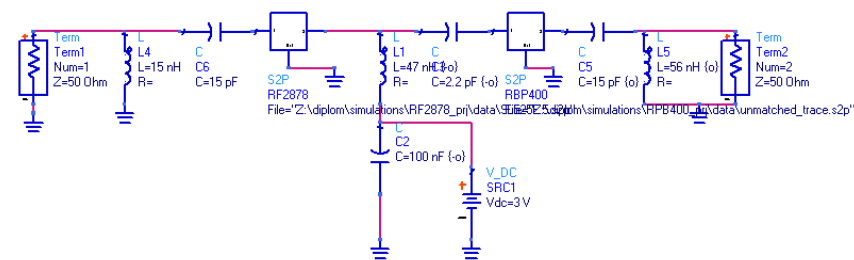


Figure L.1: Simulated matching network for the buffer section of the transmitter development circuit.

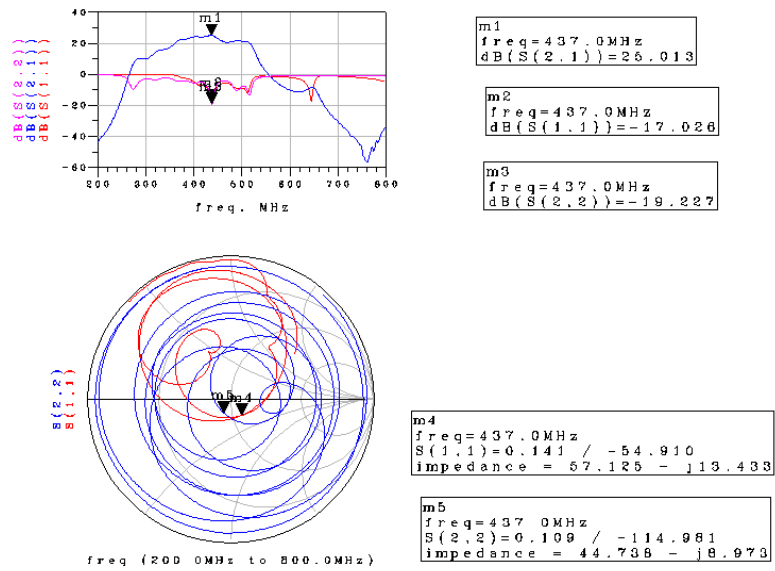
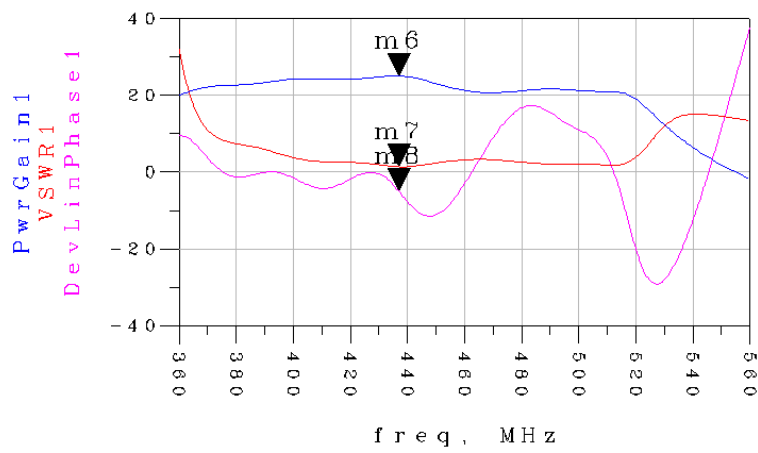


Figure L.2: Simulated s-parameters of the buffer section on the transmitter development circuit.



m6 freq = 437.0 MHz PwrGain1 = 25.013	m7 freq = 437.0 MHz VSWR1 = 1.328
m8 freq = 437.0 MHz DevLinPhase1 = -5.033	

Figure L.3: Simulated Phase and Power response for the buffer section of the transmitter development circuit.

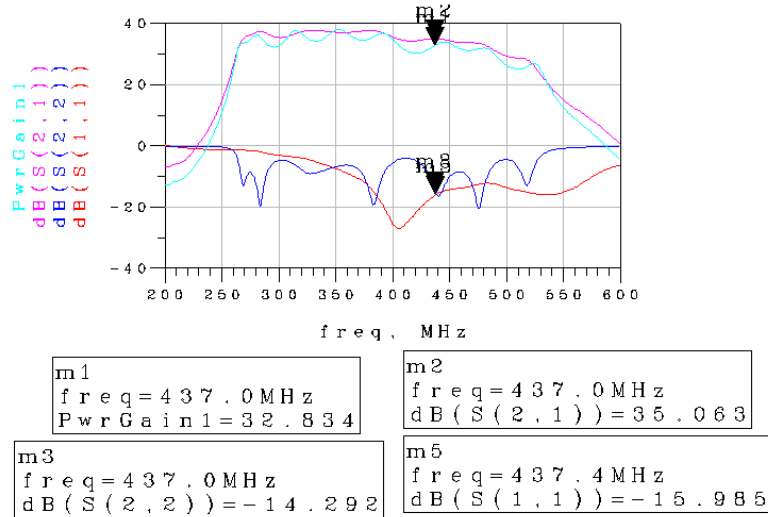


Figure M.2: S-parameter and power gain simulation results for the first stage of the receiver development circuit.

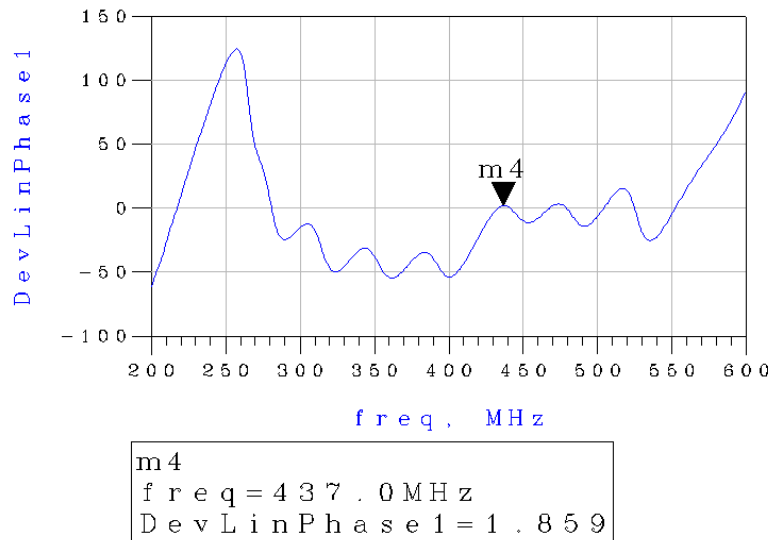


Figure M.3: Simulated phase response for the first stage of the receiver development circuit.

Appendix N

Student satellite Project Documents

Below follows the documentation and presentations made for the System Review, and the presentation made for the recruitment campaign.

N.1 System Design Review; Invitation and Agenda

Innkalling til «System Design Review»

Stad: Rom F404, Elektrobygget Gløshaugen, NTNU

Tid: 1000 – 1430 (merk at vi startar på heil time...)

Bakgrunn

Prosjektet er igangsett for å lage ein oppfølgjar til NCUBE, som var eit samarbeidsprosjekt mellom fleire universitet og høgskular i Noreg. Det nye prosjektet vil vere lokalt styrt ved NTNU for å prøve å halde det meir oversiktleg. Prosjektet vil vere med på NAROM sin studentsatellitt-konkurranse for å få tildelt resursar til oppskyting og testing. Det er venta at NAROM kjem med ei ny utlysing til denne konkurransen i løpet av våren.

Denne møtet vert det første større møtet i samband med satellittprosjektet ved NTNU. På møtet vert prosjektet presantert, saman med den foreløbige tekniske spesifikasjonen for kvart delsystem. I tillegg vert diplomoppgåvene som er under arbeid i vår gjennomgått i meir detalj.

Formålet med møtet er å kvalitetsikre arbeidet som er gjort, deltakarane på møtet vert invitert til å komme med innspel og kritikk til det som vert gjennomgått.

Agenda

10.00 – 10.15	Introduksjon
10.20 – 12.00	Gjennomgang av spesifikasjon (sjå liste under)
12.00 – 12.30	Lunsj
12.30 – 14.00	Individuell gjennomgang av oppgåver
14.00 – 14.30	Eventuelt (PR, rekruttering)

Før lunsj:

Mechanical

Thermal

Payload (Kamera, Langmuirprobe)

Power

Data (OBDH)

Etter lunsj:

Communication

ADCS

Gi gjerne tilbakemelding om du kan komme eller ikkje.

Vel møtt!

Med helsing,

Elisabeth, Erik, Kjell, Jan og Roger

N.2 System Design Review; mechanical Systems Presentation



The CubeSat standard

- Developed by California Polytech. Institute
- A universal standard for small "piggy-back"-launched satellites.
- Designed to minimize complications and interference with the carrying vessel.
- Specifies:
 - Dimensions
 - Weight and mass center
 - Initial Operation and Communication restrictions

2

The CubeSat standard

- Up to 3 satellites are contained in a "P-POD", and simultaneously ejected by a tensioned spring.
- 1, 2 and 3 liter platform sizes available
- 6,5 mm of space available for external components on all sidewalls
- The rails are the only parts allowed in contact with the P-POD at any time

3

The Poly-Picosat Orbital Deployer (P-POD)

4

2 Liter CubeSat:

- 10x10x227 cm, 2 kg
- Advantages to a 1 liter cube:
 - Larger surface means more power
 - Easier to integrate antenna systems
 - Easy adaptation to different missions.
 - Can handle larger and more power intensive payloads, thus more versatile.
- Downsides:
 - More expensive to launch than a single cube
 - Fewer available launches

5

Labels in the diagram include: Topside solar panel, Topside PCB panel, Frame Components, 437MHz antenna reflector, 145 MHz Dipole, Frontside Solar Panels, 437 MHz dipole, Nadir PCB panel, Camera, Rear Solar Panels, Magnetic Coils imprinted on the inside of PCBs, and Internal Modules stacked vertically, mounted in grooves in the structure (Battery mounted above).

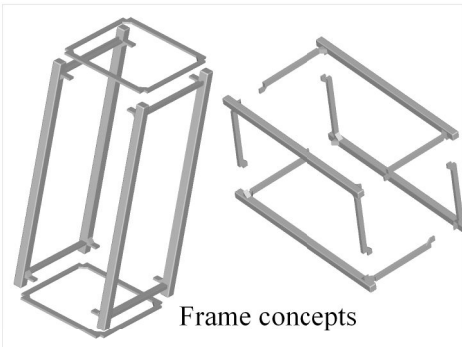
Preliminary Mass budget

Component	Type	Preliminary Dimensions	Quantity	Unit weight	Maximum allowed weight	Total weight
Chassis	7074 Aluminum	100x100x227	1	300	300	300
Sidewalls	FR4 PCB	100x83x1.55	4	40	160	160
Nadir wall	FR4 PCB	100x100x1.55	1	30	30	30
Zenith wall	FR4 PCB	100x100x1.55	1	30	30	30
Solar cells	Si Cells, mounted on sidewalls	80x160x0.5	80	1.2	70	70
Batteries	LiIon 2000 mAh	TBD	2	100	200	200
Battery mounts	7074 Aluminum	TBD	1	50	50	50
Magnetic coils	Printed on sidewall PCB's	TBD	3	0	0	0
437MHz transmitter	PCA	80x80x15	1	50	50	50
149MHz transceiver	PCA	80x80x15	1	50	50	50
ADCS	PCA and sensors	80x80x15	1	80	80	80
OSDH system	PCA and sensors	80x80x15	1	70	70	70
Power management system	PCA and sensors	80x80x15	1	60	60	60
Camera payload	PCA	80x80x15	1	40	40	40
Antenna release system	PCA and mechanics	TBD	1	60	60	60
437 MHz antenna	Antenna and mounting	330x4x1	1	5	5	5
437 MHz reflector	Reflector and mounting	340x4x1	1	5	5	5
145 MHz antenna	Antenna and mounting	1500x4x1	1	20	20	20
Flight Pin	TBD	TBD	1	10	10	10
Connector	TBD	TBD	1	10	10	10
Kill switch	TBD	TBD	2	4	10	10
Misc. Connecting hardware	TBD	TBD	1	100	100	100
SUM						1410

Mechanical Challenges

- Chassis demands:
 - conformity with the CubeSat standard
 - as light as possible
 - Must endure launch and space environment
 - Must not be susceptible to harmonic vibration during launch

8



Antenna challenges

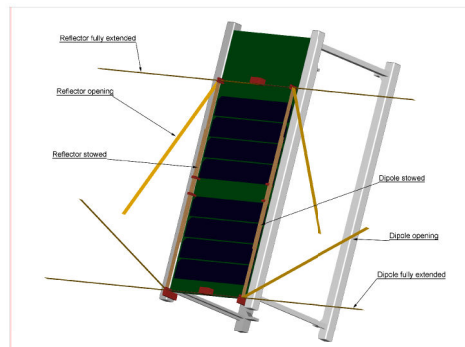
- The antenna must be stowable
- The mechanism must endure launch and space environment
- Mounting solution must not conflict with other parts, such as solar panels.
- The materials used must be able to withstand space conditions.

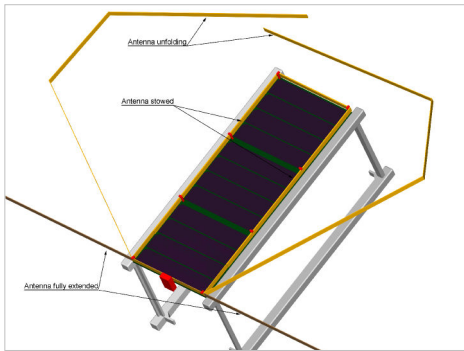
10

Antenna Deployment Mechanism

- A successful antenna deployment is essential for satellite operation
- The mechanical aspect makes antenna deployment a critical factor
- A possible solution makes use of leafspring antenna elements, held down by nylon threads
- The nylons are melted by NiChrome wires, releasing the elements


11





More information:

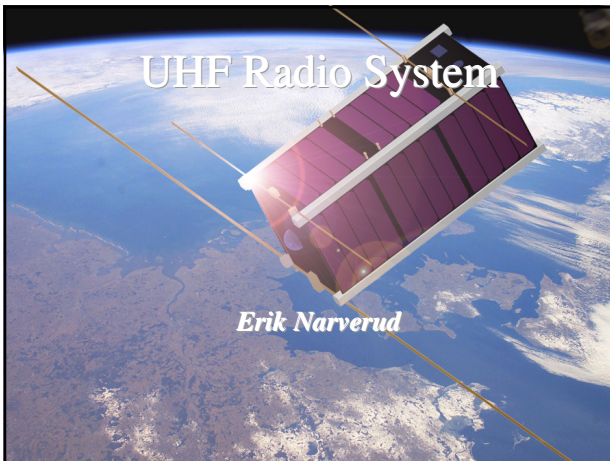
- <http://org.ntnu.no/studsat>
- Studsat@list.stud.ntnu.no

 **NTNU**
Innovation and Creativity

14

The image shows a satellite in orbit above the Earth's horizon. The satellite is a small, rectangular object with a purple and white color scheme. The background is a dark blue sky with the Earth's surface visible below. The text 'More information:' is at the top left, followed by two lines of contact information. The NTNU logo and name are at the bottom left, and the number '14' is at the bottom right.

N.3 System Design Review; UHF Radio System Presentation



Known parameters

- Assumed Carrier frequency 437.305 MHz
- Assumed allowed bandwidth 25 KHz
- +/- 12 KHz Doppler
- Half-duplex transceiver
- Primary function is payload data transmitter
- Limited power available
- directive dipole antenna concept developed

Initial Link Budget

Constants	Worst Case	Best Case	Unit
Carrier Frequency	4,37E+08	4,37E+08	[Hz]
Speed of light	3,00E+08	3,00E+08	[m/s]
Carrier Wavelength	0,69	0,69	[m]
Earth Radius	6378000,00	6378000,00	[m]
Pi	3,14	3,14	
Boltzmann's constant	1,38E-23	1,38E-23	[J/K]
Parameters	Value	Value	Unit
elevation	10,00	90,00	[deg]
Orbit Height	800000,00	400000,00	[m]
Maximum Distance	2366866,61	400000,00	[m]
Output RF Power (EIRP)	0,00	0,00	[dBW]
Propagation Losses			
Free Space Loss	152,74	137,30	[dB]
Polarization Loss	3,00	3,00	[dB]
atmospheric scintillation	6,00	3,00	[dB]
Satellite antenna gain	2,00	5,77	[dB]
Power at antenna connection	-159,74	-137,53	[dBW]
Difference in received power	22,21		[dB]
Noise properties for satellite antenna			
antenna Noise bandwidth	3,50E+04	3,50E+04	[Hz]
antenna noise temperature	300,00	200,00	[K]
noise power on antenna connection	-158,39	-160,15	[dB]
C/N at antenna connection	-1,35	22,62	[dB]

Demands

- Relatively high baud rate, enabling image download during a single transmission
- High reliability
- Low power consumption
- Low complexity
- Protocol/packet handling and coding capability

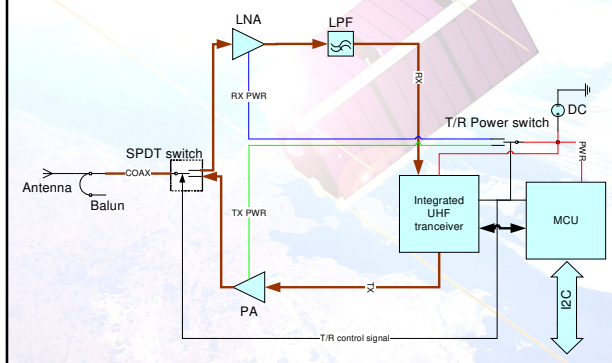
Desired features:

- Modulation with good spectral efficiency and low linearity requirements, due to the narrow band and low output power
- Highly integrated "Off-the-Shelf" components for higher reliability and low power consumption
- Good noise performance
- As many Hardwired parameters as possible

Alternative 1: fully integrated system

- Based on short range transceivers such as Nordic or Chipcon/TI products
- Advantages:
 - Very few parts
 - Low power consumption
- Disadvantages:
 - Design constrained by few degrees of freedom
 - Poor noise performance
 - Software defined – vulnerable to SEU/latch-up

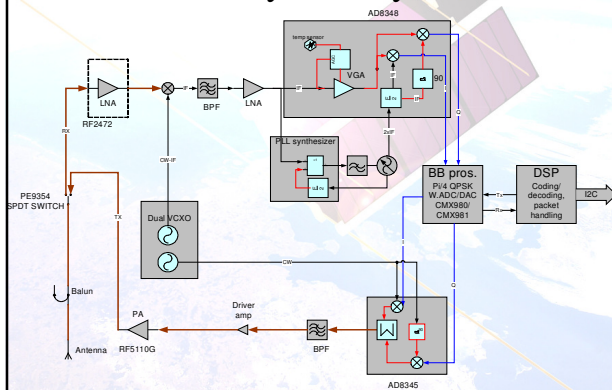
Fully integrated system layout



Alternative 2: Component assembled system with DSP

- Based on off-the-shelf components designated for hand-held systems and base-stations, with a designated DSP
- Advantages:
 - Enables custom design and modulation
 - Good Noise performance
- Disadvantages:
 - High power consumption due to DSP
 - High complexity
 - Software defined modem vulnerable to SEUs/latch-up

DSP system layout



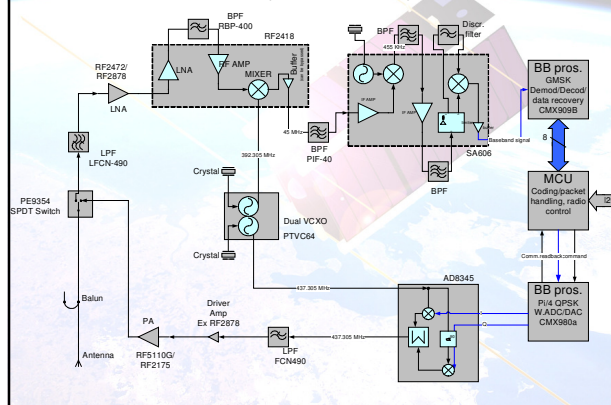
Alternative 3: Integrated system without DSP

- How to get rid of the power consuming DSP?
 - PI/4-DQPSK modulator available; DSP needed only for demod
 - No need for high-speed uplink
 - No need for QPSK modulated uplink
 - Half-duplex, RX powered down when transmitting and vice versa, enables use of two baseband processors
- Decision made to use GMSK modulation uplink
 - DSP replaced with PI/4-DQPSK modulator and GMSK demodulator(modem), both available off-the-shelf.

Key features:

- Transmitter:
 - 19,2 KBPS raised cosine pi/4-DQPSK modulation
 - Coding, packet handling and FEC
 - Potentially 1.5 W output power
 - Potentially 50% DC efficiency
- Receiver:
 - Double superhet 9600 BPS GMSK
 - Decoding, Packet handling and FEC
 - IF system similar to VHF receiver

Final system Layout



Power consumption

Transmitter	Voltage	Current, mA		Power mW	
		transmit	standby	transmit	standby
MCU	3	10	0	30	0
CMX80A baseband processor	3	20	0	60	0
ADB345 modulator/converter	3	65	0,07	195	0,21
VXCO	3	40	0	120	0
PA driver amp	3	20	0	60	0
Power amp with 50% DC efficiency	3	900	0,01	2700	0
PE9354 SPDT switch	3	0,02	0	0,06	0
Receiver		standby	receive	standby	receive
MCU	3	0	10	0	30
CMX909 modem	3	0	2,5	0	7,5
SA606	3	0	4	0	12
VXCO	3	0	40	0	120
RF2418 LNA/mixer	3	0	12	0	36
RF2472 LNA	3	0	6	0	18
PE9354 SPDT switch	3	0	0,02	0	0,06
TOTALS:	DC/DC eff	Transmit	receive	Transmit	receive
	90 %	1172,244	82,88889	3516,733	246,6333

Downlink budget

Constants	Worst Case	Best Case	Unit
Carrier Frequency	4,37E+08	4,37E+08	[Hz]
Speed of light	3,00E+08	3,00E+08	[m/s]
Carrier Wavelength	0,69	0,69	[m]
Earth Radius	6378000,00	6378000,00	[m]
Pi	3,14	3,14	
Boltzmann's constant	1,38E-23	1,38E-23	[J/K]
Parameters	Value	Value	Unit
elevation	10,00	90,00	[deg]
Orbit Height	800000,00	800000,00	[m]
Maximum Distance	2366866,61	800000,00	[m]
Propagation Losses			
Free Space Loss	152,74	143,32	[dB]
Polarization Loss	3,00	3,00	[dB]
Atmospheric scintillation	6,00	3,00	[dB]
Total Path Loss	161,74	149,32	[dBW]
Noise properties for Ground Station			
Receiver antenna gain	10,00	30,00	[dBW]
Noise bandwidth	3,59E+04	3,59E+04	[Hz]
antenna noise temperature	300,00	250,00	[K]
Receiver noise temperature	450,00	300,00	[K]
System Noise power	-154,71	-155,73	[dB]
Satellite Transmitter Properties			
Antenna SMA connector loss	-0,08	-0,08	[dB]
coax cable loss	-0,20	-0,20	[dB]
PCB SMA connector loss	-0,08	-0,08	[dB]
PE9354 switch loss	-0,50	-0,40	[dB]
PA output power	1,00	2,00	[dBW]
Emitted power	0,14	1,40	[dBW]
Satellite antenna gain	2,00	5,77	[dB]
dBW	2,14	7,17	[dB]
TOTALS			
Received Power	-149,60	-122,16	[dB]
Estimated SNR	5,11	23,61	[dB]

Receiver Gain/noise performance

Component	name	Gain[dB]	NF[dB]	Noise temp[K]	Cascade	
					Gain[dB]	Noise temp[K]
Antenna connection	SMA	-0,06	0,06	4,034301864	-0,06	4,034301864
coax cable	0,25 m	-0,1	0,1	6,754967761	-0,16	10,88324059
connection	SMA	-0,06	0,06	4,034301864	-0,22	15,06894341
switch	PE9354	-0,4	0,4	27,97867688	-0,62	44,5014477
Filter	FCN490	-0,75	0,75	54,66564596	-1,37	107,5557122
LNA	RF2472	20	1,5	119,6358879	18,63	271,5623695
2 LNA	RF2418	14	1,8	148,932762	32,63	273,6040616
Filter	RBP_400	-1,5	1,5	119,6358879	31,13	273,6693538
RF-amp/mixer	RF2418	6	10	2510	37,13	275,8814119
Filter	PIF-40	-0,4	0,4	27,97867688	36,73	275,6868298
2. Mixer stage	SA606	17	6,2	918,9212121	53,73	275,8819392
Filter	CFUKF455KA2X	-4	4	438,4470651	49,73	275,8837966

Uplink Budget

Constants	Worst Case	Best Case	Unit
Carrier Frequency	4,37E+08	4,37E+08	[Hz]
Speed of light	3,00E+08	3,00E+08	[m/s]
Carrier Wavelength	0,69	0,69	[m]
Earth Radius	6378000,00	6378000,00	[m]
Pi	3,14	3,14	
Boltzmann's constant	1,38E-23	1,38E-23	[J/K]
Physical Temperature	290,00	290,00	[K]
Parameters	Value	Value	Unit
elevation	10,00	90,00	[deg]
Orbit Height	800000,00	800000,00	[m]
Maximum Distance	2366866,61	800000,00	[m]
Reference EIRP	0,00	0,00	[dB]
Propagation Losses			
Free Space Loss	152,74	143,32	[dB]
Polarization Loss	3,00	3,00	[dB]
atmospheric scintillation	6,00	3,00	[dB]
Satellite antenna gain	2,00	5,77	[dB]
Power at antenna connection	-158,74	-143,32	[dBW]
Noise properties for satellite antenna			
System Noise bandwidth	3,59E+04	3,59E+04	[Hz]
brightness noise temperature	300,00	250,00	[K]
antenna efficiency	1,00	1,00	
Noise on Antenna connection	298,00	250,00	[K]
SNR at Antenna connection	-1,22	15,03	
Satellite receiver properties			
Receiver noise temperature	275,88	275,88	[K]
Receiver Gain	49,73	49,73	[dB]
Sensitivity on 2nd Stage IF input	-107,00	-112,00	[dB]
Required SNR on 2nd stage IF input	17,00	12,00	[dB]
TOTALS			
Noise temperature (ref. Ant. Connection)	575,98	525,88	[K]
Total power on 2nd. IF stage input	-110,98	-93,82	[dBW]
SNR on 2nd stage IF input	-4,19	12,40	[dB]
MARGINS			
Sensitivity margin	-3,98	18,18	[dB]
SNR margin	-21,19	0,40	[dB]

UHF Antenna System

- Request for a directive antenna in order to increase data throughput
- Potentially inaccurate attitude control requires wide main lobe.
- GOAL: Design a wide, uniform main lobe with a minimum of backwards radiation, realizable as a robust, simple antenna.
- Designed as a dipole with a passive reflector**

Key features

- Maximum gain of 5.77 dB
- 151x76 degree 3dB lobe width
- 32 MHz effective bandwidth
- Perfect impedance match of 50 Ohms** (simulated VSWR<1.01)
- Higher gain than a regular dipole for scan angles up to 125 degrees
- Usable as an omnidirectional antenna if the reflector is kept folded.** (VSWR=1.8)

N.4 System Design Review; Account

Referat System Review, 13 mars 2007, rom F404, Gløshaugen

Deltakrar:

Erik Narverud, Jan Rohde, Kjell Rohde, Roger Birkeland, Elisabeth Blom (studentar)
Håkon Indseth, Eystein Sedberg (Norspace)
Arne Pedersen (UiO)
Rune Sandbakken (Conax)
Odd Gutteberg, Jan Tommy Gravdahl, Morten Olavsbråten, Jon Anders Aas (faglærarar)
Torgrim Gjelsvik (Sintef)
Lasse Borja (IET)
Sverre Hendset, Bjørn B. Larsen (ITK og IET, før lunch)

Agenda

Referat System Review, 13 mars 2007, rom F404, Gløshaugen.....	1
Introduksjon.....	2
Erik Narverud: Mekanisk system.....	2
Roger Birkeland: Termisk system.....	2
Kjell Rohde: Power Management.....	3
Jan Rohde: OBDH (On Board Data Handling).....	4
Arne Pedersen, UiO: Langmuirprobe	6
Jan og Kjell Rohde, ITK: ADCS, Sensorar, Kalmanfilter og aktuatorar.....	7
Roger Birkeland, IET: VHF TTC-radio, Hardware.....	7
Erik Narverud, IET: UHF nyttelastradio.....	7
Avsluttende ord.....	8

Introduksjon

Sjå vedlagt presentasjon, vedlegg 0.

Odd Gutteberg ynskta velkommen og gjekk gjennom bakgrunn for prosjektet. Sjå introduksjonspresentasjon.

Roger Birkeland presanterte ei oversikt over prosjektet, meir bakgrunn, mål og korleis gjennomføring er tenkt.

Erik Narverud: Mekanisk system

Sjå vedlagt presentasjon, vedlegg 1.

Spørsmål og kommentarar:

Rune Sandbakken: Er metoden for innfesting og plassering av komponentar ein standard struktur?

Eystein Sedberg: Må få analysert og testa mekanisk struktur, jo før jo heller. Dette er ikkje ei lita oppgåve!

Utfordring når det gjeld antenne:

- Folding
- Oppskyting
- Ikkje øydelegge noko anna (vibrering som går utover solceller)

Rune Sandbakken: Kontrollere massebudsjettet fortløpande. Kontrollere at ein ikkje går opp mot kritiske grenser.

Arne Pedersen: Kan ein prøve å få hjelp til tilbakemelding/vurdering frå ESA? Dei har program som støttar studentprosjekt. Få kommentarar på design, marginar på system med meir. Kva med mekanisk testing? Skal det gjerast lokalt eller kanskje på Kjeller.

Odd Gutteberg: Vi har tidlegare studentar hos ESA vi kunne ta kontakt med.

Erik: FFI har sagt seg villige til å vere med på testing.

Grunngiving for frekvensvalg: Arv etter nCube, det er desse vi sansynlegvis får tildelt frå NAROM. Kan søke om eigne. Då vert andre, kanskje meir praktiske, antennetypar aktuelle.

Lasse Borja: Har prototype på foldbar patch, men den vil kanskje bli vel kompleks i dette prosjektet.

Roger Birkeland: Termisk system

Sjå vedlagt presentasjon, vedlegg 2

Det er generelle krav til struktur og komponenter. Kun passiv regulering. Ca 17 C likevektstemperatur med 2-5W intern varmeproduksjon.

40 minutt eklipse gir ca -25 C.

Kommentarer:

- Rotasjon av satellitten er viktig så ikkje ei side blir varm medan andre vert avkjølte.
- Ei omfattande termisk analyse er ynskelig og svært viktig.
- Torgrim Gjelsvik: Til dømes bruke oppvaring frå forsterkarar til oppvarming av batteribank.
- Rune Sandbakken/Arne Pedersen: Få hjelp frå ESA? Dei har truleg utstyr og programvare til dette. Bruke ekstern hjelp er viktig!

Kjell Rohde: Power Management

Sjå vedlagt presentasjon, vedlegg 3

Tre oppgåver:

- Ladeovervaking
- Overvåke effektbruk
- Prediktere effektbruk

Forslag til prioritetsliste: Stenge ned system om det ikkje er nok power i satellitten.

1. Lading
2. ADCS
3. ODBH
4. Service Transmission
5. Payload
6. Payload Transmission

Eystein Sedberg: Kvifor står Service Transmission så langt ned? Det er jo definert høgt opp mellom mission goals. Kva skjer om HW eller SW feilar? Må ha ein slags safe-mode. Kva om de-tumbling ikkje fungerer?

Kjell: Denne lista er når satellitten er i drift, dette vil avvike frå initiell operasjon. Må gi de-tumbling ei maksimum-tid.

Torgrim Gjelsvik: Power management bør vere støttesystem til OBDH, slik at OBDH er master og tek avgjersle om opp/ned-kobling.

Erik presanterar effektbudsjett. (sjå vedlegg)

Lasse Borja: Ver klar over at verknadsgrad på IFE-cellene er best-case 10% (Si).

Erik: Målet er GaAs! Vi jobbar med å skaffe dette.

Rune Sandbakken: Kva batteri er det tenkt brukt?

Erik: Li-Ion polymerceller fra Danionics har blitt benyttet i tidligere prosjekter, og oppfyller de ønskede spesifikasjonene. Disse eller lignende bør vurderes.

Jan Rohde: OBDH (On Board Data Handling)

Sjå vedlagt presentasjon, vedlegg 4

Vi vil gå for distribuert bussløsning framfor sentralisert FCU (Flight Computer Unit). Kan tole fleire feil på den måten; Ikkje alle systema i satellitten vil feile om FCU feilar. OBDH kan få power management til å kutte straum til eit system om det sluttar å fungere.

Reloading av programvare kan vere noko å tenkje på, men det er kompleks.

Det kan vere ein fordel å tilretteleggje så til dømes ein av radioane kan overta som master på bussen (I2C) om OBDH feilar skikkeleg. Kompleksitet er også her eit problem.

Håkon Indseth: Vurder Loop-back. Direkte kommunikasjon mellom radio sendar/mottakar.

Jan: Dette er ei kompleks oppgåve, mykje arbeid står igjen.

Kjell: Bit-flips i minne på grunn av høg-energistråling kan vere eit problem. Kan ha ei algoritme som køyrer kontinuerleg som sjekkar pariteten til minne.

Lasse Borja: Atmel har rad-hard 8MB til 1700 dollar... Det er dyrt.

Lasse Borja: Kva er estimatet på bit-flips? På "denne bana". (Bana vår er ukjent pr. i dag)

Erik: Det finst data på dette, men vi har ikkje dei konkrete. Område som den Søramerikanske anomali gjev problem, sannsynlegheit for single-event-upset, latchup eller bit-flip er ikkje lik for alle baneposisjonar. Kan ha ein bootloader-prosedyre i minne som vert kontrollert, så ein kan omprogrammere mikrokontrollerar om dei feilar.

Jan Tommy Gravdal: Bit-flips var vurdert som lite sannsynleg for nCube, med tanke på levetid (relativt kort) på satellitten.

Eystein Sedberg: Må ha ein ting på ein radio med minst mogleg elektronikk som kan køyre power down og power up på heile systemet, om ein får latch-up i CMOS-kretsar. MEN: den må ikkje kunne låse seg så den slår av og på power heile tida!

Bjørn B. Larsen: Kan bruke Rad-Hard komponentar til ei slik løysing. Kanskje verdt å spandere pengar på det.

Erik: Vi vil bruke Rad-Hard RX/TX-switch. Det er ein viktig komponent som ikkje toler å feile!

Torgrim Gjelsvik: Det er ein fin balanse mellom anarki og meir eit bestemt styre. Fleire masterar kan vere rissikabelt. Det er mykje spennande som kan skje om ein kan sykle power frå radiomottakar. Mykje spennande som kan skje!

Eystein Sedberg: Må ha fokus på det som er viktig. Når Dagrevyen melder om at satellitten er oppe, så er nyhenda at vi har fått radiokontakt. Ha minst mogleg nyttelast ombord. Få inn redundans i alle ledd. Begrens talet flotte funksjonar. Analyser heile satellitten med tanke på redundans. Analyser kvar komponent i satellitten for å sjå kva konsekvens ein feil får. FMECA-analyse.

Odd Gutteberg: Dette (tid, og kapasitet til gode feilanalyser) er problemet med studentsatellittprosjekt. Studentane har berre eit år på å designe, produsere og teste.

Eystein Sedberg: Analyse kan godt gjerast av nye studentar med friske auge!

Lasse Borja: "Blind og dum satellitt". Ta med 200 gram autonom hardware som kan svare på ping og gi ein temperatur. Heilt andre frekvensar? 2,4 eller 5,6 GHz patch-antenne til dømes?

Jan Tommy Gravdal: Hugs at målet er å eit ping! Dette var suksesskriteret frå nCube.

Eystein Sedberg: Viktig med analyse i alle ledd. Worstcase-analyse. Temperaturanalyse og termisk sykling må testast. Ikkje tenk på levetid i dette prosjektet. Kan få mange analysene ved å test modellar. FMECA på kritiske element. I visse delar av satellitten må vi ikkje ha moglegheit for feil. (Døme: ei buss-linje som er avkobra til jord --> Er den avkobra med ein kondensator som kortsluttar, dør bussen. Må ha to kondensatorar i serie!)

Lasse Borja: Kan Norspace gi ut eit eksempel på ei slik analyse? Er det proprietære system/programvare?

Eystein Sedberg: Dette er ikkje store og avanserte program. Ein ser på kvar komponent. Feilmodus: komponenten kan ha to feiltilstandar; "short"/"open". Vurdere kva skjer i kvart av dei to tilfella, kva konsekvensar ein slik feil får. Målet er å beskytte seg mot single point of failures.

Lasse Borja: Kan studentar komme ned til Norspace for å sjå på slike prosessar? Opprett dialog med Norspace for å få gjennomført dette!

Eystein Sedberg: Døme på system der ein ikkje vil ha single point of failure er powersystem og kommandomottakar. Ein løysing er å ha to radioar, to batteri i parallell, diode i mellom batteria så det eine ikkje kan kortslutte det andre osv.

Det er bra å lage ein engineering-modell. Testing, testing og testing er viktig. Om denne modellen blir testa skikkeleg, kan ein løyse designproblem tidleg. Når satellitten er montert, testa og skrudd saman, så er det ikkje lov med "skal bare ordne litt"... Ein kan ikkje opne satellitten for å gjere endringar på eit delsystem. Gjere ein det, må heile satellitten testast pånytt etterpå!

- Fokuser på primærfunksjon
- FMECA
- Redundans

- Test sluttproduktet

Erik: Vakuumtest er eit krav i spesifikasjonen. CalPoly har slike testar som vert utført av deira personell før launch. Vi vil også gjere slike testar sjølv. Både på engineeringmodellar og sluttprodukt.

Lasse Borja: CalPoly sine testar handlar om å sjå at alt står fast, ingen lause skruar m.m. samt utgassing. Testane er for å sjå at ein ikkje skadar moderfartøyet eller andre satellitar ombord. Ein testar ikkje *funksjonalitet* der. Det må vi gjere sjølv.

Odd Gutteberg: Kva med testrapportane frå nCube, dei kunne vore nyttig å sett. Dei har vi ikkje.

Arne Pedersen: Test og test er bra, men testar må gå lenge. Termisk sykling tildømes.

Eystein Sedberg: Typisk testprogram:

- Vibrasjon
- Termisk sykling med overvåking. Kan avdekke sprekkar, dårlege loddepunkt osv.

Instituttet Romfysikk i Kiruna: Dei har noko dei kallar ein solsimulator. (Eigentleg eit termisk vakuum-kammer).

Torgrim Gjelsvik: Kva skjer før og under launch med termisk og power? Kva er det termiske miljøet då? Vil batteri stå lenge og bli utlada?

Erik: Fysisk miljø under launch er avh. av typen bærerakett.

Eystein Sedberg: Ein kan sikkert få profilar på bærerakettar frå ESA for å få vite termiske og mekaniske profilar.

Jan: Opprette kontakt med ESA og Norspace er viktig.

Arne Pedersen, UiO: Langmuirprobe

I ettertid har vi mottatt et proposal fra UIO angående dette forslaget til payload, dette finnes i vedlegg 5.

Ein ynskjer å kartlegge strukturar i ionosfæra med ulik ladningstettleik. Desse strukturane påverkar propagasjon til radiobylgjer. Sjå vedlegg 5 for nærmare informasjon.

Instrumentet er laga av to stenger, prober, som til dømes kan stå ca 15 cm frå toppen av satellitten. Desse er forspent ulike spenningar og vil registrere ladning på grunn av elektronstrukturar satellitten går gjennom. Ein kan på den måten måle slike elektronstrukturar i størelsesorden meter. Ein treng å gjere ca 4000-5000 samples/sekund, kanskje i 16 bit oppløysing. Målingane treng ikkje vere kontinuerlege. Mest interessant ved pol-områdene? Kan danne eit bilete av nordlysovalen. Nytteverdien av målingane kan vere å danne seg eit bilde over område der slike elektron kan påvirke radiokommunikasjon slik som GPS og Galileo. Vektanslag er mellom 100 og 150 gram.

Treng truleg lite effekt, og begrensa med datakraft.

Satellitten må vere stabilisert; probene kan ikkje vere skjult bak strukturen, må ha fri-sikt i fartsretningen. Kan isolerast i stor grad frå resten av det mekaniske systemet.

Jan og Kjell Rohde, ITK: ADCS, Sensorar, Kalmanfilter og aktuatorar

Sjå vedlagt presentasjon, vedlegg 6.

Det vert nytta ulike sensorar for å estimere orientasjonen til satellitten; magnetometer og sol-sensor. Har fått magnetometer og tilhøyrande software tilsent gratis. Komponentane har eit lågt straumforbruk.

Det skal brukast fotodioder for å finne kva retning av satellitten som peikar mot sola. Ein må ta høgde for Earth Albedo error, dvs. at sensoren ikkje må slå ut på reflektert solstråling frå jorda.

Har laga eit overslagsvis effektbudsjett, og ser ut til å bruke mindre enn tildelt. Det er bra; Effekt kan heller brukast på til dømes radioar.

Til estimering vert det brukt eit Extended Kalman filter som krevar mykje reknekraft. Nyttar Gauss-Newton algoritmen.

Vurderer å bruke ein låg-effekt mikrokontroller frå Texas.

Innspel frå Lasse Borja: Er PicoPower-serien til Atmel vurdert?

Gravitasjonsbom kan vise seg å vere nødvendig for å ha god stabilitet på satellitten utan å måtte regulere heile tida. Ynskjer å styre bommen med ein DC-motor. Då har ein moglegheit til å ha ei kontrollert ut- og inntrekking av gravitasjonsbom.

Magnetiske koiler (aktuatorar) av same storleik som brukt på nCube.

Spørsmål og innspel:

- Kan ein laste ned data frå estimatoren for å sjå korleis denne jobbar? Nyttig for rekonfigurering og seinare lærdom.
- Gravitasjonsbom og motor vert sett på som eit kompliserane element med fleire utfordringar som må vurderast.

Roger Birkeland, IET: VHF TTC-radio, Hardware

Sjå vedlagd presentasjon, vedlegg 7

Spørsmål og innspel:

- Lasse Borja*: nCube hadde problem med reserverte ord som del av data. Bruke fleire bits ord? Vurdere å lage eit sjølstendig radiofyr på ein anna frekvens som er heilt autonomt og isolert frå resten av systemet.
- Håkon Indseth*: FSK gir det beste resultatet i smalband pga atmosfæriske effektar. Implementere moglegheit for tone-ranging for å måle avstand til satellitten. Utnytte bakkestasjoner verden rundt til overvåking og kommunikasjon med satellitten.
- Lasse Borja*: Ein får baneparameter frå NORAD.

Erik Narverud, IET: UHF nyttelastradio

Sjå vedlagt presentasjon, vedlegg 8

Kommentarar:

- *Lasse Borja*: 300 kB for et semikomprimert VGA-bilde.
- *Håkon Indseth*: Sjekket fasegangen i filtrene?
- *Erik*: Ja, det er kontrollert og skal gå bra. Men må måle og verifisere på lab.

Målet er å ha ein opplink operativ heile tida.

Avsluttende ord

Referat og presentasjonar skal sendast ut.

Kommentarar:

- *Odd Gutteberg*: Kunne tenke seg å køyre dette som eit “profesjonelt” prosjekt, men det er vanskeleg å gjennomføre skikkeleg pga. at studentane vert skifta ut etter som prosjektet går framover.
- *Erik* viste prosjektdatabasen, og sa litt om framtidige oppgåver og organisering. Ein treng omlag 10 studentar minimum frå hausten av for å ta tak i dei oppgåvene som ventar.

PR: Ønsker input.

- Interessant å vite om for radioamatører. Lag en hjemmeside med skikkelige faguttrykk.

Møtet slutt

N.5 Future Assignments



Future Assignments

- Most work to be done as 9th semester project and masters theses
- This enables students to be engaged in the project during two consecutive semesters
- Tasks include:
 - Design
 - Simulation
 - Construction
 - Test

2

OnBoard Data Handling

- IDI, IET, ITK
- The satellite must have an integrated common bus, a central processing unit and central storage. All payload and electrical subsystems must operate on the bus, making it easy to connect modules without excessive re-configuring. High priority, autumn 2007
- Extent: Project/diploma. 1 or 2 persons.

3

Power Management System

- IDI, IET, ITK
- Design and build a power management system to control solar panels, battery bank and power consumption. High priority, autumn 2007
- Extent: Project/diploma. 1 or 2 persons.

4

Antenna System

- IET
- An antenna system is designed. This system must be verified, tested and adjusted if needed. The deployment mechanism must be designed and tested. High priority, autumn 2007
- Extent: Project. 1 person.

5

Ground Station

- IET, IDI, ITEM
- We would like to have our own ground station here at NTNU. The station must be specified and constructed. The work can be done in co-operation with Akademisk RadioKlubb here in Trondheim.
- Extent: Project/diploma. 1 or 2 persons.

6

Error Detection And Correction, EDAC

- IDI
- It is desirable to develop an EDAC algorithm for the satellite memory, as radiation may cause irregular errors, known as "bit-flips" in the memory registers. The assignment may also include development of memory access protocols. A study of how to minimize the risk of critical latch-ups and other software related problems can also be included.
- Extent: Project/diploma. 1 person.

7

TT&C CODEC

- IET, IDI, ITEM
- Operation Procedures, Protocols and Commands
- An important part of the TT&C-system is the software part. The coder and decoder must send and receive data and commands to and from the TT&C radio hardware. The software controlling the satellite, running on the ODBH micro controller, must be developed. Protocols for internal communications, as well as internal and external commands and operating procedures must be defined. The task can be done in combination with the EDAC algorithm development.
- Extent: Project/diploma. 1 or 2 persons.

8

Mechanical Modelling and Production

- IPM
- Both the satellite frame structure and the internal layout must be further developed. Some work has already been carried out. Important issues: Vibration, thermal extending/contraction, easy mounting of modules, weight and balance. The design must comply with the CubeSat standard.
- Extent: Project/(diploma). 1 or 2 persons.

9

Thermal Modelling

- IFY, IPM
- Although a simple thermal analysis has been conducted, more knowledge of the satellites thermal environment is desirable. A full analysis of the structure would be useful in order to detect possible temperature related problems before launch. Can be done in relation with the mechanical design task.
- Extent: Project/diploma. 1 person.

10

Scientific Payload

- IFY, UiO
- The satellite will be built as a "reusable" platform. Other groups are invited to suggest possible payloads. The payload must comply with the existing power, weight and size requirements. Interfaces for power and internal communication must be developed.
- Extent: Project/diploma

11

Recruitment

- The assignments outlined is minimum needed workload
- Is it possible? Are the teachers and students motivated?
- We need to start internal PR campaign in a few weeks
- This work will go on for two more years

12

Why?

- Multidisciplinary project to every extent!
- PR for education at NTNU
- Use theories in practice!
- A more tidy project than NCUBE. Locally managed
- Ambitious project...
- ...and FUN!

13

More Information:

<http://org.ntnu.no/studsat>
studsat@list.stud.ntnu.no



14